Agenzia nazionale per le nuove tecnologie,
l'energia e lo sviluppo economico sostenibile

MINISTERO DELLO SVILUPPO ECONOMICO

Ricerca di Sistema elettrico

Installazione della sezione di prova HERO nella facility CIRCE: sviluppo nodalizzazioni e progettazione della campagna sperimentale

V. Narcisi, F. Giannetti, G. Caruso,
D. Rozzia, A. Del Nevo, M. Tarantino

Report RdS/PAR2015/044

INSTALLAZIONE DELLA SEZIONE DI PROVA HERO NELLA FACILITY CIRCE: SVILUPPO NODALIZZAZIONI E PROGETTAZIONE DELLA CAMPAGNA SPERIMENTALE

V. Narcisi, F. Giannetti, G. Caruso (CIRTEN- UNIRM1)
D. Rozzia, A. Del Nevo, M. Tarantino (ENEA)

Settembre 2016

Report Ricerca di Sistema Elettrico

Accordo di Programma Ministero dello Sviluppo Economico - ENEA
Piano Annuale di Realizzazione 2015
Area: Generazione di Energia Elettrica con Basse Emissioni di Carbonio
Progetto: Sviluppo competenze scientifiche nel campo della sicurezza nucleare e collaborazione ai programmi internazionali per il nucleare di IV Generazione.
Linea: Collaborazione ai programmi internazionali per il nucleare di IV Generazione
Obiettivo: Termoidraulica del Refrigerante
Responsabile del Progetto: Mariano Tarantino, ENEA

Il presente documento descrive le attività di ricerca svolte all'interno dell'Accordo di collaborazione "Sviluppo competenze scientifiche nel campo della sicurezza nucleare e collaborazione ai programmi internazionali per i nucleare di IV Generazione"
Responsabile scientifico ENEA: Mariano Tarantino
Responsabile scientifico CIRTEN: Giuseppe Forasassi

Titolo

INSTALLAZIONE DELLA SEZIONE DI PROVA HERO NELLA FACILITY CIRCE: SVILUPPO NODALIZZAZIONI E PROGETTAZIONE DELLA CAMPAGNA SPERIMENTALE

Descrittori

Tipologia del documento: **Rapporto Tecnico**
Collocazione contrattuale: Accordo di programma ENEA-MSE su sicurezza nucleare e reattori di IV generazione
Argomenti trattati: Generation IV reactors, Termoidraulica dei reattori nucleari, Tecnologia dei Metalli Liquidi

Sommario

Nell'ambito del progetto LEADER (Lead-cooled European Advanced DEmonstration Reactor) è stata proposta una nuova configurazione per lo Steam Generator (SG) del ALFRED ALFRED (Advanced Lead Fast Reactor European Demonstrator): il super-heated steam double wall bayonet tube type con monitoraggio delle perdite. A causa delle caratteristiche innovative di questa tipologia di SG, è necessaria un apposito task di R&D per investigare, sviluppare e migliorare gli SG con tubi a baionetta a doppia parete e sviluppare nel contempo un database per la validazione dei codici. Per questo scopo, ENEA ha progettato e costruito la sezione di prova HERO (Heavy liquid mEtal pRessurized water cOoled tubes). Questa sezione di prova è installata nella facility CIRCE ed è costituita da sette tubi a baionetta che rappresentano i tubi del SG di ALFRED in piena scala. Il report ha lo scopo di descrivere la test-section HERO CIRCE ed i calcoli di pre-test sviluppati con i codici RELAP5/Mod3.3 e RELAP5-3D.

Note

Autori:
Vincenzo Narcisi, Fabio Giannetti, Gianfranco Caruso
(CIRTEN-"SAPIENZA" UNIVERSITY OF ROME)
D. Rozzia, A. Del Nevo, M. Tarantino (ENEA)

Copia n. **In carico a:**

REV.	DESCRIZIONE	DATA		REDAZIONE	CONVALIDA	APPROVAZIONE
2			NOME			
			FIRMA			
1			NOME			
			FIRMA			
0	EMISSIONE	26/09/16	NOME	A. Del Nevo	I. Di Piazza	M. Tarantino
			FIRMA			

(Page intentionally left blank)

SUMMARY

In the framework of the Lead-cooled European Advanced DEmonstration Reactor (LEADER) project a new configuration of Steam Generator (SG) has been proposed for ALFRED (Advanced Lead Fast Reactor European Demonstrator): the super-heated steam double wall bayonet tube type with leakage monitoring. This concept allows the double physical separation between the primary lead in the pool and steam-water primary coolant that flows in the tubes. To these purposes, ENEA designed and constructed the HERO (Heavy liquid mEtal pRessurized water cOoled tubes) test section. This device is actually located in CIRCE and consists of seven double wall bayonet tubes that represent the ALFRED SG tubes (1:1 in length). The present report is aimed to describe the HERO-CIRCE test section and the pre-test calculations conducted by means of RELAP5/Mod 3.3 and RELAP5-3D.

(Page intentionally left blank)

List of contents

LIST OF FIGURES

LIST OF TABLES

(Page intentionally left blank)

ACRONYMS

ALFRED	Advanced LFR European Demonstrator
CIRCE	CIRcolazione Eutettico
DHR	Decay Heat Removal
ENEA	Agenzia nazionale per le nuove tecnologie, l'energia e lo sviluppo economico sostenibile
FPS	Fuel Pin Simulator
HERO	Heavy liquid mEtal – pRessurized water cOoled tube
HLM	Heavy Liquid-Metal
HS	Heat Source
HX	Heat Exchanger
LBE	Lead-Bismuth Eutectic
LEADER	Lead-cooled European Advanced DEmonstration Reactor
LFR	Lead cooled Fast Reactor
NPP	Nuclear Power Plant
R&D	Research and Development
SG	Steam Generator
SGBT	SG Bayonet Tube
TC	Thermocouple

(Page intentionally left blank)

1 Introduction

In the framework of the Lead-cooled European Advanced DEmonstration Reactor (LEADER) project a new configuration of Steam Generator (SG) has been proposed for ALFRED (Advanced Lead Fast Reactor European Demonstrator): the super-heated steam double wall bayonet tube type with leakage monitoring[1] [2] [3]. This concept allows the double physical separation between the primary lead in the pool and steam-water primary coolant that flows in the tubes.

There are two primary reasons for this separation. The first is to increase the safety margin of the NPP by reducing the probability of interaction coolant-hot fluid. The second is that this configuration allows the possibility to monitor eventual leakages from the coolant or from the hot fluid by pressurizing the separation region (i.e by helium). On the other hand, since it is required to monitor the leakages (using a low conductivity material as a gas) and get high thermal performance of the unit, the annular space that separates the fluids should be filled with a porous heat transfer enhancer (i.e. powder).

Due to the innovative features of this concept, R&D is mandatory to develop, investigate and improve double wall bayonet tube bundle SGs as well as to establish a comprehensive database for code validation.

To these purposes, ENEA designed and constructed the HERO (Heavy liquid mEtal pRessurized water cOoled tubes) test section. This device is actually located in CIRCE and consists of seven double wall bayonet tubes that represent, as much as possible, the ALFRED SG tubes (1:1 in length)[4] to [7].
The present report is aimed to describe the HERO-CIRCE test section and the pre-test calculations conducted by means of RELAP5/Mod 3.3 and RELAP5-3D.

(Page intentionally left blank)

2 CIRCE-HERO overview

CIRCE is a multipurpose facility dedicated to the study of innovative nuclear system cooled by heavy liquid metal (HLM). It consists of a main cylindrical vessel (S100) with an outer diameter of 1200 mm and a height of 8500mm. The main vessel can be filled with about 70 tons of molten Lead-Bismuth Eutectic (LBE) and it has been designed to host different test sections welded to and hung from bolted vessel heads for the study of thermal-hydraulic issues related to the HLM pool system.

The main vessel is equipped with auxiliary systems for eutectic circulation, with argon cover gas and recirculation system, LBE heating and cooling system.

The facility is completed with a LBE storage tank (S200), used for the liquid metal storage during maintenance phases, a small LBE transfer tank (S300) and the data acquisition systems[4] to [7].

In Fig. 1 an isometric view of the facility is shown. The main parameters relevant to the test vessel are listed in Tab. 1.

The test section is equipped with the heat source which is coupled with the facility by an appropriate mechanical structure. The HS and the mechanical structure which surrounds it make up the so called Fuel Pin Simulator (FPS). It consist of a pin bundle made by electrical heaters with a nominal thermal power of 800 kW and a total thermal power of 925 kW. The design has been aimed at achieving a difference temperature through the HS of 100°C, a fuel power density of 500 W/cm3 and average liquid metal velocity of 1 m/s.

HERO test section is implemented in CIRCE. The aim is to study the behaviour of a 1:1 bayonet tube/s under operational condition of ALFRED SG.

HERO is composed by a hexagonal shroud that contains 7 SGBT of the same geometry of the ALFRED SG (Fig. 2). The main parameters of the shroud geometry is listed in Tab. 2.

The steam generator tubes are fed by LBE, which flows by gas enhanced circulation, from the top by means of fissures that communicate with the internal zone of the separator. The LBE flows inside the tube bundle for six meters (as in the ALFRED SG) and then it leaves the device from the bottom. In the secondary side, feed-water enters the SG from its top head and is distributed to the bayonet tubes through an upper plate. It crosses each tube in down-flow and then in up-flow. The rising annular zone is insulated from the inner down flow zone by an air gap. The annular riser is designed to remove the heat from the LBE, that flows in countercurrent, and to generate superheated steam. So, gap between rising annular zone and LBE zone is filled by pressurized helium and high thermal conductivity powder with to enhance the heat exchange capability. This solution provides a double physical separation that avoid LBE-water interaction and the possibility of detecting the rupture by monitoring He pressure.

Finally the steam leaves the SG at its top nozzles, located below the bayonet tube top plate. The heat exchange capability of HERO is 504 kW.

Parameters	Value
Outside diameter [mm]	1200
Wall thickness [mm]	15
Material	AISI 316L
Max LBE inventory [kg]	90000
Electrical heating [kW]	47
Cooling air flow rate [Nm^3/s]	3
Temperature range [°C]	200 to 500
Operating pressure [kPa]	15 (gauge)
Design pressure [kPa]	450 (gauge)
Argon flow rate [Nl/s]	15
Argon injection pressure [kPa]	600 (gauge9

Tab. 1 – CIRCE S100 main parameters

Parameters	Value
L [m]	0,0726
Trasversal area [m^2]	0,0137
Power [kW]	504

Tab. 2 – HERO parameters

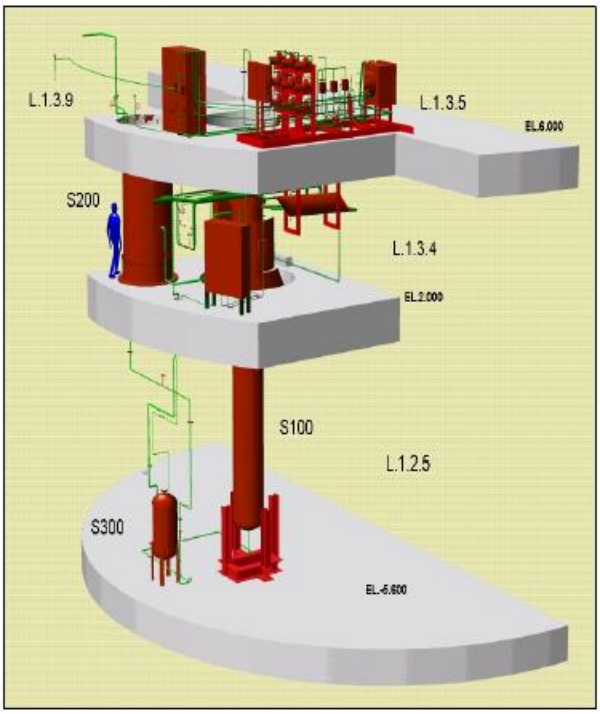

Fig. 1 – CIRCE isometric view

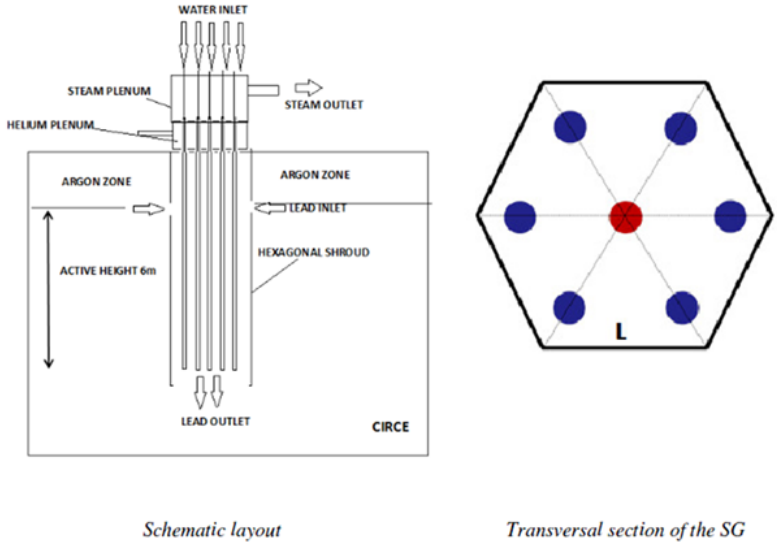

Fig. 2 – Arrangement and geometry of the seven tubes and hexagonal box

2.1 Primary system

The primary loop is characterized by:

- the Feeding Conduit;
- the Fuel Pin Simulator;
- the Release Pipe;
- the Fitting Volume;
- the Riser;
- the Separator;
- the LBE pool;
- the steam generator (HERO).

The primary circuit of CIRCE-HERO test facility is conceived in order to model a pool type reactor. All components are placed within CIRCE pool and submerged by LBE.

Primary coolant flow in downward through the pool into the lower plenum. From the lower plenum the fluid is pushed into the feeding conduit and passes through the Venturi-nozzle flow meter. The LBE, flowing upward, increases its temperature passing through the FPS. The hot fluid reaches a fitting volume and hence the riser that bring LBE at the separator, placed in the upper region of the main vessel. The circulation is enhanced by the argon injection in the bottom of the riser. So, the two-phases mixture flow upwards in the riser and collects in the separator. Here the mixture is separated and LBE flow into HERO where hot fluid is cooled and flows downward into the pool.

The CIRCE-HERO unit is shown during installation phases in Fig. 3.

The Fig. 4 shows the path of the primary fluid. It is indicated the dead volume. This component performs two main functions: the first one is to guarantee the placement and cooling of the FPS and the location of power and instrumentation cables; the second one is to limit the volume that has to be filled with the LBE.

A detailed description of the primary system components is provided in the following sections.

Fig. 3 – CIRCE-HERO unit

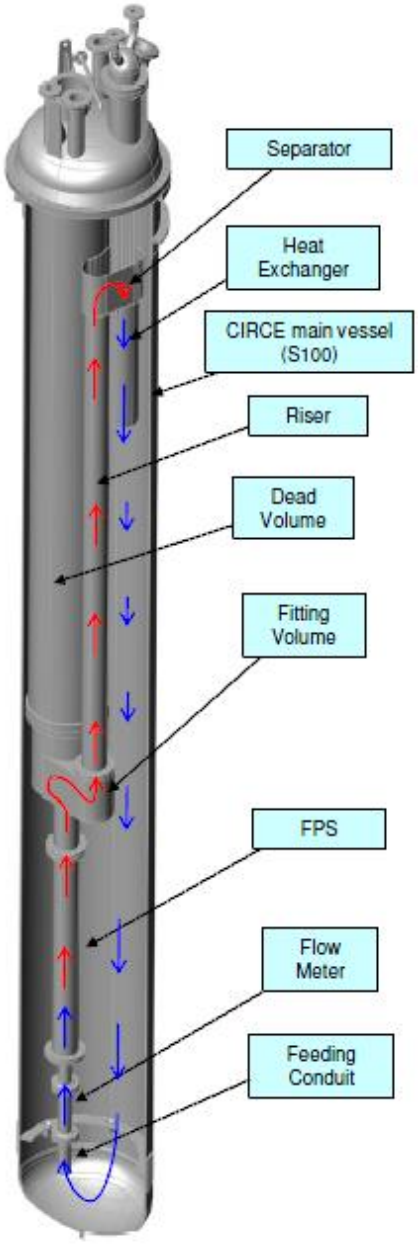

Fig. 4 – CIRCE primary flow path

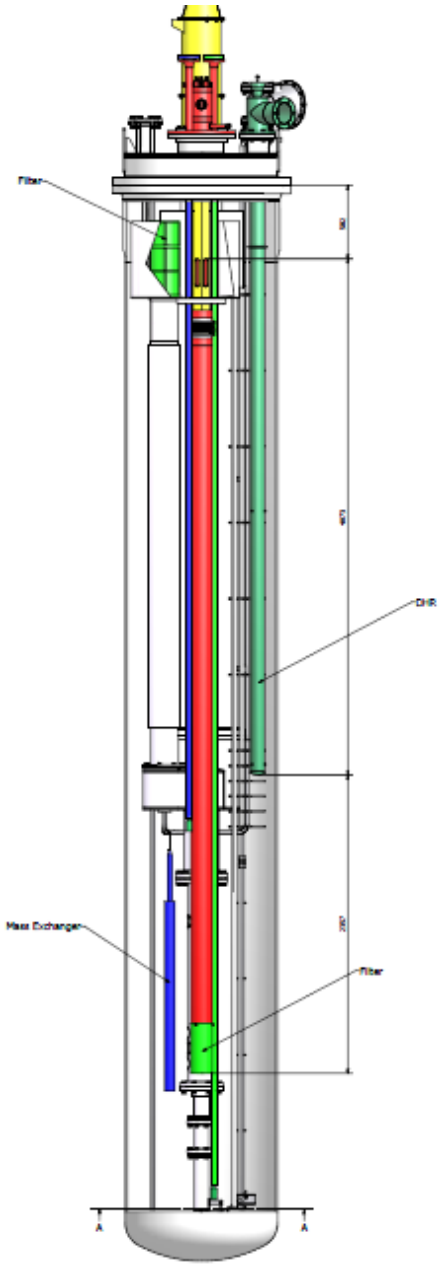

Fig. 5 – CIRCE HERO test section

2.1.1 Feeding Conduit

The feeding conduit is composed by three parts connected by 4" flanges; two of these (the bottom and the upper ones) are 4 "sch. 40 pipes with a length of 300 and 270 mm respectively. Between these two parts a Venturi flow meter is foreseen. It has been shown, through experimental activity previously carried out on the CIRCE facility, that a pressure drop of about 25 kPa is expected for a mass flow of 55.2 kg/s.

The flow measurement is performed through two pressure measurement lines. A further pressure line is foreseen in the upper tube of the feeding conduit.

2.1.2 Fuel Pin Simulator

The FPS is compound by 37 electrically heated pins and by a rated power of about 800 kW. The design of the FPS is aimed at providing, with the LBE having an average speed of 1 m/s, a coolant temperature gradient of 100 °C/m and a pin power density of 500 W/cm^3.

The electrically heated pins are enclosed into a hexagonal lattice with a pitch to diameter ratio equal to 1.8.

The electrical pin adopts a double wire solution geometry for the pin manufacturing, as reported in Fig. 7. The input voltage of 200 V and the current of 125 A are foreseen.

The Bifilar-type pins, adopted within the internal geometry, make a not uniform thermal flux around the pins. The power supply allows a maximum thermal power of about 25 kW and a heat flux, at the pin wall, of 1 MW/m^2. Each pin is characterized by an outer diameter equal to 8.2 mm and a total length of 1885 mm; the active zone is limited to 1000 mm. The other 885 mm constitute the upstream and downstream mixing zones, placed immediately below and over the heating region. These two mixing zones are respectively characterized by a length of 300 and 485 mm.

The pins are kept in their correct position by means of three spacer grids. Moreover, a lower grid, which guarantees the LBE inlet, and an upper grid, which acts as FPS cap, are placed at the bottom and upper pins edges.

The three spacer grids are located as follow:

- the first and the third ones are located at heights corresponding to the interfaces of the heating region and the mixing zones;
- the second spacer grid is located at the center of the heating zone.

The FPS hexagonal wrapper is included in a cylindrical shroud, where holes for the instrumentation connections are obtained. After positioning the instrumentation, holes are closed and the gap, between the inner hexagonal wrapper and the outer cylindrical shroud, is filled with stagnant LBE.

The FPS instrumentation is shown in Fig. 12 and it is characterized by:

- 3 TCs through the grids (one of each grid);
- 3 TCs located at 60 mm downstream the lower spacer grid (Fig. 10 shows the sub-channels in which the instrumentations are installed);
- 3 TCs placed at 120° and 10 mm upstream the pins hot part (Fig. 13);
- 9 TCs located at 20 mm upstream the middle spacer grid (3 arranged at sub-channel center and 6 placed on 6 different pins);
- 6 TCs arranged below the middle spacer grid;
- 9 TCs located at 60 mm upstream the upper spacer grid (3 arranged at sub-channel center and 6 placed on 6 different pins);
- 3 TCs placed at 120° and 10 mm by the end of the pins hot part.

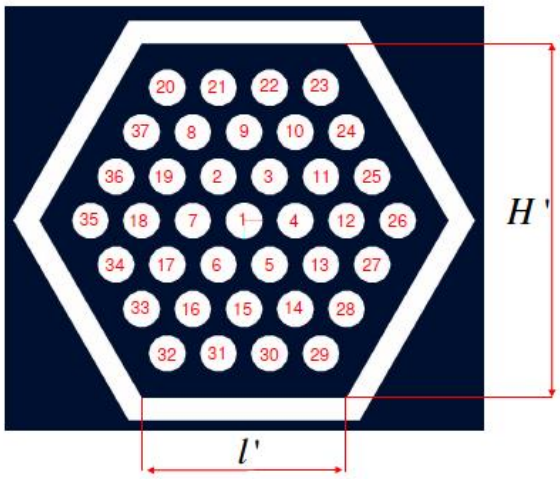

Fig. 6 – FPS cross section

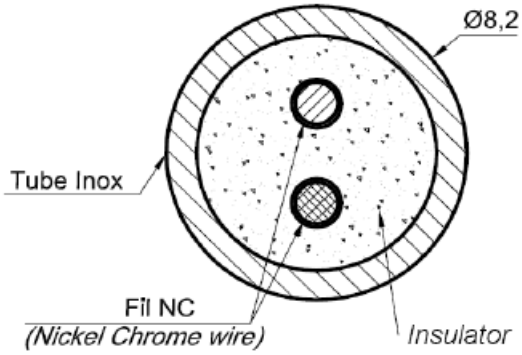

Fig. 7 – Cross section of the pin Bifilar-type

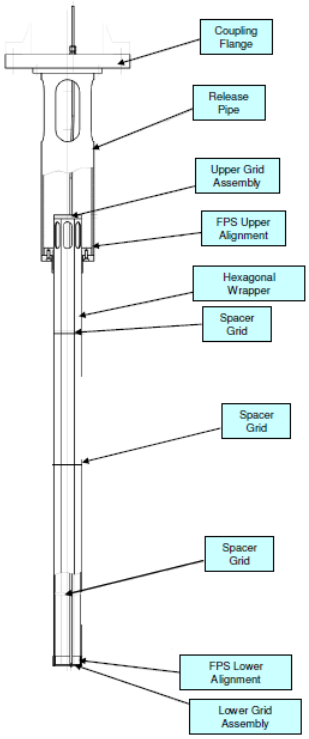

Fig. 8 – FPS mechanical drawing

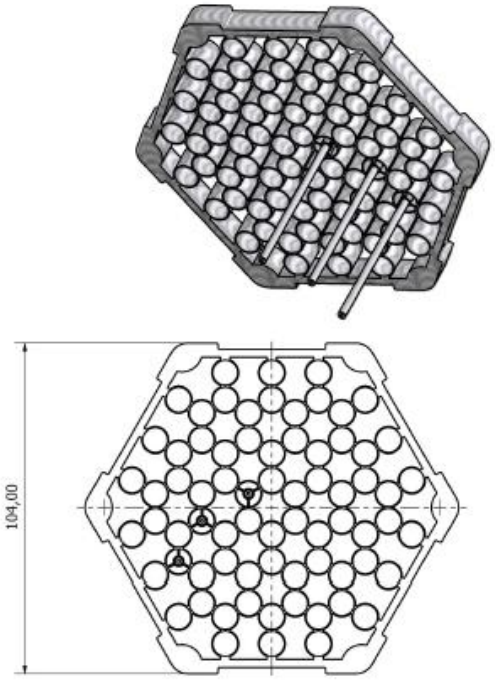

Fig. 9 – Spacer grid

Fig. 10 – Cylindrical wrapper

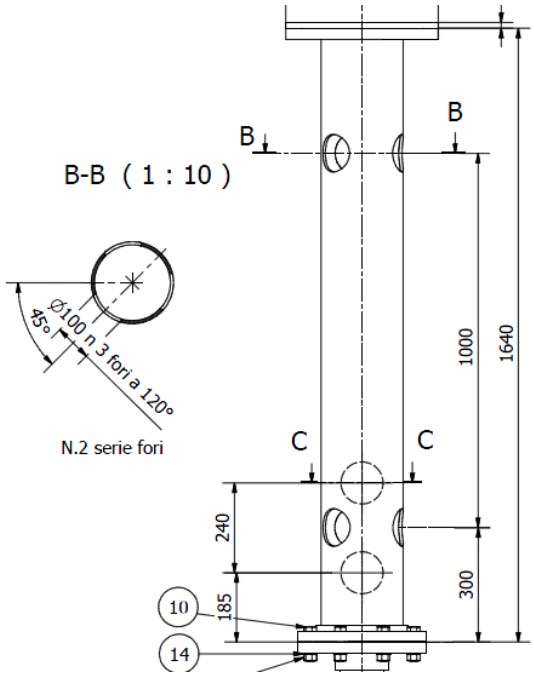

Fig. 11 – Cylindrical wrapper – mechanical drawing

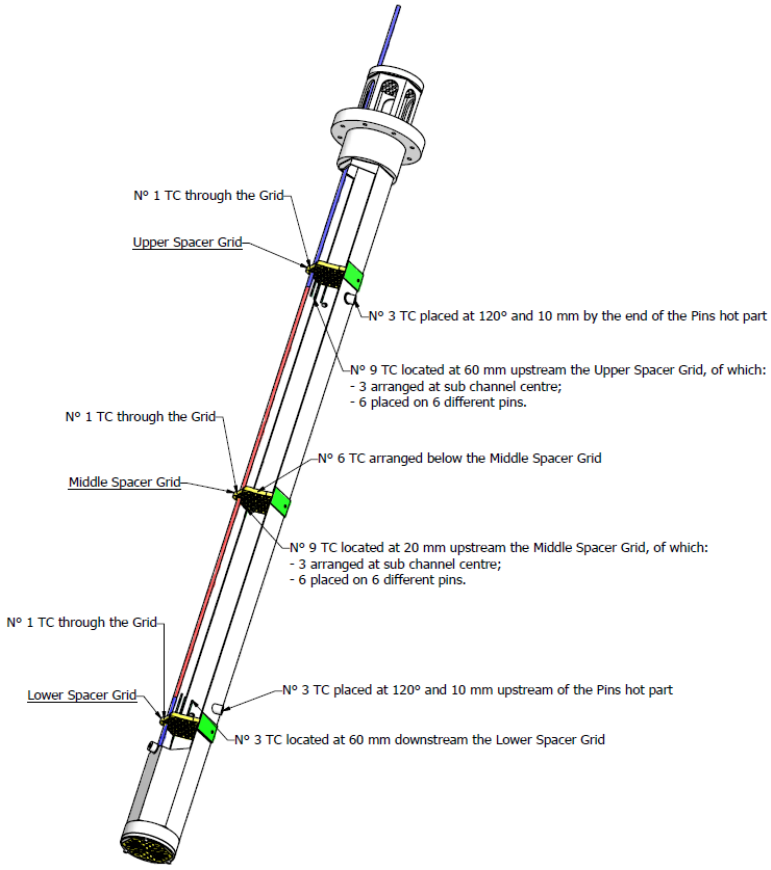

Fig. 12 – FPS instrumentation

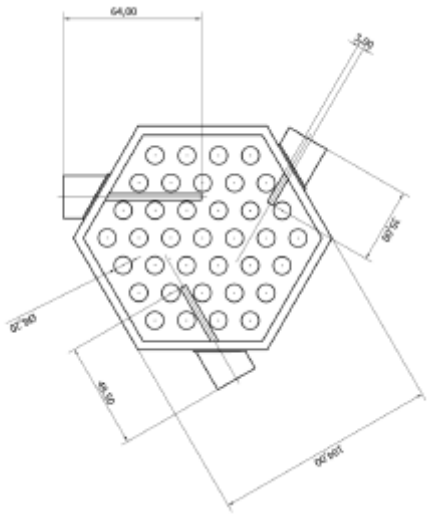

Fig. 13 – TCs arrangement at the inlet and outlet section of the FPS

2.1.3 Release Pipe

The release pipe is a 8" sch. 40 pipe. It is included inside the fitting volume (see next paragraph) with which it is in communication by means of four holes. Each hole is characterized by a flow area of 238.54 cm2.

Three thermocouples are placed in the openings that connect the release pipe to the fitting volume.

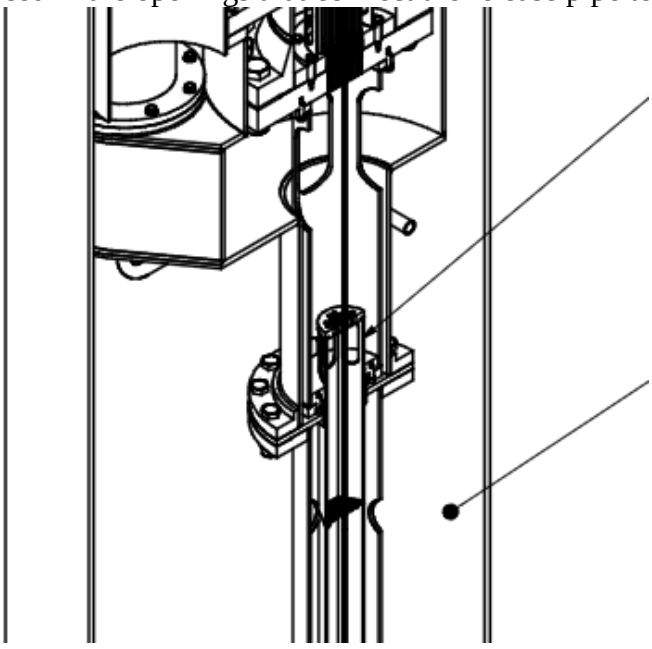

Fig. 14 – Release pipe-overview

2.1.4 Fitting Volume

The main task of the fitting volume is to connect the release pipe to the riser. Once the LBE, exiting from the release pipe, reaches the fitting volume, it is driven to the riser inlet.

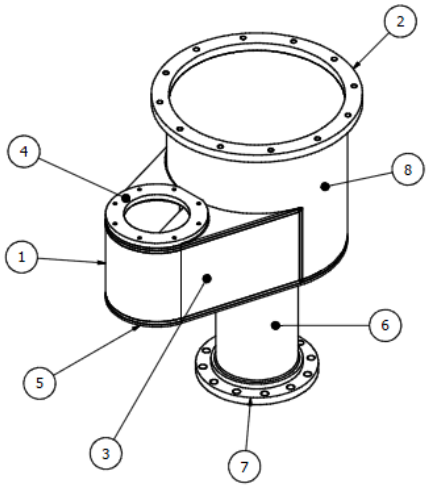

Fig. 15 – Fitting volume

2.1.5 Riser

The riser is a double-wall pipe characterized by an overall length of 3.81 m. It allows the LBE to flow upward, thanks to the gas-injection enhanced circulation, from the fitting volume to the separator. In order to reduce the hot fluid heat loss towards the main pool, a double-wall pipe has been selected for the riser. The inner tube has an inner diameter of 203 mm and it is included, for a length of 3020 mm, into a larger tube, as shown in Fig. 17. The gap between the two pipes is filled with air in order to reduce the heat loss. The riser is equipped by an axial bellow with a maximum length of 310 mm. The upper edge of the riser, which reaches the separator penetrating it of 102 mm, is coupled with a filter. Heat loss through the riser can be evaluated with TCs installed:

- 2 TCs placed in the inner section;
- 2 TCs placed in the outer section (Fig. 16).

Fig. 16 – TCs arrangement at the outlet section of the riser

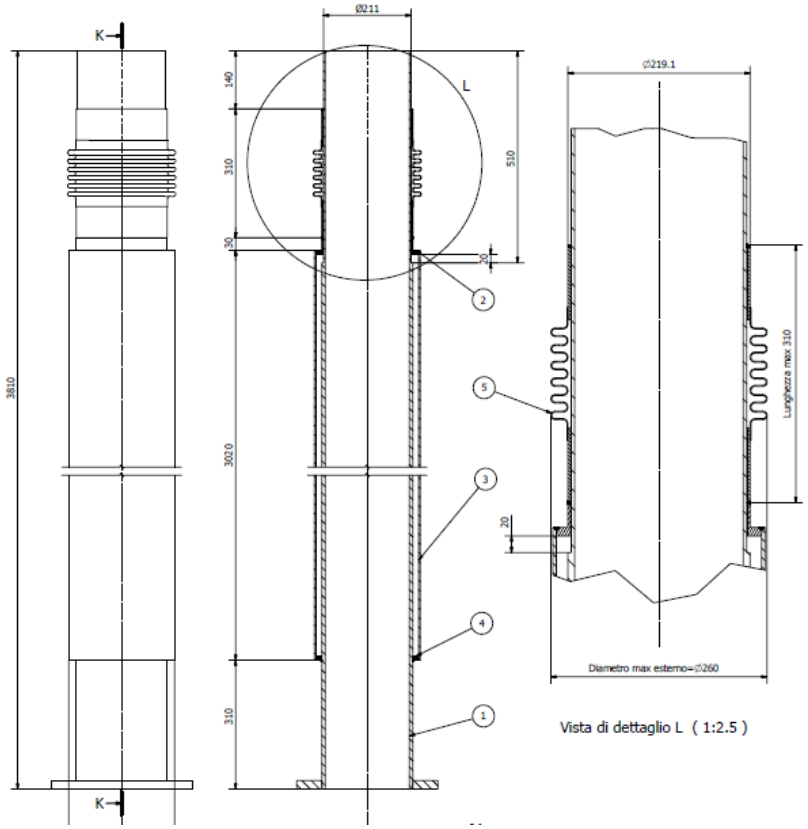

Fig. 17 – Riser overview

2.1.6 Separator

The separator, made by metal sheets, creates a volume dedicated to the separation of the hot LBE and the argon gas. The separation occurs since the hot LBE is driven downward, towards the heat exchanger inlet, while the argon can flow upward reaching the cover gas upper volume.

At the same time the separator guarantees the connection between the riser and the HERO-SGBT test section (Fig. 16). The flow path connection is obtained through 6 openings present on the heat exchanger shroud; each of them is characterized by a flow area of 84.566 cm2 (Fig. 18).

The separator walls force the LBE to flow through the heat exchanger sub-channels for reaching the downcomer. In order to avoid that LBE would overcome the separator, the separator walls have a height of 0.608 m.

Moreover, the separator has the function of an expansion tank, allowing the LBE to change its volume during transients.

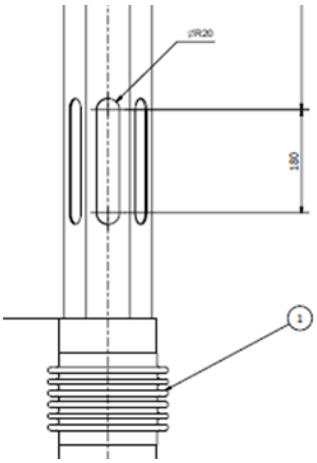

Fig. 18 – HERO inlet section: Mechanical drawing

2.1.7 Pool

The CIRCE pool is characterized by the vessel inner volume, specifically volumes that are not occupied by circuit and/or auxiliary components. At the top there is the upper plenum, completely filled with argon, which is used as cover gas. Then the pool constitutes the downcomer. Finally the LBE is collected in the lower plenum. Aimed at measuring thermal stratification during transients within the S100, pool is equipped with 119 TCs located at different heights as shown in Fig. 19.

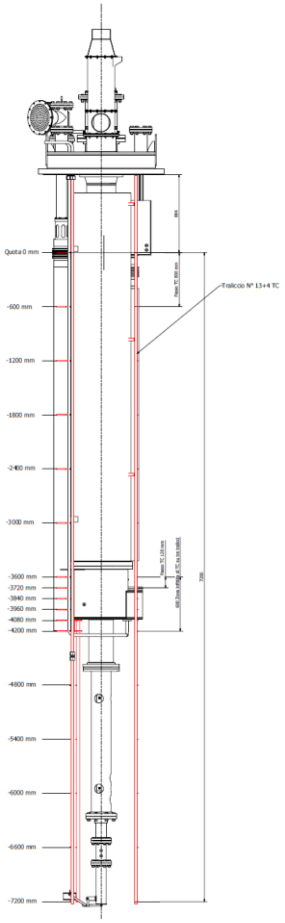

Fig. 19 – TCs arrangement at the pool

2.1.8 HERO steam generator – LBE side

HERO primary side represents the void volume between the hexagonal shell and the bayonet tubes. The hot LBE flows downwards along the steam generator, decreasing its temperature. In nominal conditions, LBE enters the heat exchanger through 6 fissure inlet (Fig. 20) at the temperature of 480°C.

The active length of the steam generator is 6,145 m, analogous to the ALFRED SG, and the flow area is 7616 mm2.

The bayonet tubes are kept in their position by means of 5 spacer grids, characterized by a free-area coefficient of 0,41.

In order to reduce the heat loss towards the main pool, a double-wall pipe has been selected to contain LBE into the heat exchanger. The insulator is obtained with an air gap of average thickness of 14,75 mm.

The test section is instrumented with 65 thermocouples, 21 differential pressure transducers, 2 absolute pressure transducers and 8 flow meters. The list of instrumentation is reported in Tab. 3.

Particularly, the central tube is instrumented with 31 TCs (Fig. 24):

- the water-steam path is monitored by 4 TCs with a diameter of 0.5 mm. they are placed in the center of the bulk, at different heights: at the feed-water tube inlet. At the feed-water tube end, at the annular riser active length end and in the steam plenum;
- 10 TCs are located in the annular riser active length with a distance of 300 mm, at the center of the bulk to monitor the boiling length;
- 1 TC is located at the feed-water tube inlet on its outer surface in order to monitor condensation phenomena;
- 4 TCs are placed inside the powder gap at 4 axial elevations;
- 12 TCs with a diameter of 1 mm are placed at the third tube outer wall surface (LBE side) at 4 axial elevations and 3 azimuthal positions;
- The other tubes are monitored with 18 TCs (Fig. 25):
- 2 TCs (0.5 mm) are located in each tube: 1 at its inlet and the other at its outlet;
- 6 TCs (1 mm) are placed at 3 axial elevations in the LBE side of 2 tubes.

The differential pressure transducers are installed in order to measure, per each tubes, the pressure drop across the orifice, the total pressure drop across the tube, the descended pressure drop and the ascendant pressure drop. Absolute pressure transducers are placed in the steam chamber and in the collector (see paragraph for HERO secondary side.

#	ID	Instrumentation location			Measurement	Type
		Zone	Elev. / Position	Medium	Quantity Dim.	
1	TC-C0-I00	Tube 0 – Inner tube	Inlet	Water	Temperature °C	D=0.5mm
2	TC-C0-I01	Tube 0 – Inner tube	Outlet	Water	Temperature °C	D=0.5mm
3	TC-C0-O15	Tube 0 – Second tube	1500mm	Water	Temperature °C	D=0.5mm
4	TC-C0-O18	Tube 0 – Second tube	1800mm	Water	Temperature °C	D=0.5mm
5	TC-C0-O21	Tube 0 – Second tube	2100mm	Water	Temperature °C	D=0.5mm
6	TC-C0-O24	Tube 0 – Second tube	2400mm	Water	Temperature °C	D=0.5mm
7	TC-C0-O27	Tube 0 – Second tube	2700mm	Water	Temperature °C	D=0.5mm
8	TC-C0-O30	Tube 0 – Second tube	3000mm	Water	Temperature °C	D=0.5mm
9	TC-C0-O33	Tube 0 – Second tube	3300mm	Water	Temperature °C	D=0.5mm
10	TC-C0-O36	Tube 0 – Second tube	3600mm	Water	Temperature °C	D=0.5mm

#	ID	Instrumentation location			Measurement	Type
		Zone	Elev. / Position	Medium	Quantity Dim.	
11	TC-C0-O39	Tube 0 – Second tube	3900mm	Water	Temperature °C	D=0.5mm
12	TC-C0-O42	Tube 0 – Second tube	4200mm	Water	Temperature °C	D=0.5mm
13	TC-C0-O60	Tube 0 – Second tube	6000mm	Water	Temperature °C	D=0.5mm
14	TC-C0-O70	Tube 0 – Second tube	7016mm	Water	Temperature °C	D=0.5mm
15	TC-WO-W68	Tube 0 – Inner tube	6800mm	Wall – Water	Temperature °C	D=0.5mm
16	TC-WO-P15	Tube 0 – Second tube	1500mm / 0°	Wall – SiC	Temperature °C	D=0.5mm
17	TC-WO-P30	Tube 0 – Second tube	3000mm / 0°	Wall – SiC	Temperature °C	D=0.5mm
18	TC-WO-P40	Tube 0 – Second tube	4200mm / 0°	Wall – SiC	Temperature °C	D=0.5mm
19	TC-WO-P60	Tube 0 – Second tube	6000mm / 0°	Wall – SiC	Temperature °C	D=0.5mm
20	TC-W0-L10	Tube 0 – Third tube	1500mm / 0°	Wall – LBE	Temperature °C	D=1mm
21	TC-W0-L11	Tube 0 – Third tube	1500mm / 120°	Wall – LBE	Temperature °C	D=1mm
22	TC-W0-L12	Tube 0 – Third tube	1500mm / 240°	Wall – LBE	Temperature °C	D=1mm
23	TC-W0-L30	Tube 0 – Third tube	3000mm / 0°	Wall – LBE	Temperature °C	D=1mm
24	TC-W0-L31	Tube 0 – Third tube	3000mm / 120°	Wall – LBE	Temperature °C	D=1mm
25	TC-W0-L32	Tube 0 – Third tube	3000mm / 240°	Wall – LBE	Temperature °C	D=1mm
26	TC-W0-L40	Tube 0 – Third tube	4200mm / 0°	Wall – LBE	Temperature °C	D=1mm
27	TC-W0-L41	Tube 0 – Third tube	4200mm / 120°	Wall – LBE	Temperature °C	D=1mm
28	TC-W0-L42	Tube 0 – Third tube	4200mm / 240°	Wall – LBE	Temperature °C	D=1mm
29	TC-W0-L60	Tube 0 – Third tube	6000mm / 0°	Wall – LBE	Temperature °C	D=1mm
30	TC-W0-L61	Tube 0 – Third tube	6000mm / 120°	Wall – LBE	Temperature °C	D=1mm
31	TC-W0-L62	Tube 0 – Third tube	6000mm / 240°	Wall – LBE	Temperature °C	D=1mm
32	TC-C1-I00	Tube 1 – Inner tube	Inlet	Water	Temperature °C	D=0.5mm
33	TC-C1-O70	Tube 1 – Second tube	7016mm	Water	Temperature °C	D=0.5mm
34	TC-C2-I00	Tube 2 – Inner tube	Inlet	Water	Temperature °C	D=0.5mm
35	TC-C2-O70	Tube 2 – Second tube	7016mm	Water	Temperature °C	D=0.5mm
36	TC-C3-I00	Tube 3 – Inner tube	Inlet	Water	Temperature °C	D=0.5mm
37	TC-C3-O70	Tube 3 – Second tube	7016mm	Water	Temperature °C	D=0.5mm
38	TC-C4-I00	Tube 4 – Inner tube	Inlet	Water	Temperature °C	D=0.5mm
39	TC-C4-O70	Tube 4 – Second tube	7016mm	Water	Temperature °C	D=0.5mm
40	TC-C5-I00	Tube 5 – Inner tube	Inlet	Water	Temperature °C	D=0.5mm
41	TC-C5-O70	Tube 5 – Second tube	7016mm	Water	Temperature °C	D=0.5mm
42	TC-C6-I00	Tube 6 – Inner tube	Inlet	Water	Temperature °C	D=0.5mm
43	TC-C6-O70	Tube 6 – Second tube	7016mm	Water	Temperature °C	D=0.5mm
44	TC-W1-L11	Tube 1 – Third tube	1500mm / 120°	Wall – LBE	Temperature °C	D=1mm
45	TC-W2-L12	Tube 2 – Third tube	1500mm / 240°	Wall – LBE	Temperature °C	D=1mm
46	TC-W1-L31	Tube 1 – Third tube	3000mm / 120°	Wall – LBE	Temperature °C	D=1mm
47	TC-W2-L32	Tube 2 – Third tube	3000mm / 240°	Wall – LBE	Temperature °C	D=1mm
48	TC-W1-L41	Tube 1 – Third tube	4200mm / 120°	Wall – LBE	Temperature °C	D=1mm
49	TC-W2-L42	Tube 2 – Third tube	4200mm / 240°	Wall – LBE	Temperature °C	D=1mm
50	TC-01-L15	Sub-channel 1 centre	1500mm	LBE	Temperature °C	D=1mm
51	TC-07-L15	Sub-channel 7 centre	1500mm	LBE	Temperature °C	D=1mm
52	TC-09-L15	Sub-channel 9 centre	1500mm	LBE	Temperature °C	D=1mm
53	TC-11-L15	Sub-channel 11 centre	1500mm	LBE	Temperature °C	D=1mm
54	TC-01-L30	Sub-channel 1 centre	3000mm	LBE	Temperature °C	D=1mm
55	TC-07-L30	Sub-channel 7 centre	3000mm	LBE	Temperature °C	D=1mm
56	TC-09-L30	Sub-channel 9 centre	3000mm	LBE	Temperature °C	D=1mm
57	TC-11-L30	Sub-channel 11 centre	3000mm	LBE	Temperature °C	D=1mm
58	TC-01-L42	Sub-channel 1 centre	4200mm	LBE	Temperature °C	D=1mm

#	ID	Instrumentation location			Measurement	Type
		Zone	Elev. / Position	Medium	Quantity Dim.	
59	TC-07-L42	Sub-channel 7 centre	4200mm	LBE	Temperature °C	D=1mm
60	TC-09-L42	Sub-channel 9 centre	4200mm	LBE	Temperature °C	D=1mm
61	TC-11-L42	Sub-channel 11 centre	4200mm	LBE	Temperature °C	D=1mm
62	TC-SL-W01	Steam-chamber outlet	--	Water	Temperature °C	D=1mm
63	TC-SL-W02	Steam-chamber outlet	--	Water	Temperature °C	D=1mm
64	TC-SL-W03	Steam-chamber outlet	--	Water	Temperature °C	D=1mm
65	TC-SL-W04	Steam-chamber outlet	--	Water	Temperature °C	D=1mm
1	DP-C0-W00	Tube 0	Overall	Water	Press. diff. kPa	
2	DP-C0-W01	Tube 0	Descending	Water	Press. diff. kPa	
3	DP-C0-W02	Tube 0	Ascending	Water	Press. diff. kPa	
4	DP-C0-W00	Tube 1	Overall	Water	Press. diff. kPa	
5	DP-C0-W01	Tube 1	Descending	Water	Press. diff. kPa	
6	DP-C0-W02	Tube 1	Ascending	Water	Press. diff. kPa	
7	DP-C0-W00	Tube 2	Overall	Water	Press. diff. kPa	
8	DP-C0-W01	Tube 2	Descending	Water	Press. diff. kPa	
9	DP-C0-W02	Tube 2	Ascending	Water	Press. diff. kPa	
10	DP-C0-W00	Tube 3	Overall	Water	Press. diff. kPa	
11	DP-C0-W01	Tube 3	Descending	Water	Press. diff. kPa	
12	DP-C0-W02	Tube 3	Ascending	Water	Press. diff. kPa	
13	DP-C0-W00	Tube 4	Overall	Water	Press. diff. kPa	
14	DP-C0-W01	Tube 4	Descending	Water	Press. diff. kPa	
15	DP-C0-W02	Tube 4	Ascending	Water	Press. diff. kPa	
16	DP-C0-W00	Tube 5	Overall	Water	Press. diff. kPa	
17	DP-C0-W01	Tube 5	Descending	Water	Press. diff. kPa	
18	DP-C0-W02	Tube 5	Ascending	Water	Press. diff. kPa	
19	DP-C0-W00	Tube 6	Overall	Water	Press. diff. kPa	
20	DP-C0-W01	Tube 6	Descending	Water	Press. diff. kPa	
21	DP-C0-W02	Tube 6	Ascending	Water	Press. diff. kPa	
22	PC-00-I00	FW collector	--	Water	Press. diff. MPa	
23	PC-00-O00	Steam collector		Water	Press. diff. MPa	
1	MF-00-I00	Tube 0 – inlet	--	Water	Mass flow g/s	
2	MF-01-I00	Tube 1 – inlet	--	Water	Mass flow g/s	
3	MF-02-I00	Tube 2 – inlet	--	Water	Mass flow g/s	
4	MF-03-I00	Tube 3 – inlet	--	Water	Mass flow g/s	
5	MF-04-I00	Tube 4 – inlet	--	Water	Mass flow g/s	
6	MF-05-I00	Tube 5 – inlet	--	Water	Mass flow g/s	
7	MF-06-I00	Tube 6 – inlet	--	Water	Mass flow g/s	
8	MF-FW-I00	FW collector	--	Water	Mass flow g/s	

Tab. 3 – HERO instrumentation

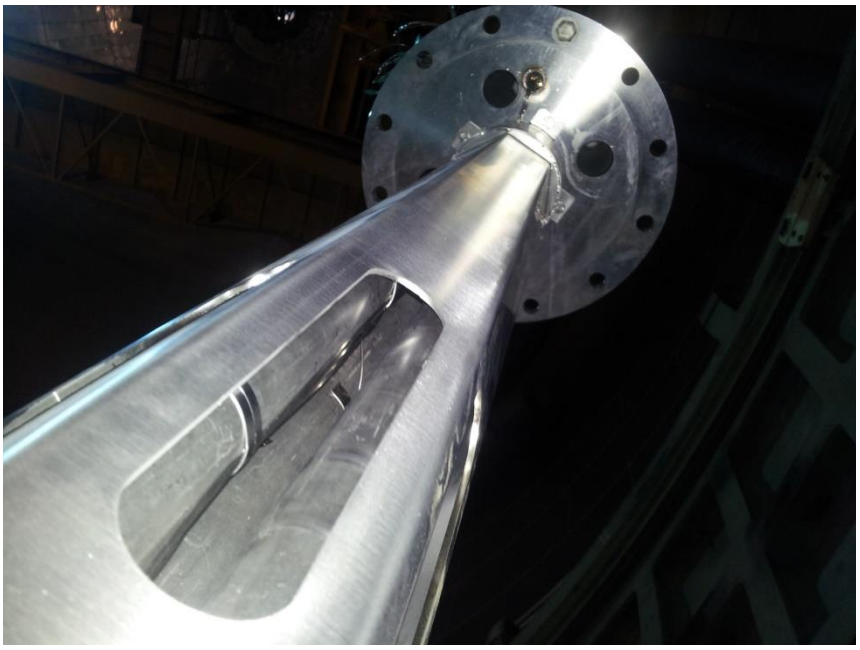

Fig. 20 – HERO inlet section

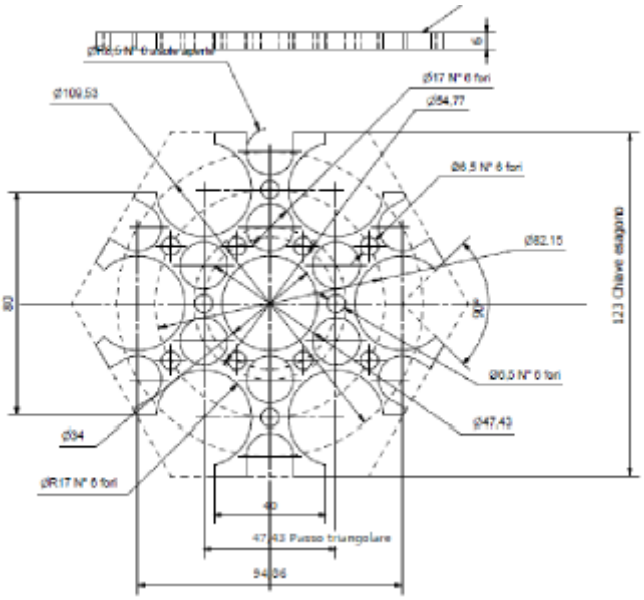

Fig. 21 – HERO spacer grid: Mechanical drawing

Fig. 22 – HERO spacer grid

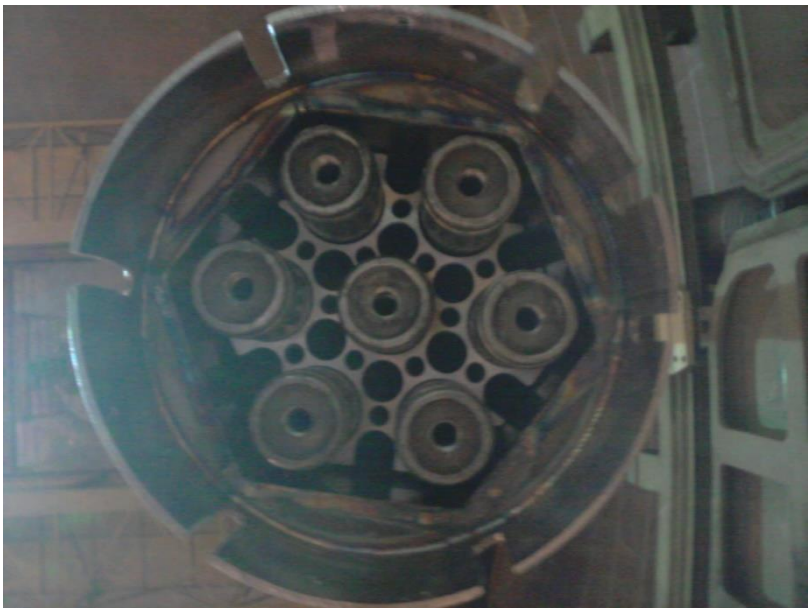

Fig. 23 – HERO outlet section

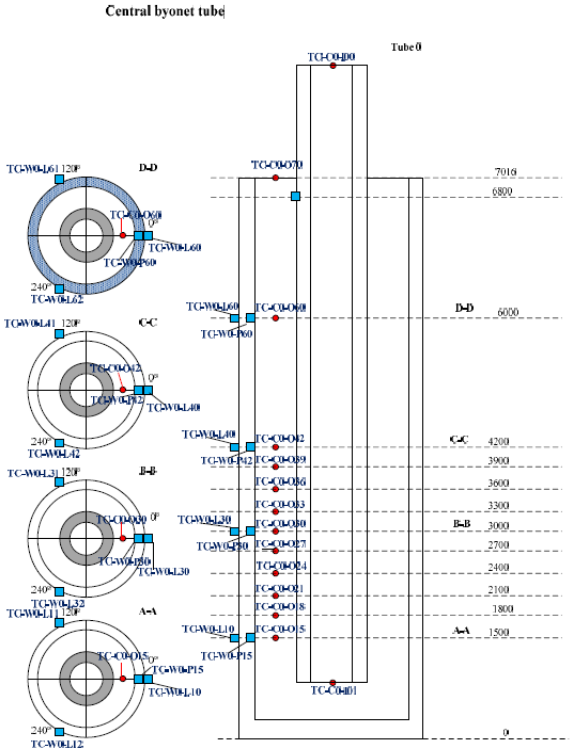

Fig. 24 – Thermocouples in the central tube

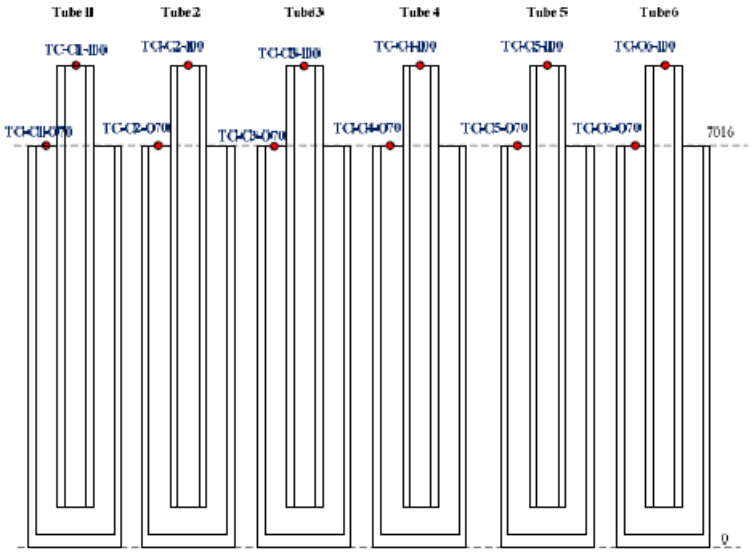

Fig. 25 – Thermocouples in the tubes

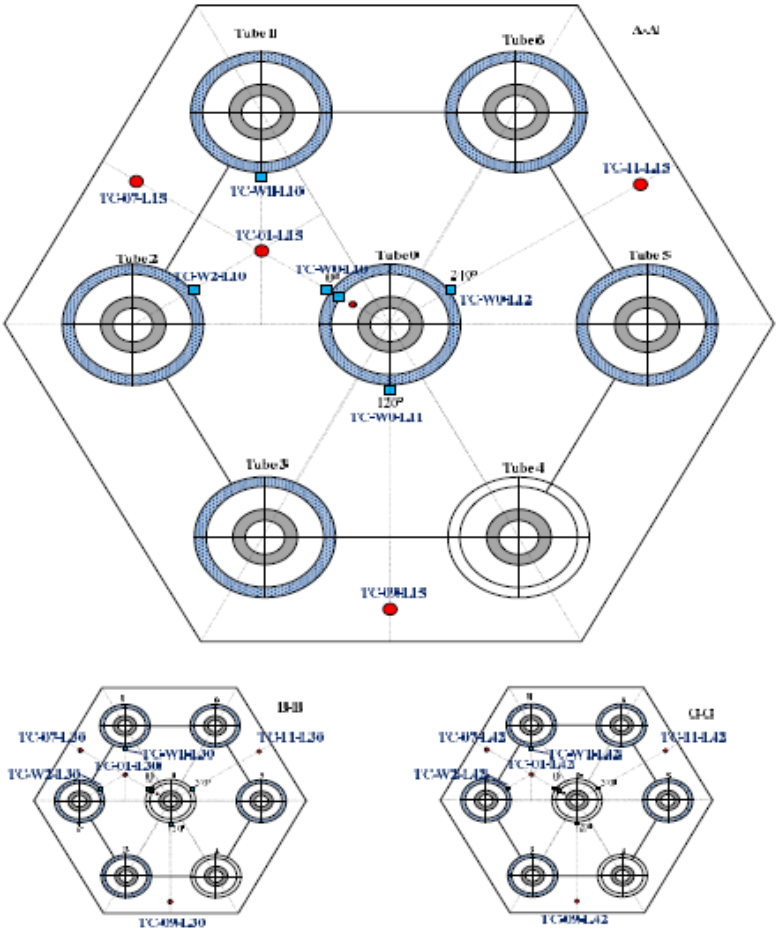

Fig. 26 – Thermocouples in the LBE channel

Fig. 27 – Thermocouples in the lead sub-channel

Fig. 28 – TCs exit

2.2 Secondary system

Secondary loop is based on an open loop circuit fed by water. The water should be pressurized at 172 bar and preheated at 335°C before entering the SGBT unit. It is required approximately 500 kW.

The preheating function is performed by an electrically heated pipe (24 m long) designed in spiral geometry. This component assures the Tmax of 450°C. The geometry and the scheme of the heater is shown in Fig. 29 and Fig. 30. Secondary system is composed by:

- the demineralizer;
- the pump;
- the spiral heater;
- the collector;
- the HERO Steam Generator Bayonet Tubes (HERO SGBTs).

The demineralized water is pressurized by a volumetric pump (with oscillation reducer) connected with a control valve. The pressurized water is sent to the pre-heated component to increase its temperature. Then water is collected in the collector. This component is designed in order to achieve as uniform as possible distribution of the feed-water to the seven bayonet tubes (two grids with no coaxial holes are provided). Finally the water enters in HERO SGBTs where it is heated and evaporated. Fig. 31 shows a schematic view of secondary loop.

Fig. 29 – Pre-heater

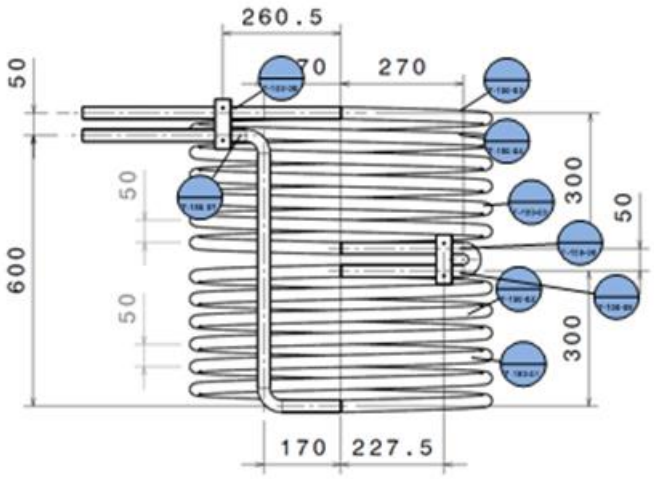

Fig. 30 – Spiral geometry

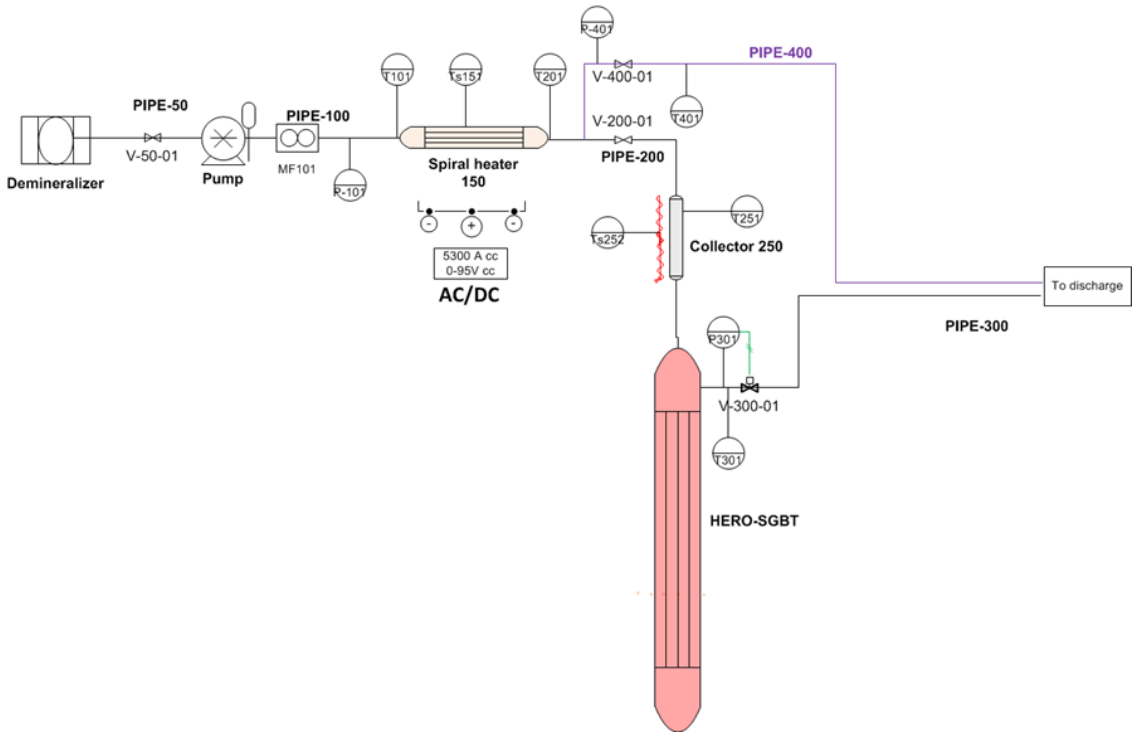

Fig. 31 – Secondary loop

2.2.1 HERO SGBT

The HERO test section assembly is shown in Fig. 32. Fig. 33 shows the bundle during installation phase.

The assembly is characterized by a 14” flange with a thickness of 30 mm (see position 1 in Fig. 32), which connects the test section to the CIRCE experimental facility. On the flange 7 holes for the bayonet tubes and 1 for the instrumentation are obtained. The flange has also to support the helium chamber, the steam chamber, the bayonet tubes and hexagonal wrapper.

The helium chamber is slightly pressurized in order to increase the heat transfer from the primary LBE to the steam flowing inside the bayonet tubes and, at the same time, to make easier the detection of possible leakage. The helium chamber, which is made of a 6" sch. 40 pipe, is welded at its bottom edge to the flange while the upper edge is welded to a septum that guarantees the separation of helium chamber and steam chamber. On both the flange and the septum, the 7 holes for passing the bayonet tubes are obtained.

The steam chamber, which has to collect the superheated steam (170 bar and 430°C) coming from the steam generator, is made by a 6" sch.120 pipe. At the top of the steam chamber, there is a plate that seals the HERO test section; on this plate the bayonet tube upper edges are fixed. The superheated steam is extracted from the chamber through a 2 ½" sch.80 outlet nozzle.

Both chambers are equipped with 1" sch.40 radial nozzles to connect cables to the internal instrumentation (i.e. thermocouples installed on the bayonet tubes).

The feed water reaches the 7 bayonet tubes through Swagelok connections that pass through the test section upper plate and through a changeable orifice plate. The bayonet tubes consist of four concentric tubes, as shown in Fig. 34. In particular it shows a detail of the bottom region of a bayonet tube.

The slave and the inner tubes pass through the steam chamber while the helium chamber is crossed by the slave, the inner and the second tubes. Hence the bayonet tubes enter the main vessel S100 through the connection flange, at which the third tube is connected through a bellows. Inside the slave tube the feed water (cold) flows downward; during the descendent path, the water is preheated.

Once the bottom edge of the slave tube is reached, the water changes its direction of 180° flowing upward between the outer wall of the inner tube and the inner wall of the second tube. In this zone the water vaporizes reaching the superheated state before entering the steam chamber. The primary coolant, the LBE, flows downward in contact with the outer wall of the third.

Two gaps are present in each bayonet tube:

- between the slave and the inner tubes;
- between the second and the third tubes.

The first gap (i.e. between the slave and inner tubes) is filled with a thermal insulator, the ZIRCOFOAM 250, in order to minimize the heat transfer between the cold feed water and the hot superheated steam; it allows to increase the thermodynamic efficiency of the steam generator. The thermal conductivity of the ZIRCOFOAM 250 as a function of the temperature is shown in Tab. 5.

The second gap (i.e. between the second and third tubes) is filled with SiC powder and slightly pressurized helium. These materials have been selected to guarantee good heat transfer performance (i.e. SiC thermal conductivity) and at the same time to possibility of detecting any leakage (i.e. connection with the helium chamber).

At the bayonet tube bottom edge, on the lower plate (see position 16 in Tab. 4), a 1/8” NPT penetration is foreseen to allow the connection of a pressure gauge transducer; if not needed it can be sealed with a swagelok cap. In Fig. 36 a view of the bayonet tube bottom end is shown.

Position	Quantity	Description
21	1	Third tube: OD 33,4 TH. 3,38 [mm]
16	1	Plate: OD 25,4 th. 9 [mm]
7	1	Slave tube: OD 9,53 th. 1,22 [mm]
6	1	Inner tube: OD 19,05 th. 1,65 [mm]
4	1	Second tube: OD 25,4 th. 2,11 [mm]

Tab. 4 – SGBT main dimentions

Temperature [K]	Thermal conductivity [W/mK]
423,15	0,06
523,15	0,071
673,15	0,088
873,15	0,113

Tab. 5 – Zircofoam 250 thermal conductivity

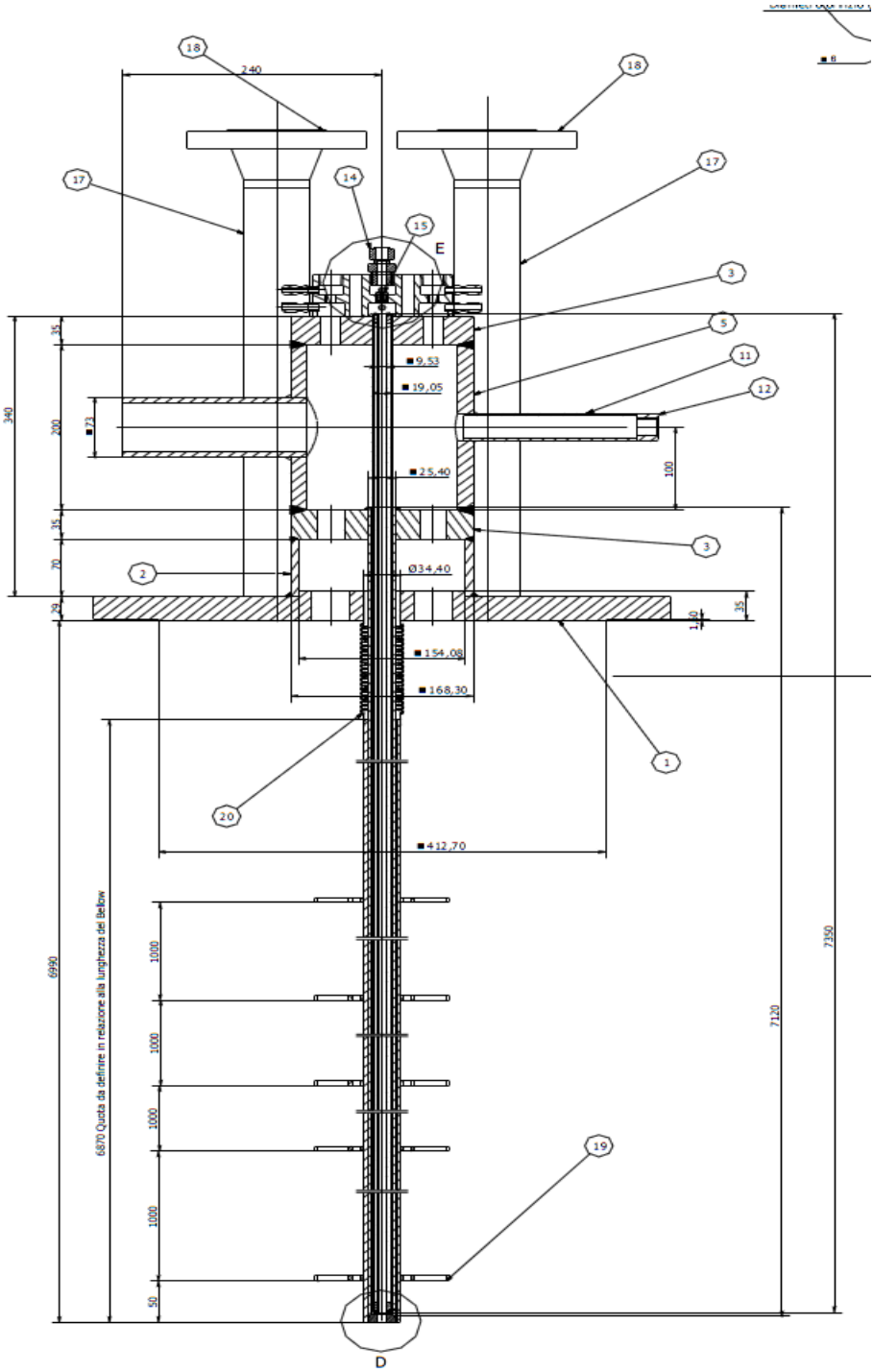

Fig. 32 – HERO SGBT: Mechanical drawing

Fig. 33 – HERO SGBTs

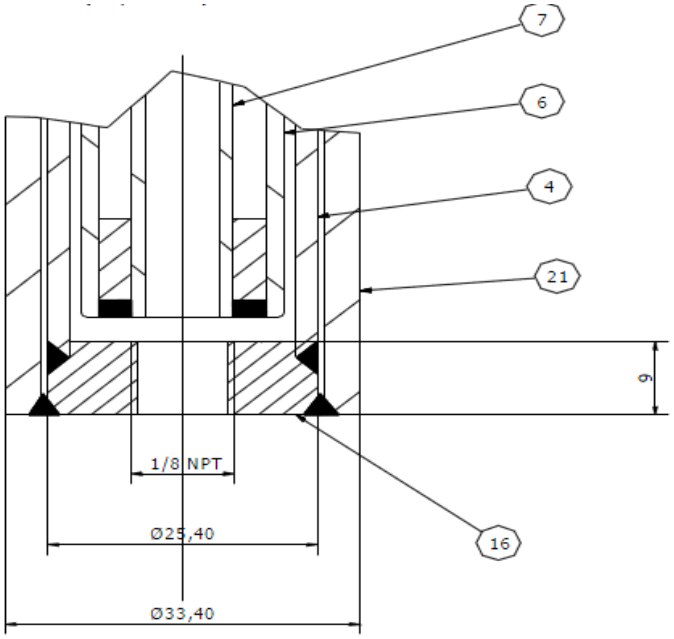

Fig. 34 – Section of bayonet tube bottom end

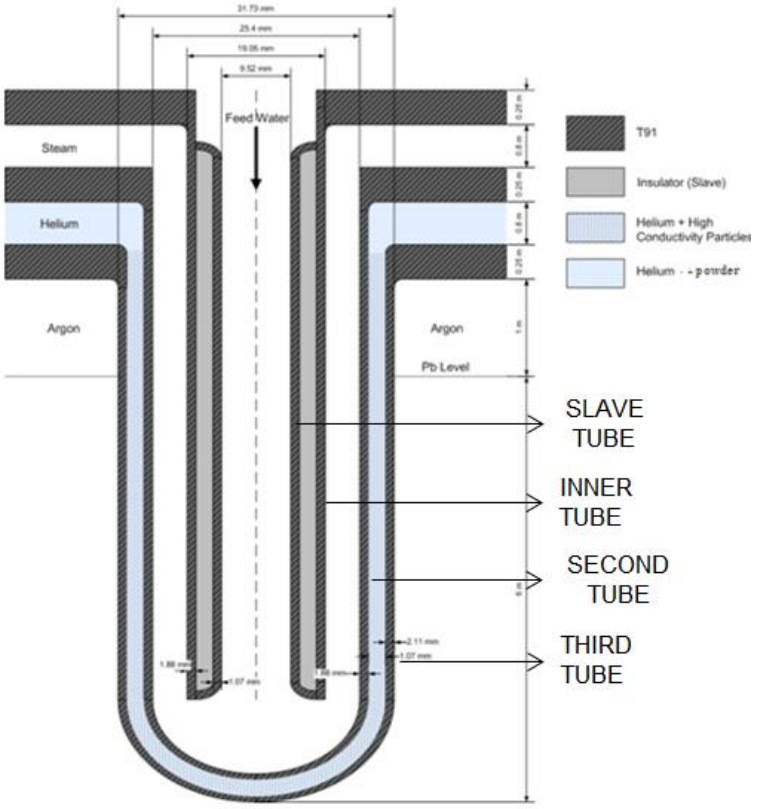

Fig. 35 – Bayonet tube

Fig. 36 – End of bayonet tubes

3 Modelling CIRCE-HERO facility by RELAP5-3D

3.1 CIRCE-HERO facility 1D nodalization

The nodalization scheme developed in the analysis of CIRCE-HERO test facility is depicted in Fig. 4.1.

The whole facility has been divided in order to obtain axial volume basic length of 150 mm. The primary loop has been divided into 156 volumes and 157 junctions. The secondary loop has been divided into 98 volumes and 97 junctions.

The volumes are thermally connected by the following heat structure:

- 1 heat structure to simulate the heat source,8 sub-structure divided into 10 axial mesh points;
- 13 heat structure to simulate heat dispersion, 161 sub-structure;
- 2 heat structure to simulate HERO SGBTs, 49 sub-structure with 20 mesh points and 40 sub-structure with 31 mesh points.

The main geometrical parameters relating to hydrodynamics components and heat structures are summarized in the following Tab. 6:

No	Region	Elevation (m)	Axial Lenght (m)	Flow Area (m^2)	Hydraulic Diameter (m)	Heated Diameter [left] (m)	Heated Diameter [right] (m)
10	Feeding conduit 1	-7.4450 -7.1450	0.3000	0.0082	0.1023	- N/A -	- N/A -
20	Venturi nozzle	-7.1450 -6.7450	0.4000	0.0082	0.1023	- N/A -	- N/A -
30	Feeding conduit 2	-6.7450 -6.5300	0.2150	0.0082	0.1023	- N/A -	- N/A -
	LOWER GRID						
40	Hexagonal wrapper (lower alig.)	-6.5300 -6.2300	0.3000	0.0060	0.0188	- N/A -	- N/A -
	MIDDLE GRID						
40	Hexagonal wrapper (lowhot)	-6.2300 -5.6800	0.5500	0.0060	0.0188	0.0000	0.025294
	MIDDLE GRID						
40	Hexagonal wrapper (uphot)	-5.6800 -5.1300	0.5500	0.0060	0.0188	0.0000	0.025294
	MIDDLE GRID						
40	Hexagonal wrapper (up align.)	-5.1300 -4.6450	0.4850	0.0060	0.0188	- N/A -	- N/A -
	N6 SLOTTED HOLES 36						
50	Release pipe 1	-4.7650 -4.6500	0.1150	0.0230	0.0922	- N/A -	- N/A -
50	Release pipe 2	-4.6500 -4.0050	0.6450	0.0304	0.0765	- N/A -	- N/A -
	N4 SLOTTED HOLES 100						
60	Fitting Volume 1	-4.2950 -4.0050	0.2900	0.3214	0.4037	- N/A -	- N/A -
70	Fitting Volume 2	-4.0050 -3.8625	0.1425	0.0549	0.0633	- N/A -	- N/A -
70	Fitting Volume 3	-3.8625 -3.7200	0.1425	0.1854	0.2600	- N/A -	- N/A -
90	Riser	-4.0050 -0.1600	3.8450	0.0309	0.1985	- N/A -	- N/A -
100	Separatore 1	-0.2620 -0.1600	0.1020	0.2338	0.2752	- N/A -	- N/A -
110-120	Separatore 2	-0.1600 0.3380	0.4980	0.2715	0.4005	- N/A -	- N/A -
140	Upper plenum 1	0.3380 0.4080	0.0700	0.7252	0.4304	- N/A -	- N/A -
140	Upper plenum 2	0.4080 0.6380	0.2300	0.9870	0.6952	- N/A -	- N/A -
140	Upper plenum 3	0.6380 0.8480	0.2100	0.9593	0.6814	- N/A -	- N/A -

No	Region	Elevation (m)	Axial Lenght (m)	Flow Area (m^2)	Hydraulic Diameter (m)	Heated Diameter [left] (m)	Heated Diameter [right] (m)
160	Pool	0.3380	0.6080	0.4471	0.2378	- N/A -	- N/A -
		-0.2700					
		-0.2700	0.0770	0.6741	0.3576	- N/A -	- N/A -
		-0.3470					
		-0.3470	3.3230	0.6670	0.3504	- N/A -	- N/A -
		-3.6700					
		-3.6700	0.3120	0.7418	0.4062	- N/A -	- N/A -
		-3.9820					
		-3.9820	0.3280	0.2290	0.1275	- N/A -	- N/A -
		-4.3100					
		-4.3100	0.2320	1.0037	0.7182	- N/A -	- N/A -
		-4.5420					
		-4.5420	0.2930	1.0221	0.8001	- N/A -	- N/A -
		-4.8350					
		-4.8350	1.1270	1.0429	0.8445	- N/A -	- N/A -
		-5.9620					
		-5.9620	0.5130	1.0652	0.9659	- N/A -	- N/A -
		-6.4750					
		-6.4750	0.9700	1.0926	1.0707	- N/A -	- N/A -
		-7.4450					
250	Lower plenum	-7.4450	0.3500	- N/A -	- N/A -	- N/A -	- N/A -
		-7.7950					
	N6 SLOTTED HOLES 20						
300	Hero	0.1410	0.1500	0.0076	0.0260	0.004046	0.041477
		-0.0090					
		-0.0090	0.1780	0.0076	0.0260	0.004046	0.041477
		-0.1870					
		-0.1870	0.1500	0.0076	0.0260	0.004046	0.041477
		-0.3370					
		-0.3370	0.1500	0.0076	0.0260	0.004046	0.041477
		-0.4870					
		-0.4870	0.1500	0.0076	0.0260	0.004046	0.041477
		-0.6370					
	GRID A						
300	Hero	-0.6370	0.1500	0.0076	0.0260	0.004046	0.041477
		-0.7870					
		-0.7870	0.1500	0.0076	0.0260	0.004046	0.041477
		-0.9370					
		-0.9370	0.1500	0.0076	0.0260	0.004046	0.041477
		-1.0870					
		-1.0870	0.1500	0.0076	0.0260	0.004046	0.041477
		-1.2370					

No	Region	Elevation (m)	Axial Lenght (m)	Flow Area (m^2)	Hydraulic Diameter (m)	Heated Diameter [left] (m)	Heated Diameter [right] (m)
		-1.2370	0.1500	0.0076	0.0260	0.004046	0.041477
		-1.3870					
		-1.3870	0.1500	0.0076	0.0260	0.004046	0.041477
		-1.5370					
		-1.5370	0.1500	0.0076	0.0260	0.004046	0.041477
		-1.6870					
		-1.6870	0.1500	0.0076	0.0260	0.004046	0.041477
		-1.8370					
		-1.8370	0.1500	0.0076	0.0260	0.004046	0.041477
		-1.9870					
	GRID B						
300	Hero	-1.9870	0.1500	0.0076	0.0260	0.004046	0.041477
		-2.1370					
		-2.1370	0.1500	0.0076	0.0260	0.004046	0.041477
		-2.2870					
		-2.2870	0.1500	0.0076	0.0260	0.004046	0.041477
		-2.4370					
		-2.4370	0.1500	0.0076	0.0260	0.004046	0.041477
		-2.5870					
		-2.5870	0.1500	0.0076	0.0260	0.004046	0.041477
		-2.7370					
		-2.7370	0.1500	0.0076	0.0260	0.004046	0.041477
		-2.8870					
		-2.8870	0.1500	0.0076	0.0260	0.004046	0.041477
		-3.0370					
		-3.0370	0.1500	0.0076	0.0260	0.004046	0.041477
		-3.1870					
	GRID C						
300	Hero	-3.1870	0.1500	0.0076	0.0260	0.004046	0.041477
		-3.3370					
		-3.3370	0.1500	0.0076	0.0260	0.004046	0.041477
		-3.4870					
		-3.4870	0.1500	0.0076	0.0260	0.004046	0.041477
		-3.6370					
		-3.6370	0.1500	0.0076	0.0260	0.004046	0.041477
		-3.7870					
		-3.7870	0.1500	0.0076	0.0260	0.004046	0.041477
		-3.9370					
		-3.9370	0.1500	0.0076	0.0260	0.004046	0.041477
		-4.0870					
		-4.0870	0.1500	0.0076	0.0260	0.004046	0.041477
		-4.2370					

No	Region	Elevation (m)	Axial Lenght (m)	Flow Area (m^2)	Hydraulic Diameter (m)	Heated Diameter [left] (m)	Heated Diameter [right] (m)
		-4.2370	0.1500	0.0076	0.0260	0.004046	0.041477
		-4.3870					
		-4.3870	0.1500	0.0076	0.0260	0.004046	0.041477
		-4.5370					
		-4.5370	0.1500	0.0076	0.0260	0.004046	0.041477
		-4.6870					
	GRID D						
300	Hero	-4.6870	0.1500	0.0076	0.0260	0.004046	0.041477
		-4.8370					
		-4.8370	0.1500	0.0076	0.0260	0.004046	0.041477
		-4.9870					
		-4.9870	0.1500	0.0076	0.0260	0.004046	0.041477
		-5.1370					
		-5.1370	0.1500	0.0076	0.0260	0.004046	0.041477
		-5.2870					
		-5.2870	0.1500	0.0076	0.0260	0.004046	0.041477
		-5.4370					
		-5.4370	0.1313	0.0076	0.0260	0.004046	0.041477
		-5.5683					
		-5.5683	0.1313	0.0076	0.0260	0.004046	0.041477
		-5.6995					
		-5.6995	0.1313	0.0076	0.0260	0.004046	0.041477
		-5.8308					
	GRID E						
300	Hero	-5.8308	0.1313	0.0076	0.0260	0.004046	0.041477
		-5.9620					

Tab. 6 – CIRCE-HERO facility: Geometrical parameters

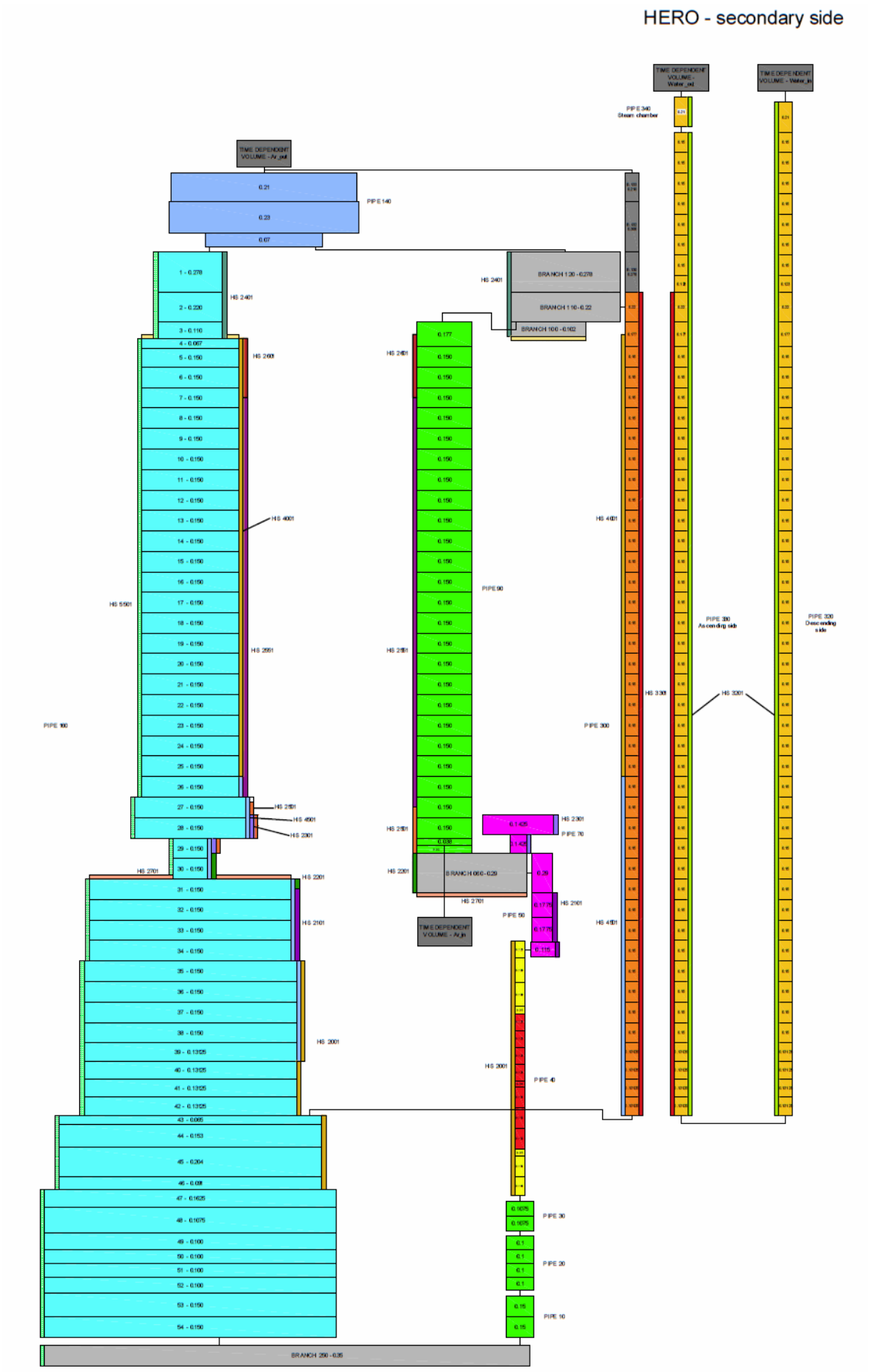

Fig. 37 – CIRCE-HERO 1D nodalization scheme by RELAP5-3D code

3.2 CIRCE-HERO facility 3D nodalization

The 1-D model is refurbished in order to simulate the 3D pool thermal-hydraulics (Fig. 39).

The 3D nodalization of CIRCE pool can be divided into 2 regions:

- 3D Region #1: it represents the CIRCE pool. It is connected to the CIRCE upper plenum, the 3D region #2 and the outlet section of HERO. The 3D region #1 contains all internals of CIRCE.
- 3D Region #2: it represents the CIRCE lower plenum. This region is connected to the 3D region #1 and the feeding conduit inlet section.

The multi-dimensional volume is defined in cylindrical geometry. The radial and angular meshes are the same for each regions. They are composed by 4 r-coordinate intervals and 8 θ-coordinate intervals.

3.2.1 3D Region #1: CIRCE pool

It represents the downcomer of CIRCE. This region contain all internals: HERO, the dead volume, the riser, the fitting volume, the FPS and the feeding conduit. It is models by 51 axial intervals with average length of 150 mm. It is constituted by 1632 volumes.

In order to take into account the internals, the volume occupied by every component are corrected with a volume factor that represent the ratio of free volume and busy volume. In the same way the junction area factor allows to indicate the area filled by internal components. If the junction area factor is equal to 0, this junction is closed.

The volumes completely filled by internals are characterized by a volume factor equal to 1. This volumes are hydraulically and thermally insulated (all junction present the factor equal to 0).

The region is connected to the outlet section of HERO by the junction 305 (Fig. 41). The junction connect the last volume of the steam generator with the downcomer at the axial level 40.

3.3 3D Region #2: CIRCE lower plenum

The 3D region #2 in Fig. 42 represents the lower plenum of CIRCE. It is composed of a single axial level (32 volumes).

The lower plenum does not contain internal components. Volume factors and junction area factors are equal to 1.

The region is connected to the inlet section of the feeding conduit by the junction 255.

Region	r_1	r_2	θ_1	θ_2	z_1	z_2	Volume factor
#1	1	1	1	8	1	23	1.000
	2	2	1	2	1	23	1.000
	2	2	3	3	1	23	0.026
	2	2	4	4	1	23	0.340
	2	2	5	5	1	23	0.630
	2	2	6	6	1	23	0.455
	2	2	7	7	1	23	0.030

Region	r_1	r_2	θ_1	θ_2	z_1	z_2	Volume factor
	2	2	8	8	1	23	1.000
	3	3	1	1	1	23	1.000
	3	3	2	2	1	23	0.267
	3	3	3	3	1	23	0.762
	3	3	4	4	1	23	0.334
	3	3	5	5	1	1	0.817
	3	3	5	5	2	23	0.640
	3	3	6	6	1	23	0.947
	3	3	7	7	1	23	0.767
	3	3	8	8	1	23	0.269
	4	4	1	1	1	23	0.859
	4	4	2	5	1	23	1.000
	4	4	6	6	1	23	0.942
	4	4	7	7	1	23	0.873
	4	4	8	8	1	23	1.000
	1	1	1	8	24	27	1.000
	2	2	1	2	24	27	1.000
	2	2	3	3	24	25	0.136
	2	2	3	3	24	27	1.000
	2	2	4	4	24	25	0.540
	2	2	4	4	24	27	1.000
	2	2	5	5	24	25	0.787
	2	2	5	5	24	27	0.328
	2	2	6	6	24	25	0.655
	2	2	6	6	24	27	0.596
	2	2	7	7	24	27	0.140
	2	2	8	8	24	27	1.000
	3	3	1	1	24	27	0.073
	3	3	2	2	24	25	0.439
	3	3	2	2	26	27	0.408
	3	3	3	3	24	25	0.843
	3	3	3	3	26	27	0.382
	3	3	4	4	24	25	0.334
	3	3	4	4	26	27	0.123
	3	3	5	5	24	25	0.640
	3	3	5	5	26	27	0.619
	3	3	6	6	24	27	0.947
	3	3	7	7	24	27	0.849
	3	3	8	8	24	27	0.439
	4	4	1	5	24	25	1.000
	4	4	1	2	26	27	1.000
	4	4	3	3	26	27	0.992
	4	4	4	4	26	27	0.804
	4	4	5	5	26	27	1.000

Region	r_1	r_2	θ_1	θ_2	z_1	z_2	Volume factor
	4	4	6	6	24	27	0.942
	4	4	7	7	24	27	0.873
	4	4	8	8	24	27	1.000
	1	1	1	1	28	31	0.174
	1	1	2	2	28	31	0.522
	1	1	3	7	28	31	1.000
	1	1	8	8	28	31	0.522
	2	2	1	1	28	31	1.000
	2	2	2	2	28	31	0.519
	2	2	3	7	28	31	1.000
	2	2	8	8	28	31	0.519
	3	3	1	1	28	31	0.869
	3	3	2	2	28	31	0.995
	3	3	3	4	28	31	1.000
	3	3	5	5	28	31	0.640
	3	3	6	6	28	29	0.947
	3	3	7	7	28	29	0.900
	3	3	6	7	30	31	1.000
	3	3	8	8	28	31	0.995
	4	4	1	5	28	29	1.000
	4	4	6	6	28	29	0.873
	4	4	7	7	28	29	0.873
	4	4	8	8	28	29	1.000
	4	4	1	8	30	31	1.000
	1	1	1	1	32	39	0.609
	1	1	2	2	32	39	0.957
	1	1	3	7	32	39	1.000
	1	1	8	8	32	39	0.957
	2	2	1	1	32	39	0.009
	2	2	2	2	32	39	0.757
	2	2	3	7	32	39	1.000
	2	2	8	8	32	39	0.757
	3	3	1	1	32	39	0.966
	3	3	2	4	32	39	1.000
	3	3	5	5	32	39	0.640
	3	3	6	8	32	39	1.000
	4	4	1	8	32	39	1.000
	1	1	1	1	40	43	0.609
	1	1	2	2	40	43	0.957
	1	1	3	7	40	43	1.000
	1	1	8	8	40	43	0.957
	2	2	1	1	40	43	0.009
	2	2	2	2	40	43	0.757
	2	2	3	7	40	43	1.000

Region	r_1	r_2	θ_1	θ_2	z_1	z_2	Volume factor
	2	2	8	8	40	43	0.757
	3	3	1	1	40	43	0.966
	3	3	2	8	40	43	1.000
	4	4	1	8	40	43	1.000
	1	1	1	8	44	51	1.000
	2	2	1	1	44	51	0.651
	2	2	2	8	44	51	1.000
	3	4	1	8	44	51	1.000

Tab. 7 – Volume factor

Region	r_1	r_2	θ_1	θ_2	z_1	z_2	Volume face	Junction area factor
#1	1	1	1	8	1	23	2	0.000
	2	2	1	2	1	23	2	0.000
	2	2	2	2	1	23	4	0.000
	2	2	8	8	1	23	4	0.000
	2	2	3	3	1	23	2	0.194
	2	2	3	3	1	23	4	0.086
	2	2	3	3	1	22	6	0.026
	2	2	4	4	1	23	2	0.361
	2	2	4	4	1	23	4	0.470
	2	2	4	4	1	22	6	0.340
	2	2	5	5	1	23	2	1.000
	2	2	5	5	1	23	4	0.470
	2	2	5	5	1	22	6	0.630
	2	2	6	6	1	23	2	1.000
	2	2	6	6	1	23	4	0.146
	2	2	6	6	1	22	6	0.455
	2	2	7	7	1	23	2	0.253
	2	2	7	7	1	22	6	0.030
	2	2	8	8	1	23	2	0.000
	2	2	7	7	1	23	4	0.000
	3	3	1	1	1	23	2	0.000
	3	3	1	1	1	23	4	0.000
	3	3	8	8	1	23	4	0.000
	3	3	2	2	1	23	2	0.920
	3	3	2	2	1	23	4	0.533
	3	3	2	2	1	22	6	0.327
	3	3	3	3	1	23	2	1.000
	3	3	3	3	1	23	4	0.130
	3	3	3	3	1	22	6	0.762

Region	r_1	r_2	θ_1	θ_2	z_1	z_2	Volume face	Junction area factor
	3	3	4	4	1	23	2	0.703
	3	3	4	4	1	23	4	1.000
	3	3	4	4	1	22	6	0.334
	3	3	5	5	1	23	2	1.000
	3	3	5	5	1	23	4	1.000
	3	3	5	5	1	1	6	0.817
	3	3	5	5	2	22	6	0.640
	3	3	6	6	1	23	2	0.847
	3	3	6	6	1	23	4	0.640
	3	3	6	6	1	22	6	0.947
	3	3	7	7	1	23	2	0.737
	3	3	7	7	1	23	4	0.532
	3	3	7	7	1	22	6	0.767
	3	3	8	8	1	23	2	0.919
	3	3	8	8	1	22	6	0.269
	4	4	1	1	1	23	4	0.949
	4	4	1	1	1	22	6	0.859
	4	4	2	2	1	23	4	1.000
	4	4	2	2	1	22	6	1.000
	4	4	3	5	1	23	4	1.000
	4	4	3	5	1	22	6	1.000
	4	4	6	6	1	23	4	0.422
	4	4	6	6	1	22	6	0.942
	4	4	7	7	1	23	4	1.000
	4	4	7	7	1	22	6	0.873
	4	4	8	8	1	23	4	1.000
	4	4	8	8	1	22	6	1.000
	1	1	1	8	24	27	2	0.000
	2	2	1	2	24	27	2	0.000
	2	2	2	2	24	27	4	0.000
	2	2	8	8	24	27	4	0.000
	2	2	3	3	24	25	2	0.489
	2	2	3	3	24	25	4	0.278
	2	2	3	3	24	25	6	1.000
	2	2	4	4	24	25	2	0.361
	2	2	4	4	24	25	4	0.646
	2	2	4	4	24	25	6	3.969
	2	2	3	4	26	27	2	0.000
	2	2	2	2	26	27	4	0.000
	2	2	4	4	26	27	4	0.000
	2	2	3	4	26	27	6	0.000
	2	2	5	5	24	25	2	1.000
	2	2	5	5	24	25	4	0.646
	2	2	5	5	24	25	6	0.787

Region	r_1	r_2	θ_1	θ_2	z_1	z_2	Volume face	Junction area factor
	2	2	5	5	26	27	2	0.796
	2	2	5	5	26	27	4	0.472
	2	2	5	5	26	26	6	0.328
	2	2	6	6	24	27	2	1.000
	2	2	6	6	24	27	4	0.343
	2	2	6	6	24	25	6	0.655
	2	2	6	6	26	26	6	0.596
	2	2	7	7	24	27	2	0.546
	2	2	7	7	24	26	6	0.140
	2	2	8	8	24	27	2	0.000
	2	2	7	7	24	27	4	0.000
	3	3	1	2	24	27	2	1.000
	3	3	1	1	24	27	4	0.117
	3	3	1	1	24	26	6	0.073
	3	3	2	2	24	25	4	0.697
	3	3	2	2	26	27	4	0.512
	3	3	2	2	24	25	6	0.439
	3	3	2	2	26	26	6	0.408
	3	3	3	3	24	25	2	1.000
	3	3	3	3	24	25	4	0.130
	3	3	3	3	24	25	6	0.843
	3	3	3	3	26	27	2	0.909
	3	3	3	3	26	26	6	0.382
	3	3	4	4	24	25	2	0.703
	3	3	4	4	24	25	4	1.000
	3	3	4	4	24	25	6	0.334
	3	3	4	4	26	27	2	0.327
	3	3	4	4	26	27	4	0.704
	3	3	4	4	26	26	6	0.123
	3	3	5	5	24	27	2	1.000
	3	3	5	5	24	27	4	1.000
	3	3	5	5	24	25	6	0.640
	3	3	5	5	26	26	6	0.619
	3	3	6	6	24	27	2	0.847
	3	3	6	6	24	27	4	0.640
	3	3	6	6	24	25	6	0.947
	3	3	7	7	24	27	2	0.739
	3	3	7	7	24	27	4	0.697
	3	3	7	7	24	26	6	0.849
	3	3	8	8	24	27	2	1.000
	3	3	8	8	24	27	4	0.117
	3	3	8	8	24	26	6	0.439
	4	4	1	5	24	25	4	1.000

Region	r_1	r_2	θ_1	θ_2	z_1	z_2	Volume face	Junction area factor
	4	4	1	5	24	25	6	1.000
	4	4	1	2	26	27	4	1.000
	4	4	1	2	26	26	6	1.000
	4	4	3	3	26	27	4	0.813
	4	4	3	3	26	26	6	0.992
	4	4	4	4	26	27	4	1.000
	4	4	4	4	26	26	6	0.804
	4	4	5	5	26	27	4	1.000
	4	4	5	5	26	26	6	1.000
	4	4	6	6	24	27	4	0.422
	4	4	6	6	24	26	6	0.942
	4	4	7	7	24	27	4	1.000
	4	4	7	7	24	26	6	0.873
	4	4	8	8	24	27	4	1.000
	4	4	8	8	24	26	6	1.000
	1	1	1	1	28	31	4	0.428
	1	1	1	1	28	30	6	0.174
	1	1	2	2	28	31	2	0.291
	1	1	2	2	28	31	4	1.000
	1	1	2	2	28	30	6	0.522
	1	1	3	7	28	31	2	1.000
	1	1	3	7	28	31	4	1.000
	1	1	3	7	28	30	6	1.000
	1	1	8	8	28	31	2	0.291
	2	2	1	1	28	31	2	0.522
	2	2	1	1	28	31	4	0.000
	2	2	8	8	28	31	4	0.000
	1	1	8	8	28	30	6	0.000
	3	3	1	1	28	31	2	1.000
	3	3	1	1	28	31	4	0.916
	3	3	1	1	28	30	6	0.869
	3	3	2	2	28	31	2	1.000
	3	3	2	2	28	31	4	1.000
	3	3	2	2	28	30	6	0.995
	3	3	3	4	28	31	2	1.000
	3	3	3	4	28	31	4	1.000
	3	3	3	4	28	30	6	1.000
	3	3	5	5	28	31	2	1.000
	3	3	5	5	28	31	4	1.000
	3	3	5	5	28	30	6	0.640
	3	3	6	6	28	29	2	0.847
	3	3	6	6	28	29	4	0.640
	3	3	6	6	28	29	6	0.947
	3	3	7	7	28	29	2	0.739

Region	r_1	r_2	θ_1	θ_2	z_1	z_2	Volume face	Junction area factor
	3	3	7	7	28	29	4	1.000
	3	3	7	7	28	29	6	0.900
	3	3	6	7	30	31	2	1.000
	3	3	6	7	30	31	4	1.000
	3	3	6	7	30	30	6	1.000
	3	3	8	8	28	31	2	1.000
	3	3	8	8	28	31	4	0.916
	3	3	8	8	28	30	6	0.995
	4	4	1	5	28	29	4	1.000
	4	4	1	5	28	29	6	1.000
	4	4	6	6	28	29	4	0.422
	4	4	6	6	28	29	6	0.873
	4	4	7	7	28	29	4	1.000
	4	4	7	7	28	29	6	0.873
	4	4	8	8	28	31	4	1.000
	4	4	8	8	28	30	6	1.000
	4	4	1	8	30	31	4	1.000
	4	4	1	8	30	30	6	1.000
	1	1	1	1	32	39	4	0.843
	1	1	1	1	32	38	6	0.609
	1	1	2	2	32	39	2	0.782
	1	1	2	2	32	39	4	1.000
	1	1	2	2	32	38	6	0.957
	1	1	3	7	32	39	2	1.000
	1	1	3	7	32	39	4	1.000
	1	1	3	7	32	38	6	1.000
	1	1	8	8	32	39	2	0.782
	1	1	8	8	32	38	6	0.957
	3	3	1	8	32	39	2	1.000
	3	3	1	8	32	39	4	1.000
	3	3	1	1	32	38	6	0.966
	3	3	2	8	32	38	6	1.000
	4	4	1	8	32	39	4	1.000
	4	4	1	8	32	38	6	1.000
	1	1	1	1	40	43	4	0.843
	1	1	1	1	40	42	6	0.609
	1	1	2	2	40	43	2	0.782
	1	1	2	2	40	43	4	1.000
	1	1	2	2	40	42	6	0.957
	1	1	3	7	40	43	2	1.000
	1	1	3	7	40	43	4	1.000
	1	1	3	7	40	42	6	1.000
	1	1	8	8	40	43	2	0.782
	1	1	8	8	40	42	6	0.957

Region	r_1	r_2	θ_1	θ_2	z_1	z_2	Volume face	Junction area factor
	3	3	1	8	40	43	2	1.000
	3	3	1	8	40	43	4	1.000
	3	3	1	8	40	42	6	1.000
	4	4	1	8	40	43	4	1.000
	4	4	1	8	40	42	6	1.000
	1	3	1	8	44	51	2	1.000
	1	3	1	8	44	51	4	1.000
	4	4	1	8	44	51	4	1.000
	1	1	1	8	44	50	6	1.000
	2	2	1	1	44	50	6	0.651
	2	2	2	8	44	50	6	1.000
	3	3	1	8	44	50	6	1.000
	4	4	1	8	44	50	6	1.000

Tab. 8 – Junction area factor

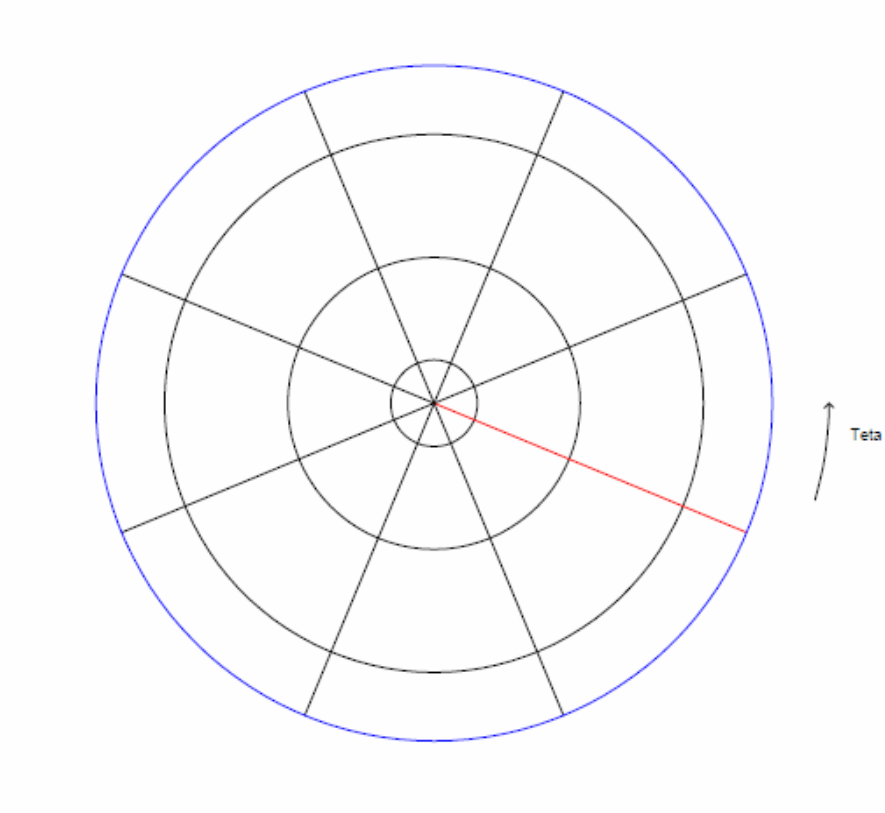

Fig. 38 – Radial and angular meshes

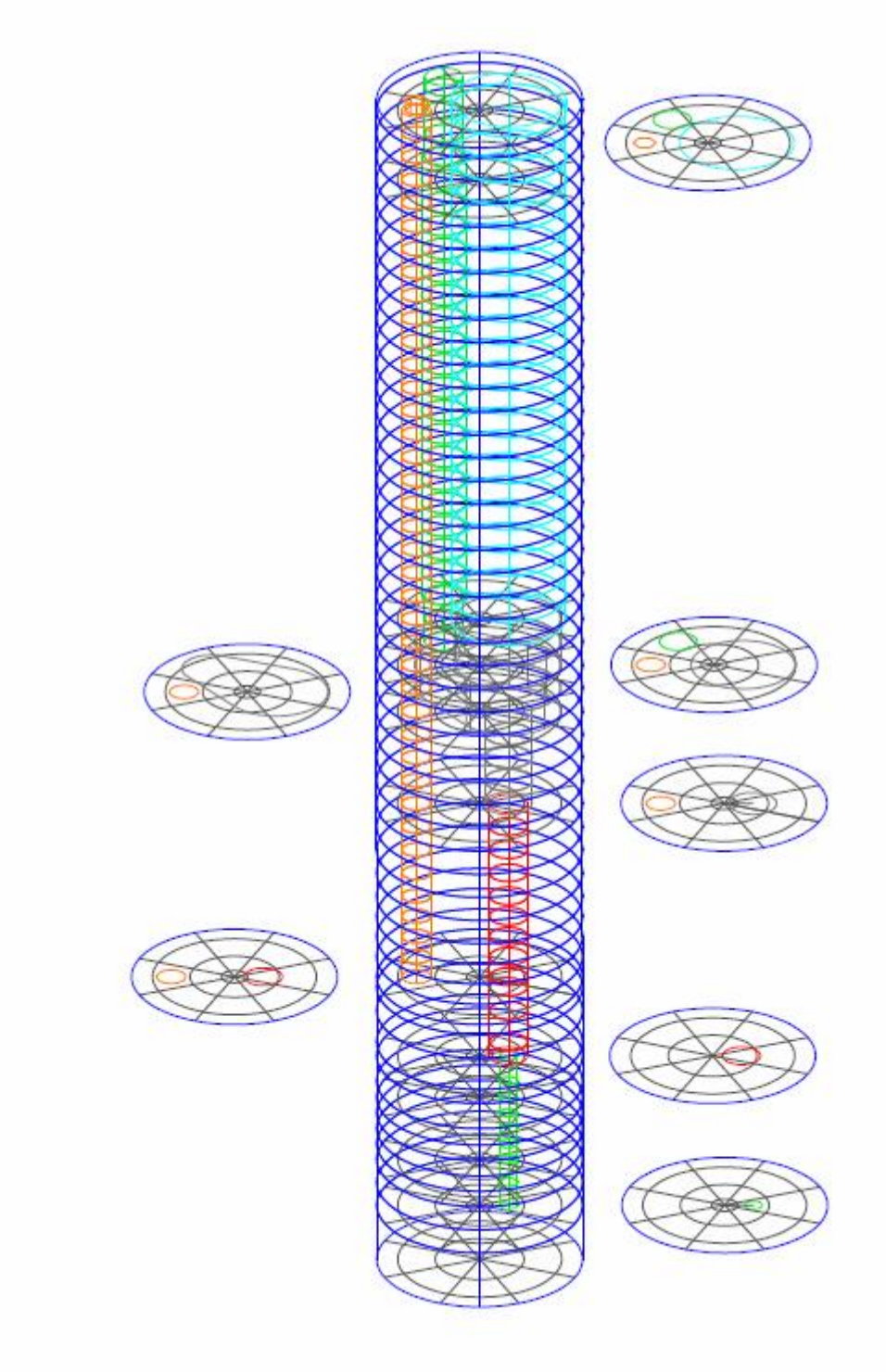

Fig. 39 – 3D models

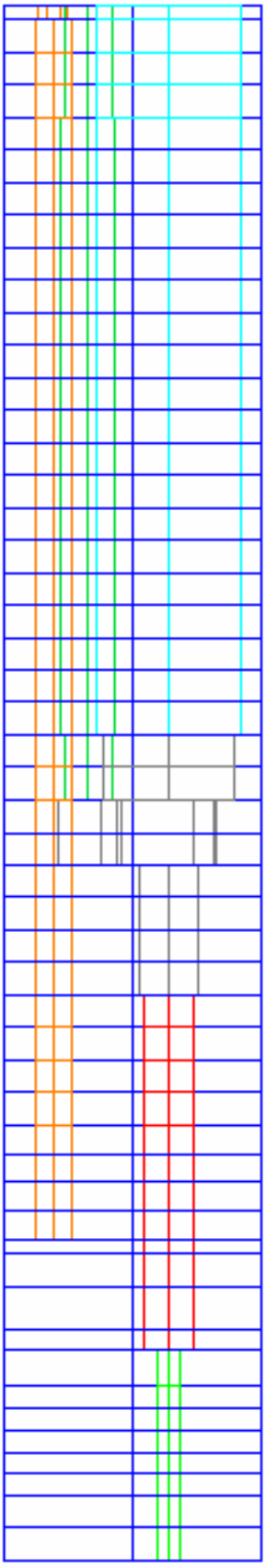

Fig. 40 – 3D Region #1

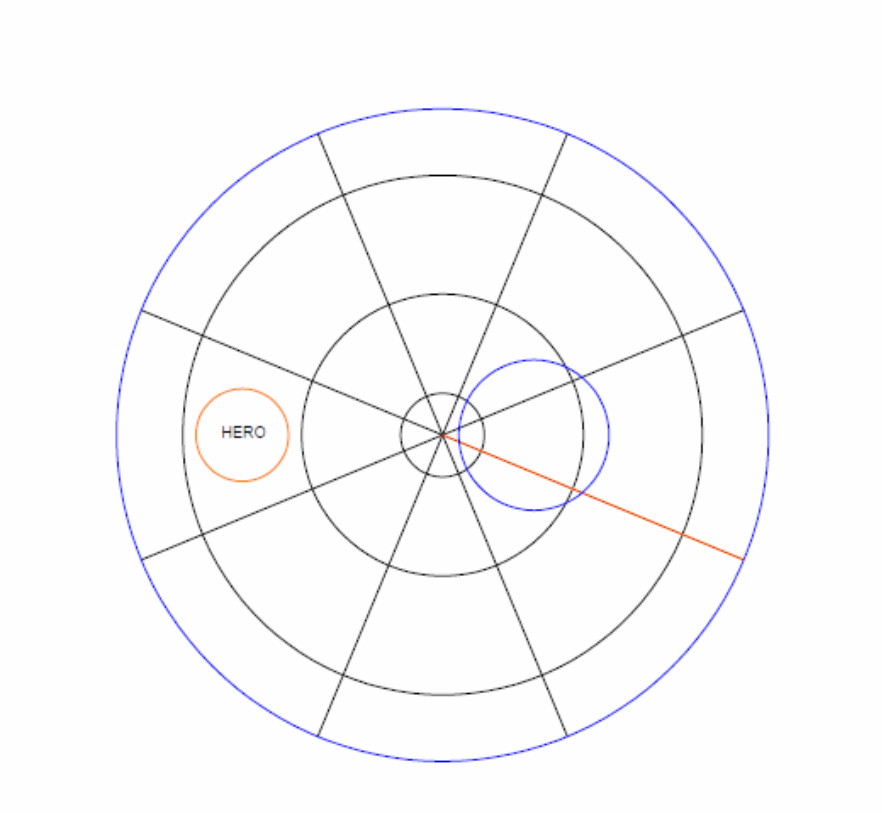

Fig. 41 – Axial level 40

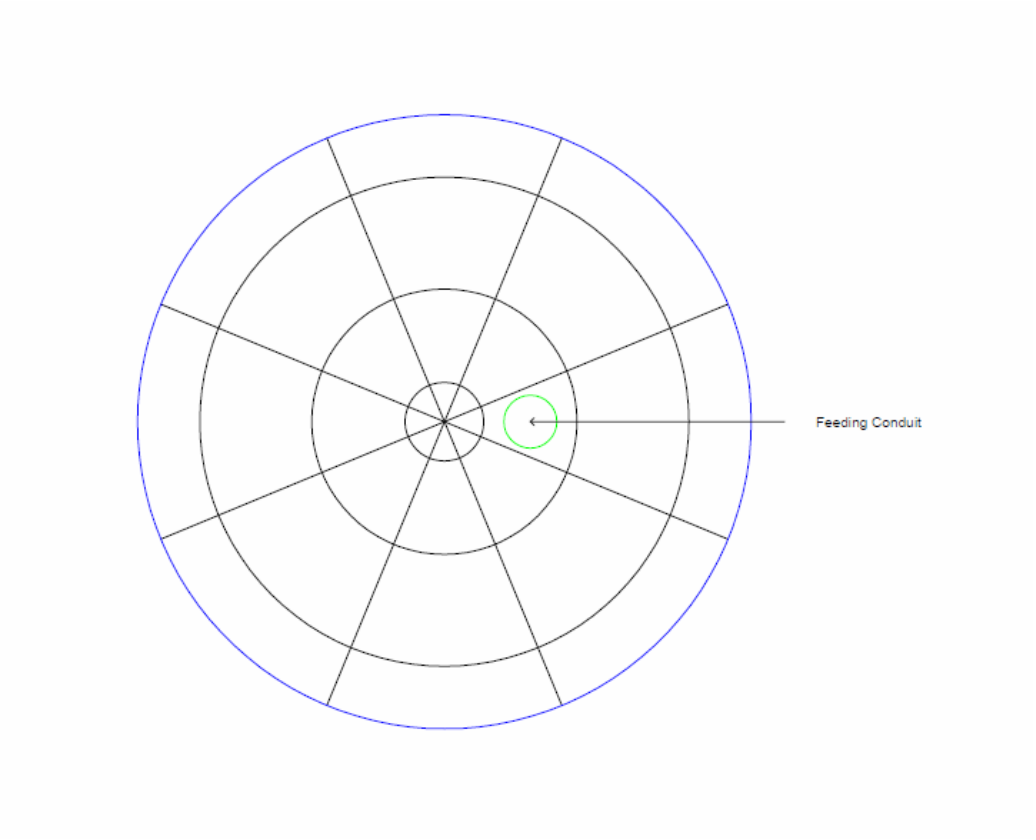

Fig. 42 – Lower plenum

4 Pre-Test Calculations

4.1 Steady state operation at full power

The multi-dimensional model has been developed to provide steady state simulation. Their main aim is to provide simulations at full power considering two different cases and the heat losses effects. The following cases are analyzed:

- Case 1: Gas enhanced circulation, full power (450kW), hot conditions (405°C) inside the pool, fixed LBE mass flow rate across the SGBT section equal to 44.7kg/s (representative of the scaled down SG of ALFRED). Heat losses are assumed equal to 45 kW (conservatively).
- Case 2: Gas enhanced circulation, full power (450kW), nominal feed-water flow rate (0.330785000 kg/s), hot conditions (405°C) inside the pool, fixed temperature drop across the FPS equal to 80°C in the range 400-480°C (representative of the temperature drop across the core ALFRED). Heat losses are assumed equal to 45 kW (conservatively).

The initial conditions are summarized in Tab. 9.

The main results are summarized in Tab. 10.

Fig. 43 and Fig. 44 highlight the evolutions of the LBE temperatures at FPS inlet (tempf 40020000), FPS outlet (tempf 40120000), HERO channel inlet (tempf 300010000) and HERO channel outlet (tempf 300400000) comparing case 1 to case 2. According to the target, case 2 shows the temperature drop across the FPS equal to 79°C while case 1 highlights a temperature drop equal to 67°C due to the higher speed of LBE.

Fig. 45 and Fig. 46 report the trend of temperatures at the HERO secondary water/steam inlet (tempf 320010000) and outlet (tempg 330400000) versus the HERO LBE channel temperature drop comparing case 1 to case 2.

Fig. 47 and Fig. 48 depicts the LBE mass flow rate at HERO channel inlet (mflowj 300010000). According to the objective, case 1 shows the mass flow rate equal to 44.9 kg/s.

Fig. 50 and Fig. 51 highlight the thermal stratification and the velocity of liquid LBE in the pool after 18000 seconds. The images show the physical quantities of the axial section represented with the red line in Fig. 49.

In both cases the LBE exits from HERO with a temperature greater than the pool and goes up through the downcomer.

In the case 1 the average temperature in the pool is included between 669 – 667 K except the lower part that reaches 665 – 666 K.

Case 2 shows slightly lower temperatures. The average temperature is included between 667 – 665 K and the lower part reaches 662 – 663 K.

In both the cases, the LBE flow out from HERO with a temperature higher than pool temperature and begin to flow upward the downcomer.

Description			RUN # Case1	RUN # Case2
Initial conditions	I1	FPS power [kW]	450	450
	I2	Pool initial T. [K]	677.75	677.75
	I3	Ar mass flow [kg/s]	0.00241	0.00151
	I4	Feed-water pressure [bar]	172	172
	I5	Feed-water inlet T. [K]	608.15	608.15
	I6	Feed-water mass flow [kg/s]	0.330785	0.330785
	I7	Heat losses [kW]	45	45

Tab. 9 – Initial conditions

Description			RUN # Case1	RUN # Case2
Results at steady state	R1	FPS inlet T. [K]	665.7	662.5
	R2	FPS outlet T. [K]	732.9	741.5
	R3	LBE - HERO inlet T. [K]	729.2	736.2
	R4	LBE - HERO outlet T. [K]	672.2	669.7
	R5	LBE mass flow HERO inlet [kg/s]	44.9	38.5
	R6	Steam max temp T. [K]	654.0	655.0
	R7	Steam outlet temp T. [K]	649.3	649.7
	R8	Power removed by heat losses [kW]	389.5	390.1

Tab. 10 – Results at steady state

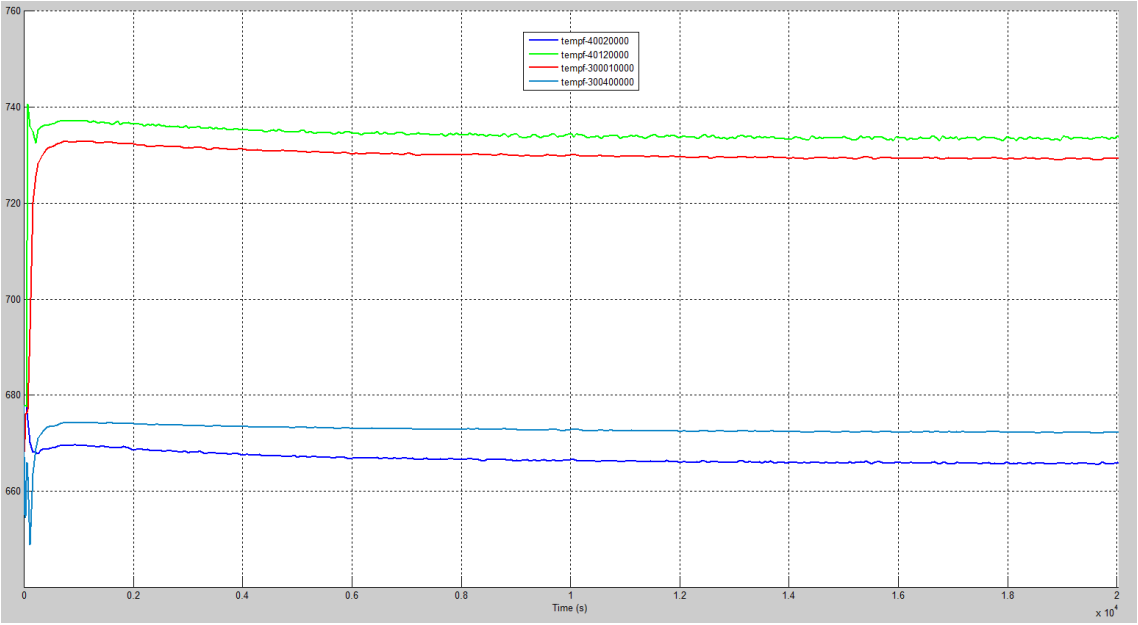

Fig. 43 – Case 1: HERO-CIRCE full power steady state preliminary simulations, LBE temperatures at FPS and HERO channels inlet/outlet

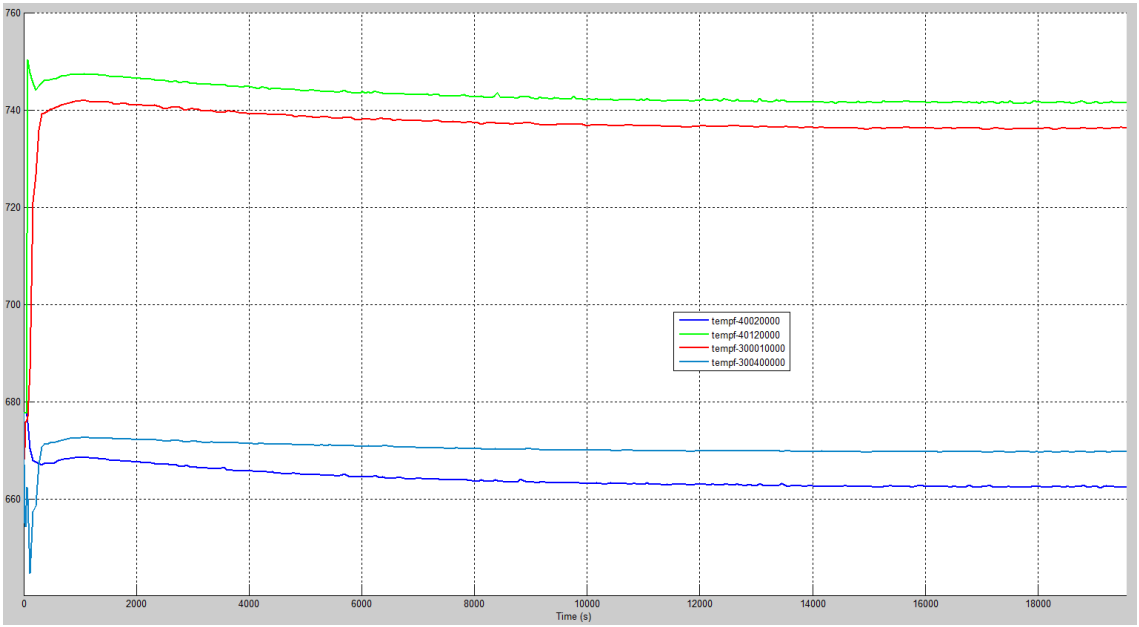

Fig. 44 – Case 2: HERO-CIRCE full power steady state preliminary simulations, LBE temperatures at FPS and HERO channels inlet/outlet

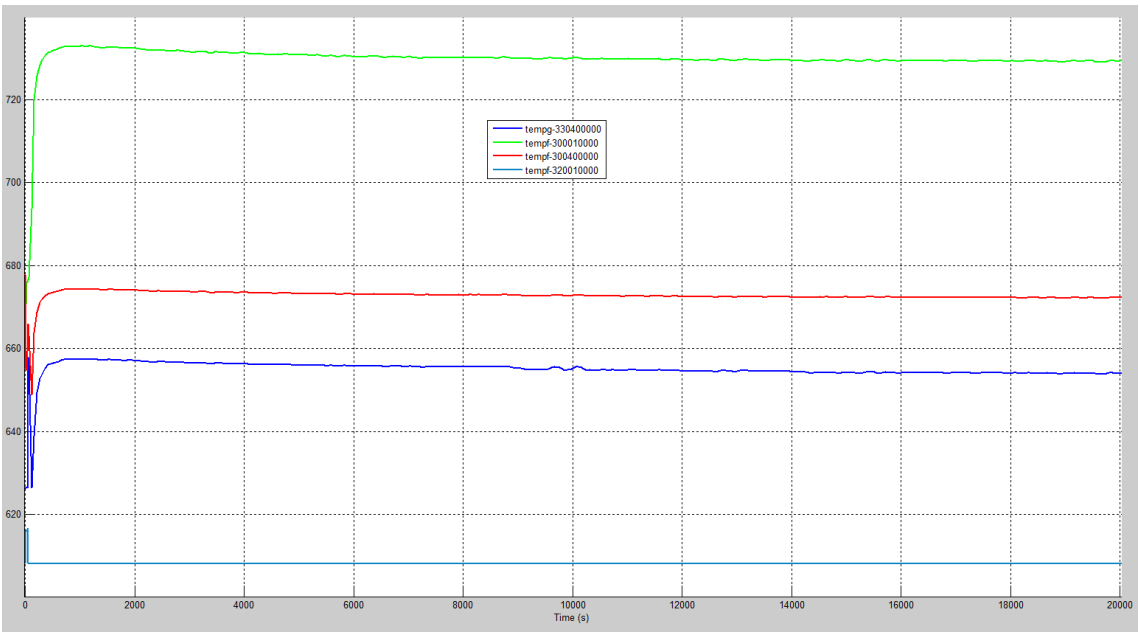

Fig. 45 – Case 1: HERO-CIRCE full power steady state preliminary simulations, temperatures at the HERO secondary water/steam inlet, outlet and LBE temperature at HERO channels inlet/outlet

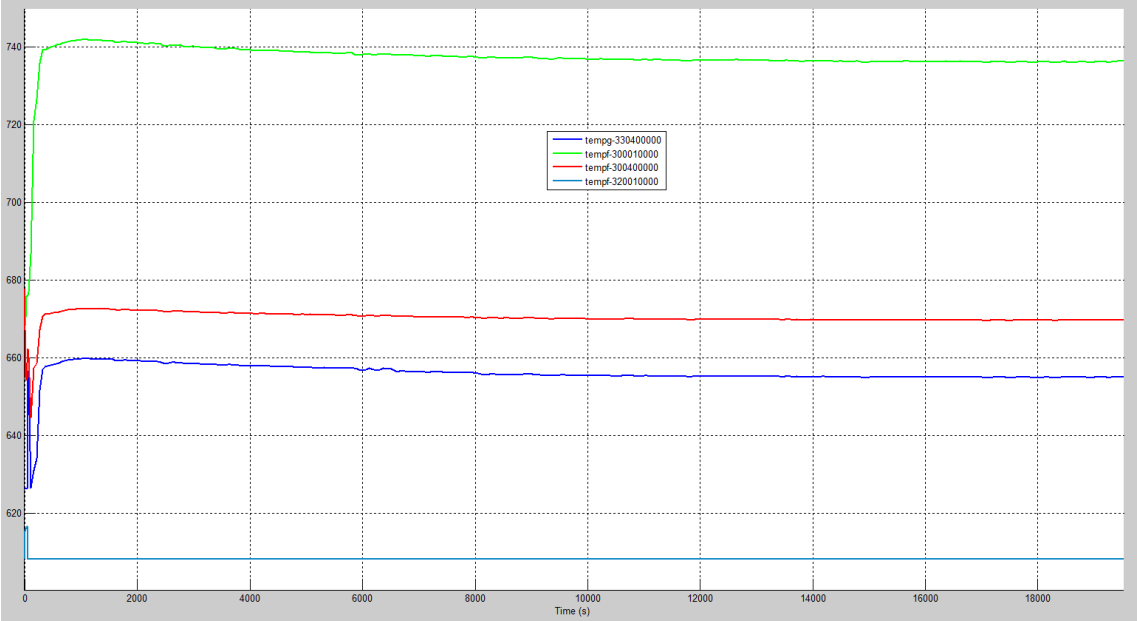

Fig. 46 – Case 2: HERO-CIRCE full power steady state preliminary simulations, temperatures at the HERO secondary water/steam inlet, outlet and LBE temperature at HERO channels inlet/outlet

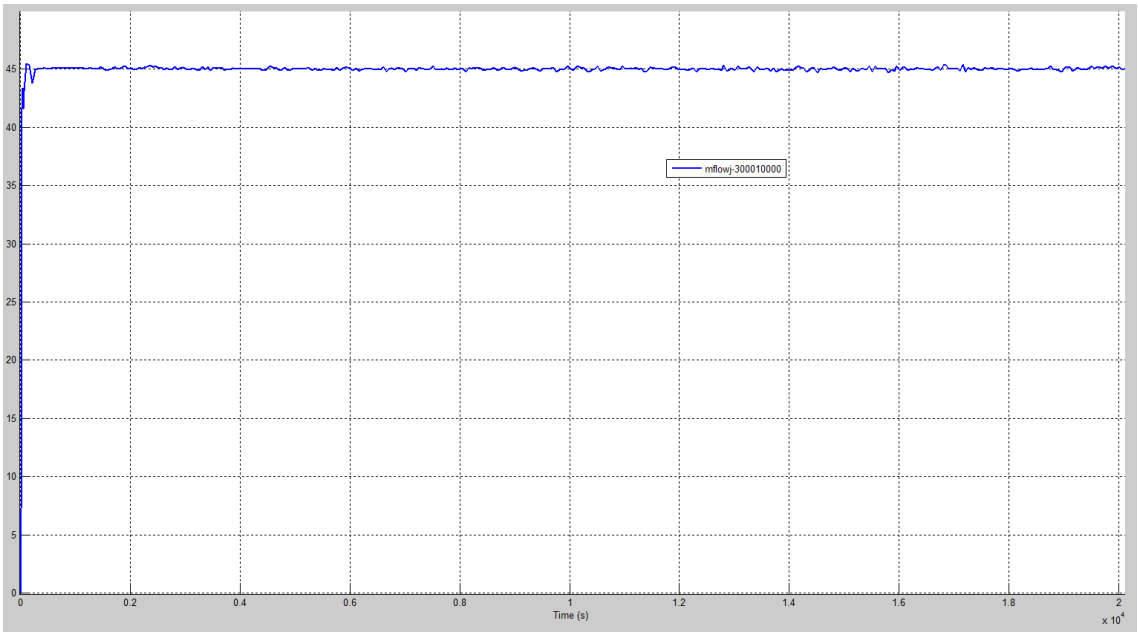

Fig. 47 – Case 1: HERO-CIRCE full power steady state preliminary simulations, LBE mass flow rate at HERO channel inlet

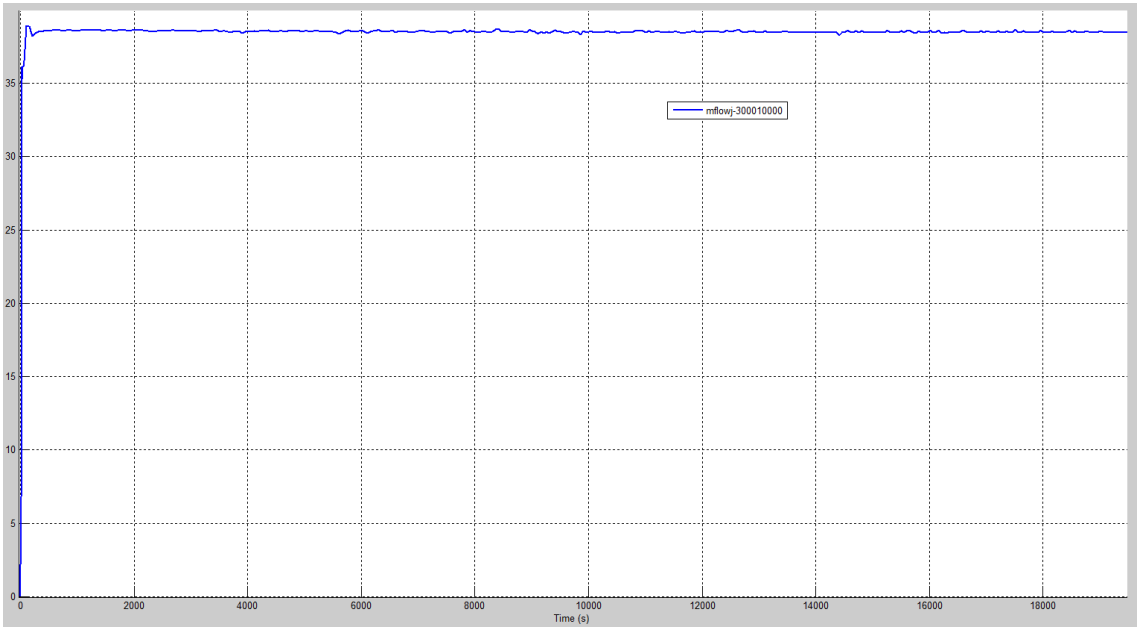

Fig. 48 – Case 2: HERO-CIRCE full power steady state preliminary simulations, LBE mass flow rate at HERO channel inlet

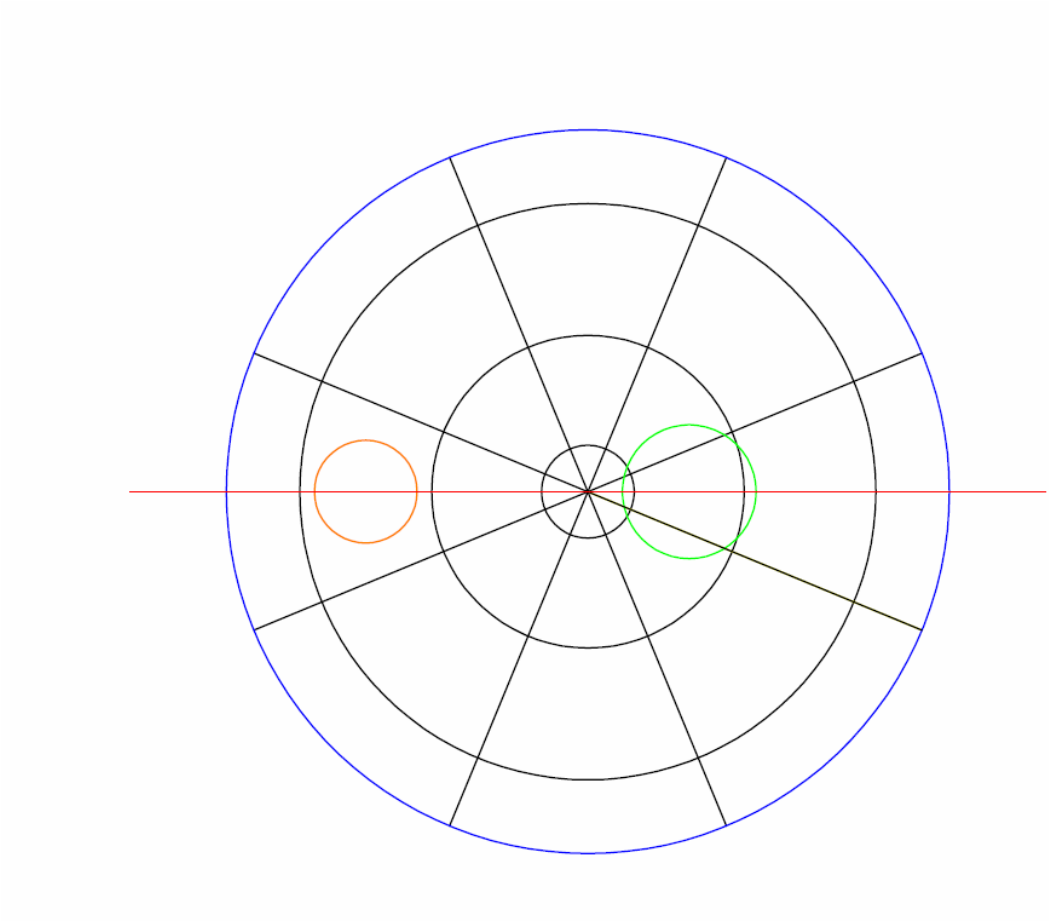

Fig. 49 – Axial section

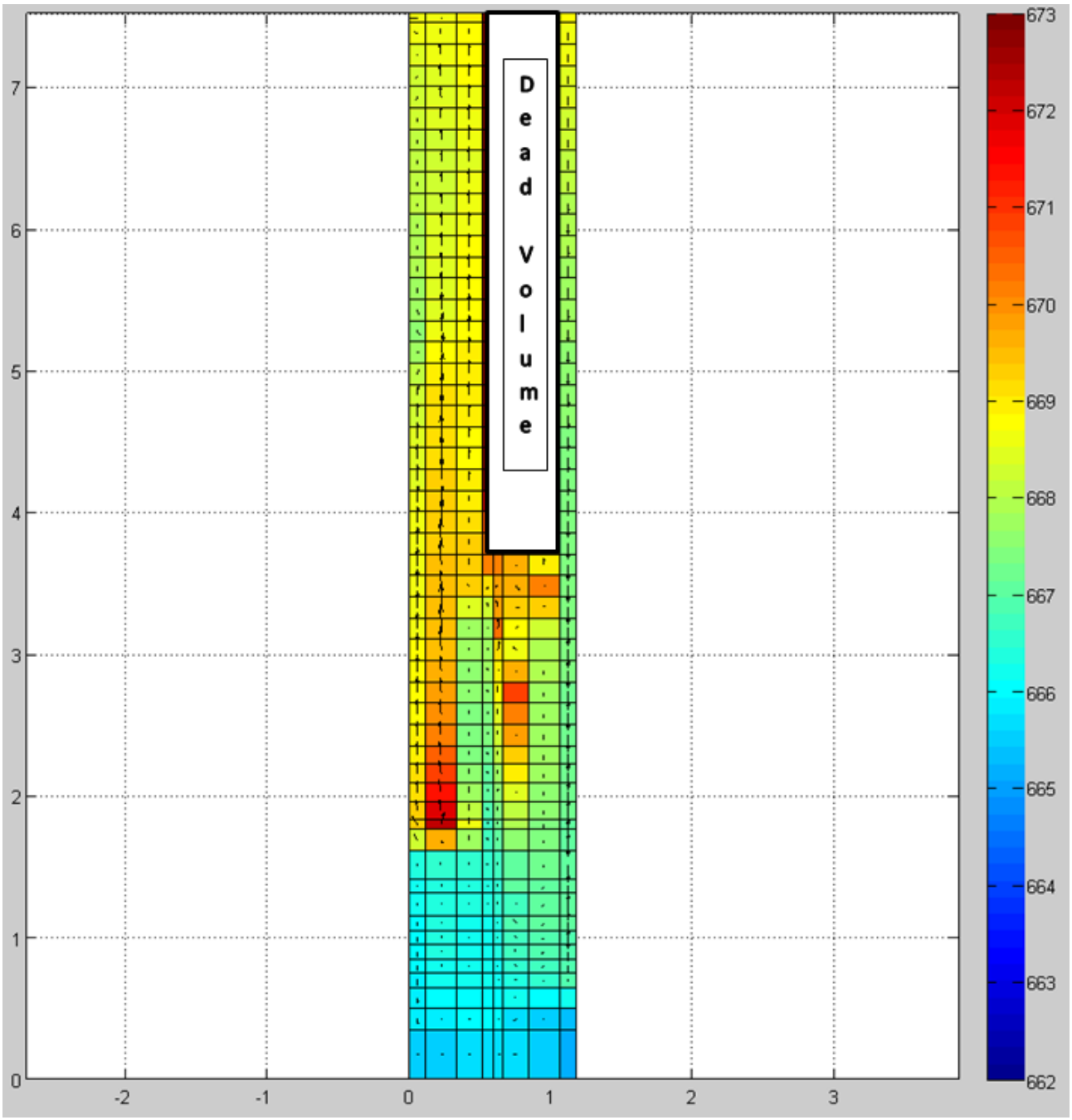

Fig. 50 – Case 1: HERO-CIRCE full power steady state preliminary simulations, LBE the thermal stratification and the velocity in the pool

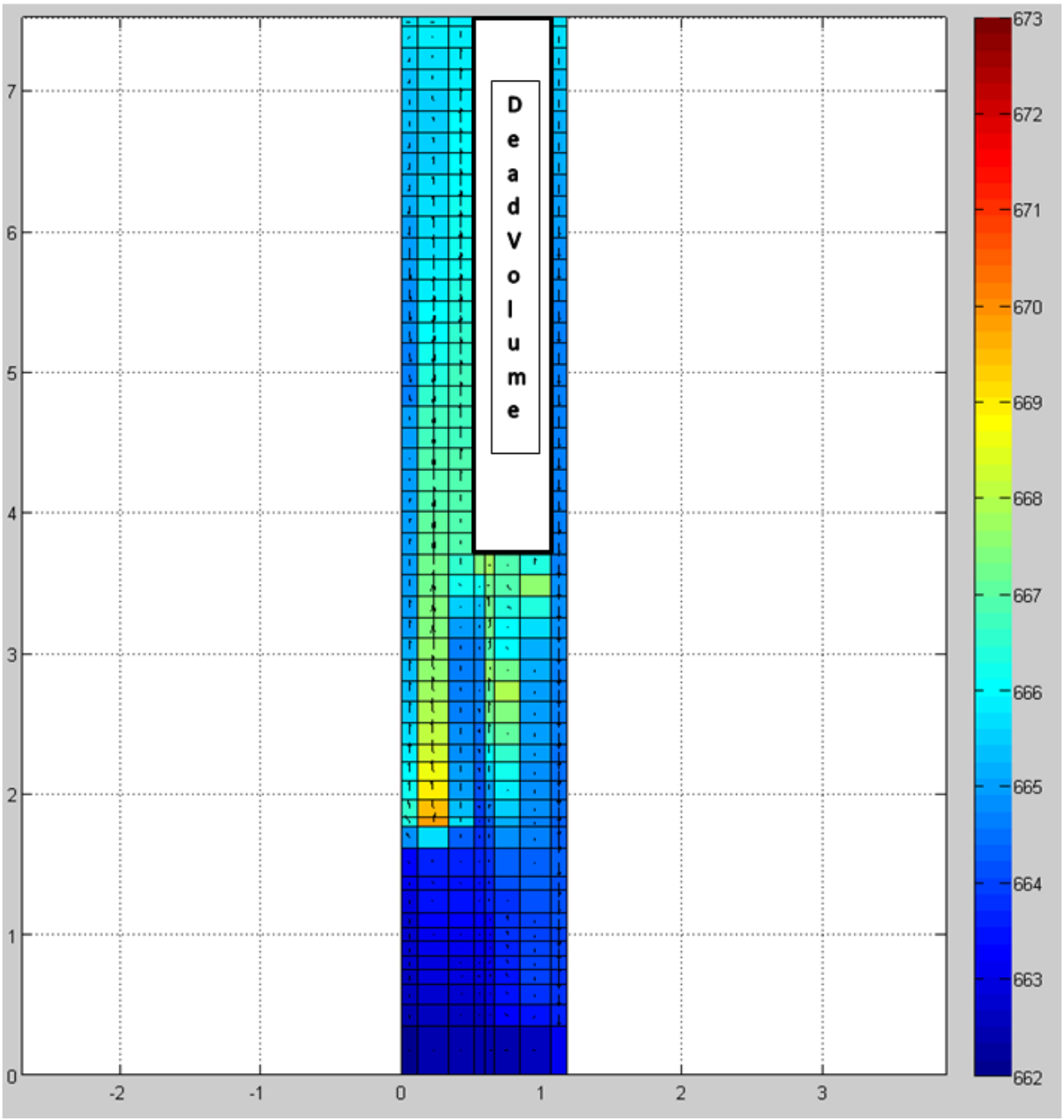

Fig. 51 – Case 2: HERO-CIRCE full power steady state preliminary simulations, LBE the thermal stratification and the velocity in the pool

4.2 Transient analysis

4.2.1 Transient test 1: Loss of flow

The starting point for transient test is considered case 1. The test basically consists in a protected loss of LBE pump: the FPS power decrease down to 5-7% (representative of decay heat), loss of Ar injection will occur followed by the activation of the DHR-1 which consists in the transition of HERO to a reduced flow rate.

The FPS power decreases in 900s according to Fig. 52, Tab. 11. The compensated FPS power accounts for the decay heat power and the heat losses from CIRCE (that are assumed 20 kW during the transient). The Ar injection decreases linearly in 10 seconds from 0.002410 kg/s to zero, the feed-water falls in from 0.330785000 to 0.033078500 linearly in 5 seconds, Tab. . The test terminates when the LBE pool temperature reaches 300°C.

Time [s]	Power shutdown curve [kW]	Compensated FPS power [kW]	Heat losses [kW]
0	450	450	45
1000	450	450	45
1001	96.99	116.99	20
1002	83.482	103.482	20
1003.5	71.073	91.073	20
1005	62.513	82.513	20
1007.5	52.932	72.932	20
1010	46.728	66.728	20
1015	38.639	58.639	20
1022.5	31.571	51.571	20
1030	27.173	47.173	20
1040	23.01	43.01	20
1050	19.948	39.948	20
1060	17.749	37.749	20
1090	13.979	33.979	20
1120	11.937	31.937	20
1180	9.738	29.738	20
1240	8.717	28.717	20
1300	8.168	28.168	20
1360	7.618	27.618	20
1420	7.225	27.225	20
1480	6.99	26.99	20
1540	6.754	26.754	20
1600	6.518	26.518	20
1660	6.283	26.283	20
1720	6.047	26.047	20
1780	5.969	25.969	20
1840	5.733	25.733	20
1900	5.576	25.576	20

Tab. 11 – HERO-CIRCE transient, FPS power

Time [s]	Power [kW]	Feed-water flow [kg/s]	Ar mass flow [kg/s]	Transient terminated
0	450	0.330785000	0.002410	When pool temperature reaches 300°C
1000	450	0.330785000	0.002410	
1005	82.513	0.0330785000	0.001205	
1010	66.728	0.0330785000	0	
1050	39.948	0.0330785000	0	
1900	25.576	0.0330785000	0	

Tab. 12 – HERO-CIRCE transient test 1, sequence of main event

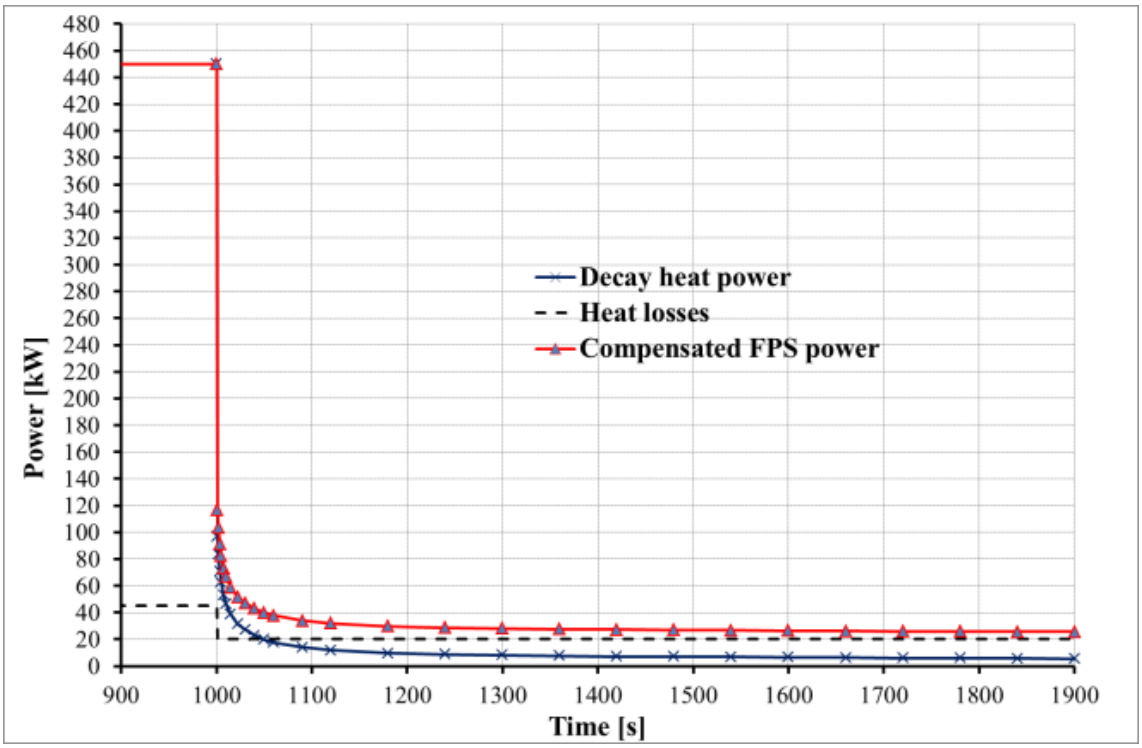

Fig. 52 – HERO-CIRCE transient, FPS power

4.2.2 Results

Fig. 53 highlights the evolution of temperature for 6000 seconds from the transient start up.

6000-6100 seconds (Fig. 54): FPS outlet temperature (tempf 40120000) decreases below 710 K in the first 50 seconds. FPS inlet temperature (tempf40020000) slightly increases to 670 K. The temperature at the HERO channel inlet (tempf 300010000) slightly decreases below 725 K in the first 50 seconds, then increases during the following 50 seconds. The temperature at the outlet section of HERO begins to decrease and reaches 655 K going below the temperature of the FPS inlet during the first 100 seconds.

6100-7000 seconds (Fig. 55): as result of the spike of FPS inlet temperature during first 1oo second ok the transient, the FPS outlet temperature increase above 725 K between 6100 – 6200 seconds and remain constant until 6280 seconds. Then the temperature begins to decrease. The temperature at the FPS inlet begins to decrease and reaches 610 K until 7000 seconds. The temperature at the HERO Channel inlet follows the trend of FPS outlet temperature reaching the temperature of 715 K. The temperature at the outlet section of HERO continues to decrease reaching a constant value of 640 K.

7000-11500 seconds (Fig. 56): All the temperatures decrease constantly. LBE mass flow rate at HERO channel inlets are given in Fig. 57.

6000-6100 seconds (Fig. 58): LBE mass flow rate quickly decrease to a minimum of about 8 kg/s and the the gradient decreases.

6100-7000 seconds (Fig. 59): LBE mass flow rate continues to decrease until reaching an average value of 4 kg/s that remain constant until 7000 seconds.
7000-11500 seconds (Fig. 60): LBE mass flow rate constantly increase to a value of 7.5 kg/s.

Fig. 61 highlights the thermal stratification and the velocity of liquid LBE in the pool at 6060 seconds, when the LBE temperature of the FPS inlet section shows the peak.

Fig. 62 represent the thermal stratification and the velocity of liquid LBE in the pool at 6200 seconds, when the LBE at the inlet section of HERO presents the maximum value. The two representations are compared with Fig. 50. After the protected loss of LBE pump, the average value of LBE temperature in the pool increase to the value between 669-670K. At this moment, the temperature of LBE at the outlet section of HERO quickly decrease and goes below the LBE temperature in the pool. As a consequence, the cooler LBE flow down towards the lower plenum.

The following Figs show the thermal stratification and the velocity of liquid LBE in the pool at different instants:

- Fig. 63: 6500 seconds;
- Fig. 64: 6800 seconds;
- Fig. 65: 7000 seconds;
- Fig. 66: 8000 seconds;
- Fig. 67: 9000 seconds;
- Fig. 68: 10000 seconds;
- Fig. 69: 11000 seconds;
- Fig. 70: 11500 seconds.

In order to show the evolution of pool temperature during the transient, the Fig.s use a wide temperature scale. About the temperature, the Fig.s shows that the thermal stratification is constantly increasing over time. At 6500 the temperature drop between the lower plenum and the central part of the pool is about 3 degrees. In the end of the simulation, the temperature drop increase to 25 K. The thermal stratification is presented at the level of the HERO outlet section from which the cooler LBE goes down.

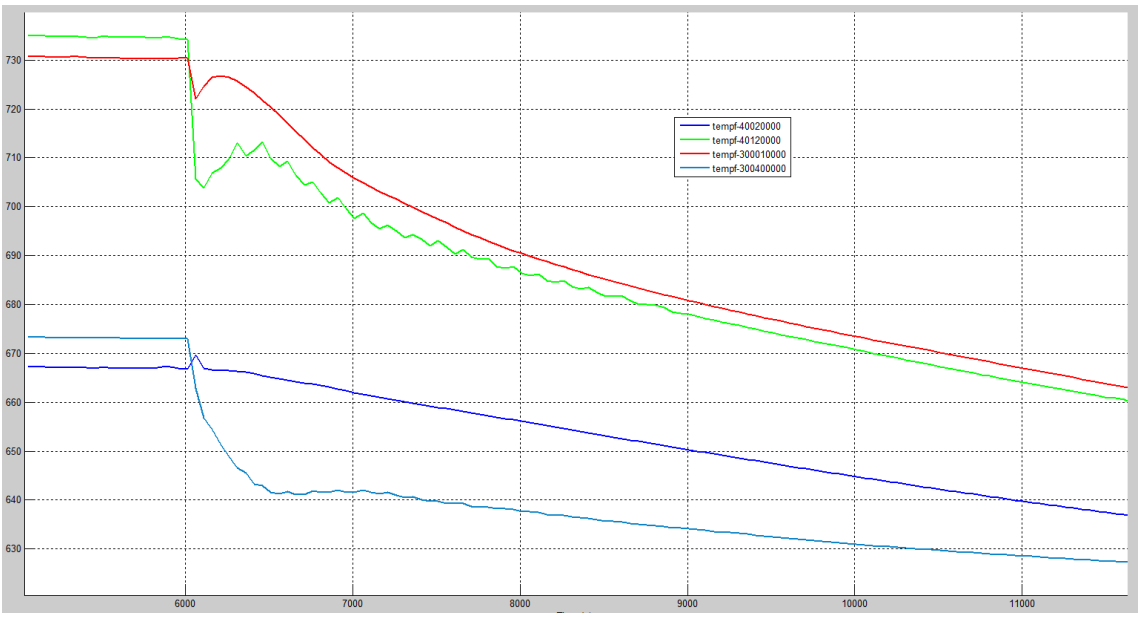

Fig. 53 – HERO-CIRCE transient, FPS and HERO channel LBE inlet-outlet temperatures

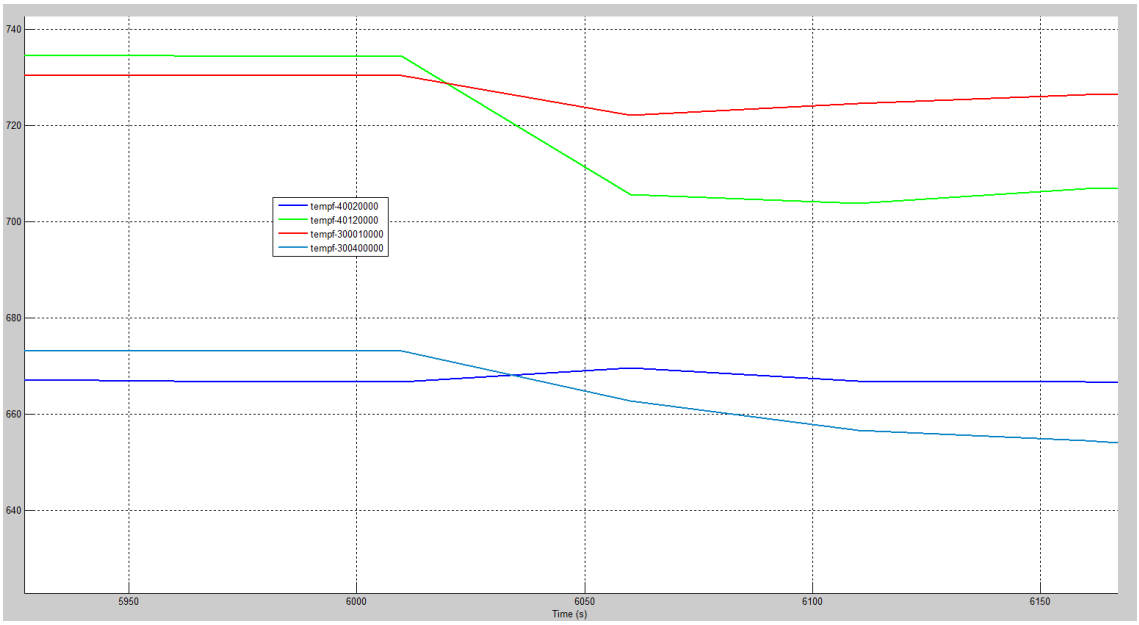

Fig. 54 – HERO-CIRCE transient, FPS and HERO channel LBE inlet-outlet temperatures: 6000-6100 seconds

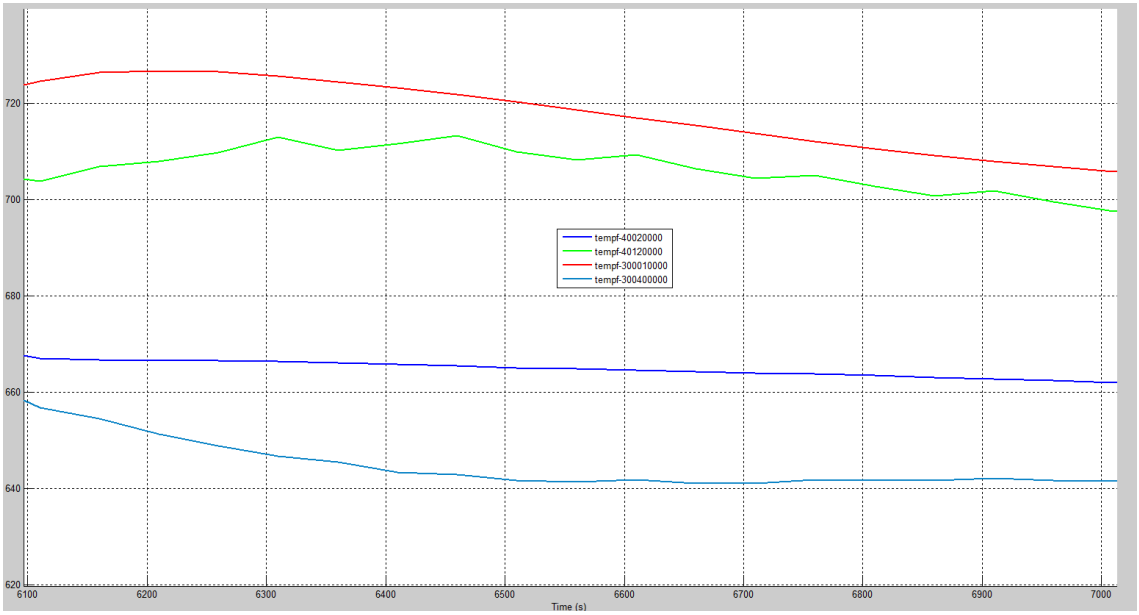

Fig. 55 – HERO-CIRCE transient, FPS and HERO channel LBE inlet-outlet temperatures: 6100-7000 seconds

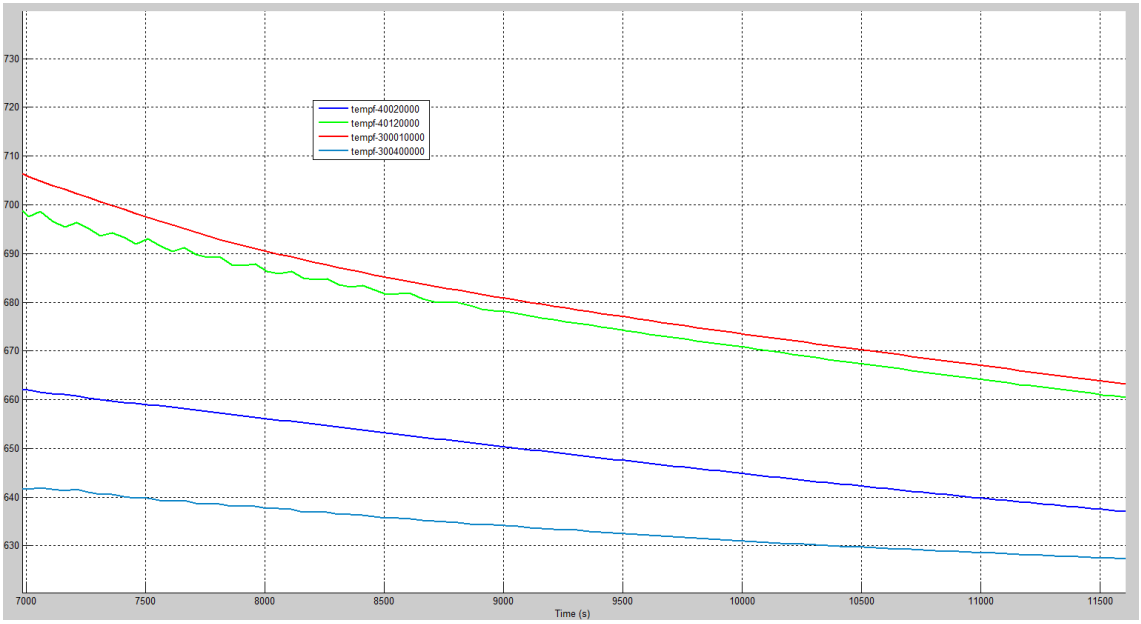

Fig. 56 – HERO-CIRCE transient, FPS and HERO channel LBE inlet-outlet temperatures: 7000-11500 seconds

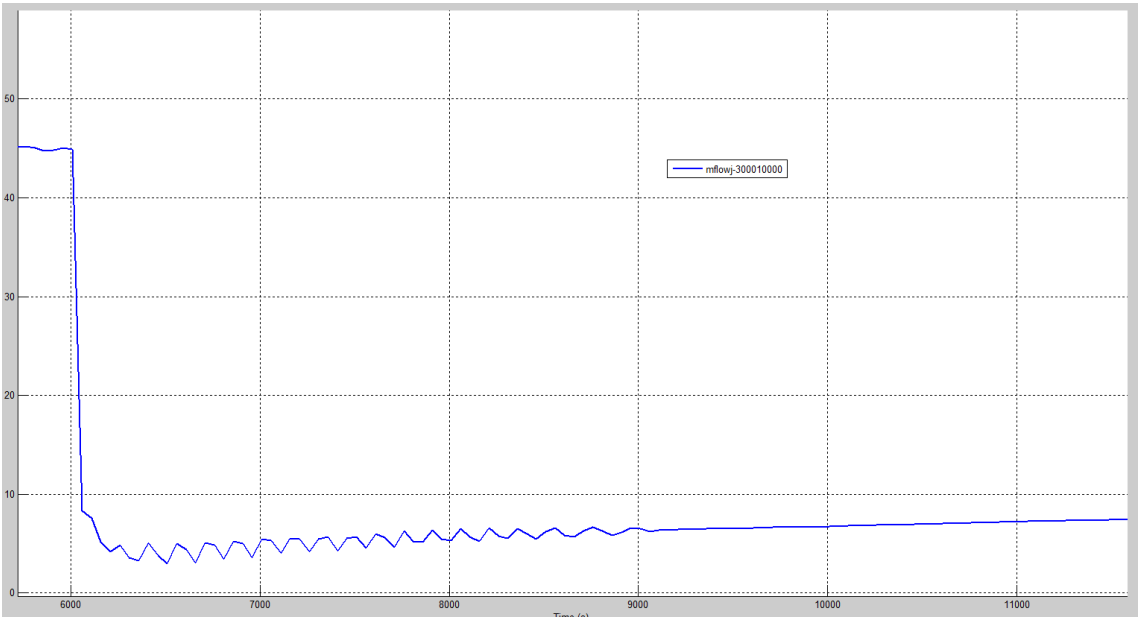

Fig. 57 – HERO-CIRCE transient, LBE mass flow rate at HERO LBE channel inlet

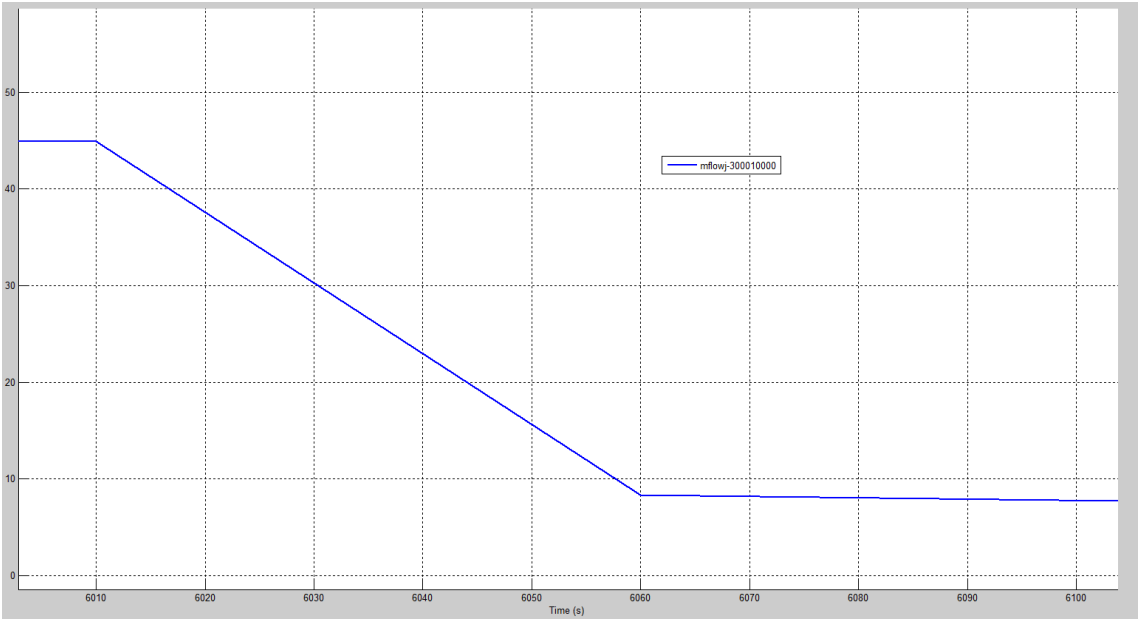

Fig. 58 – HERO-CIRCE transient, LBE mass flow rate at HERO LBE channel inlet: 6000-6100 seconds

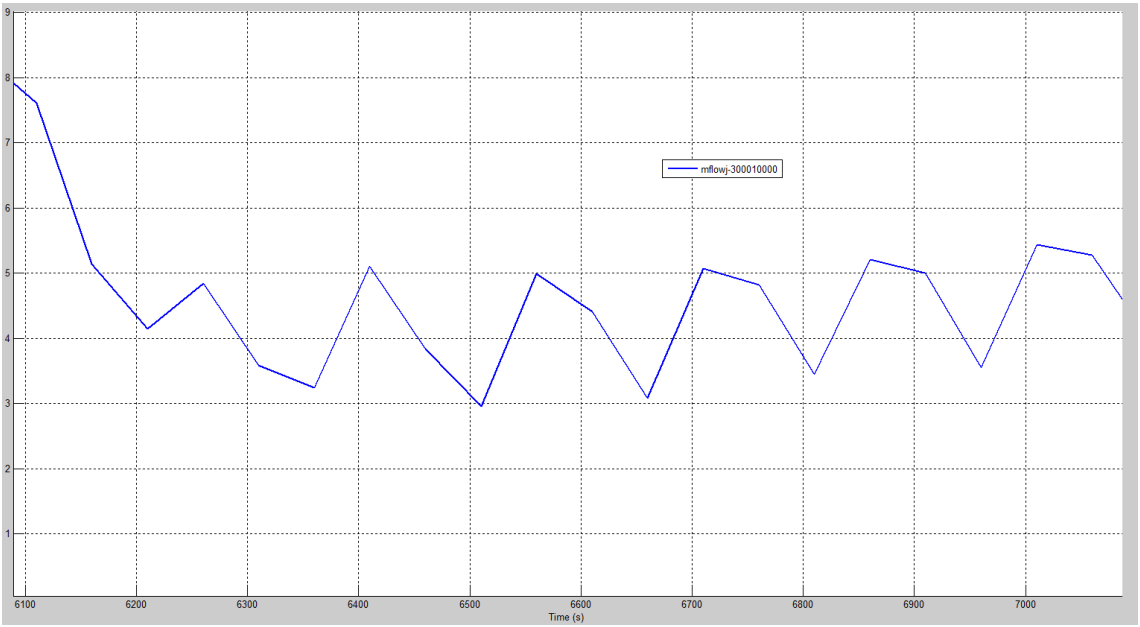

Fig. 59 – HERO-CIRCE transient, LBE mass flow rate at HERO LBE channel inlet: 6100-7000 seconds

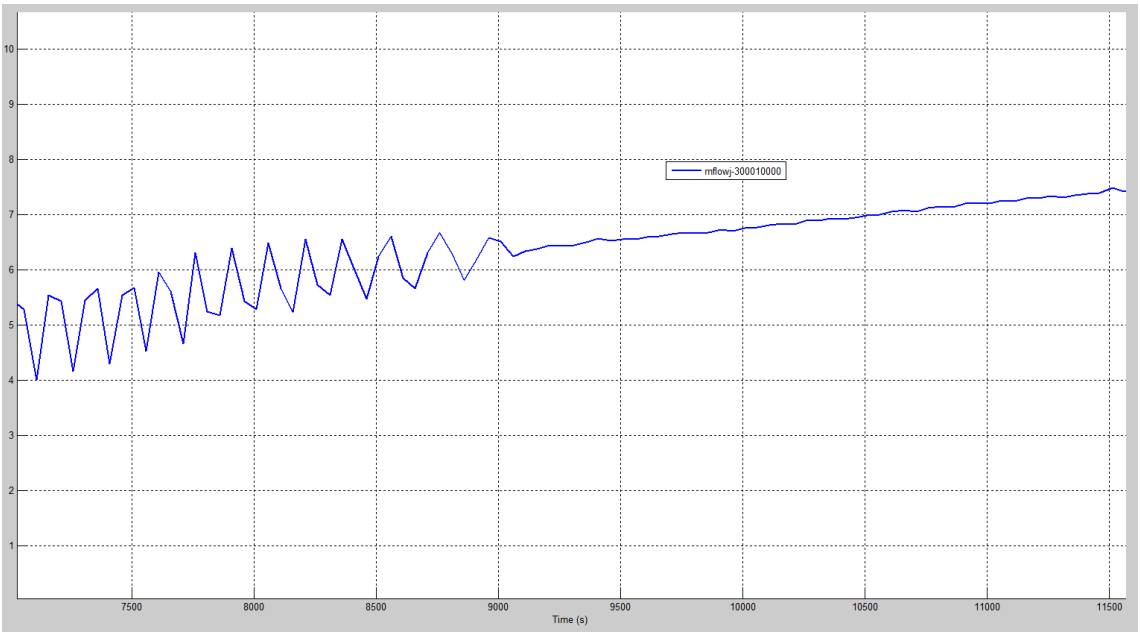

Fig. 60 – HERO-CIRCE transient, LBE mass flow rate at HERO LBE channel inlet: 7000-11500 seconds

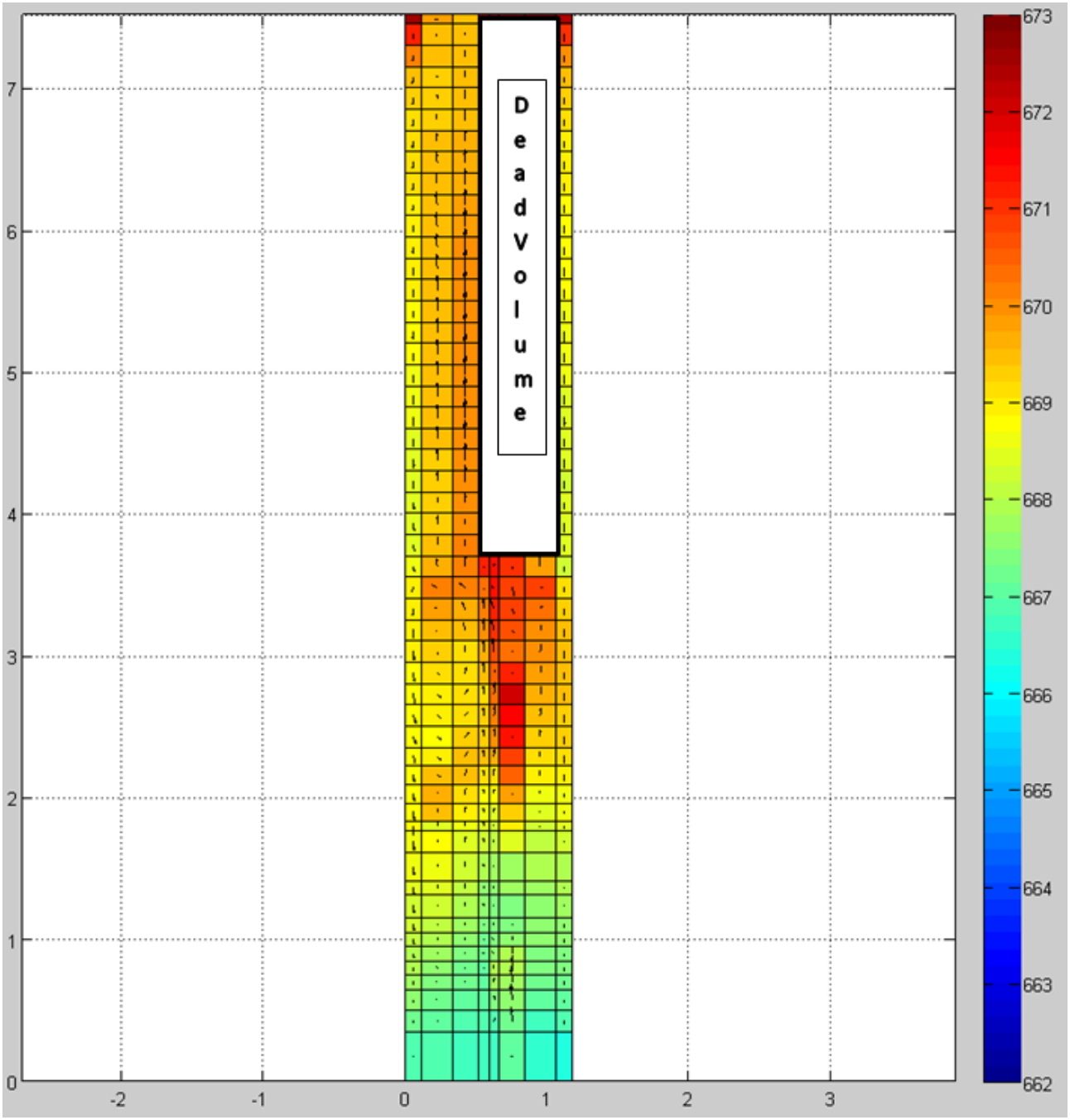

Fig. 61 – HERO-CIRCE transient, LBE the thermal stratification and the velocity in the pool: 6060 seconds

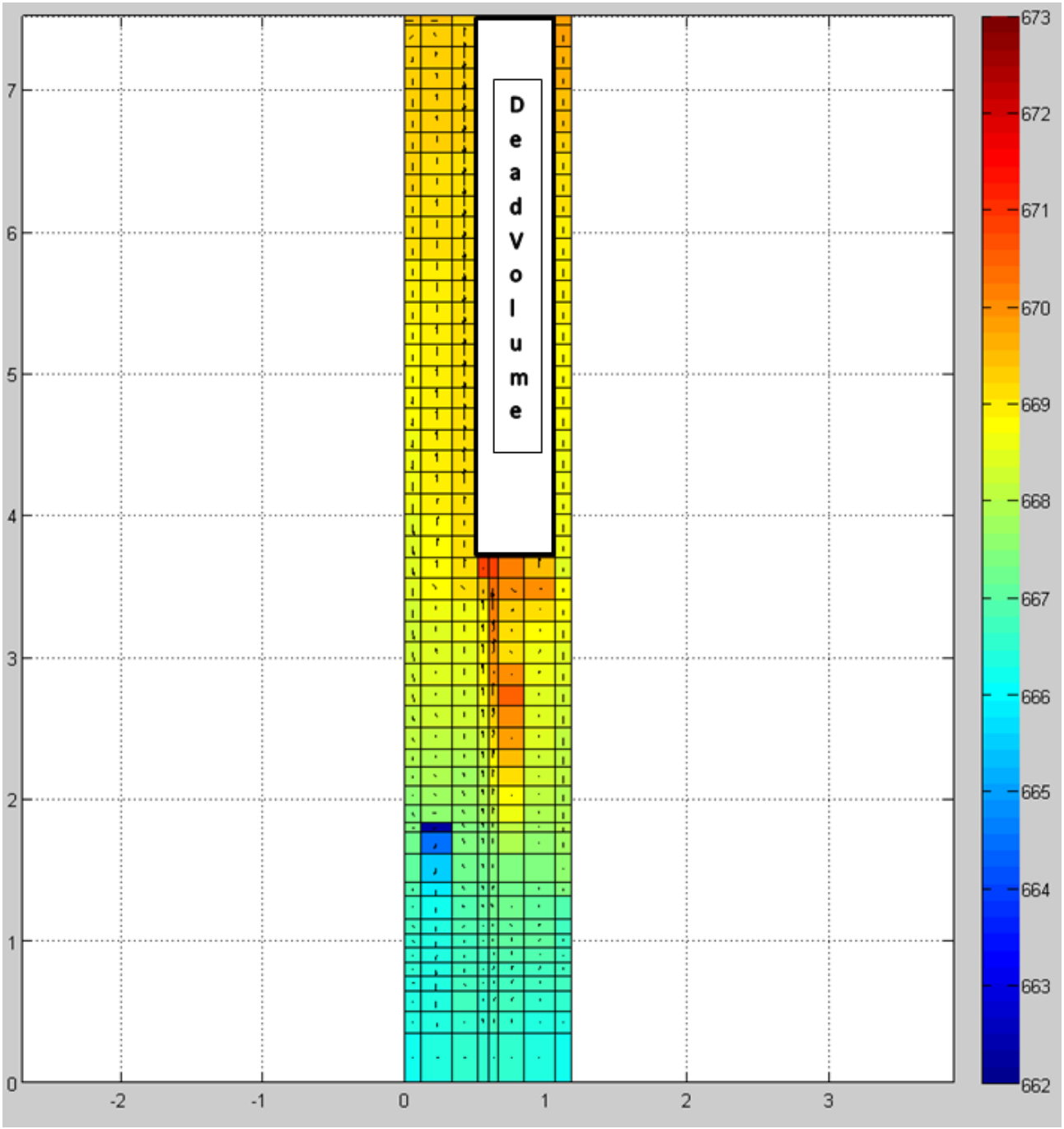

Fig. 62 – HERO-CIRCE transient, LBE the thermal stratification and the velocity in the pool: 6200 seconds

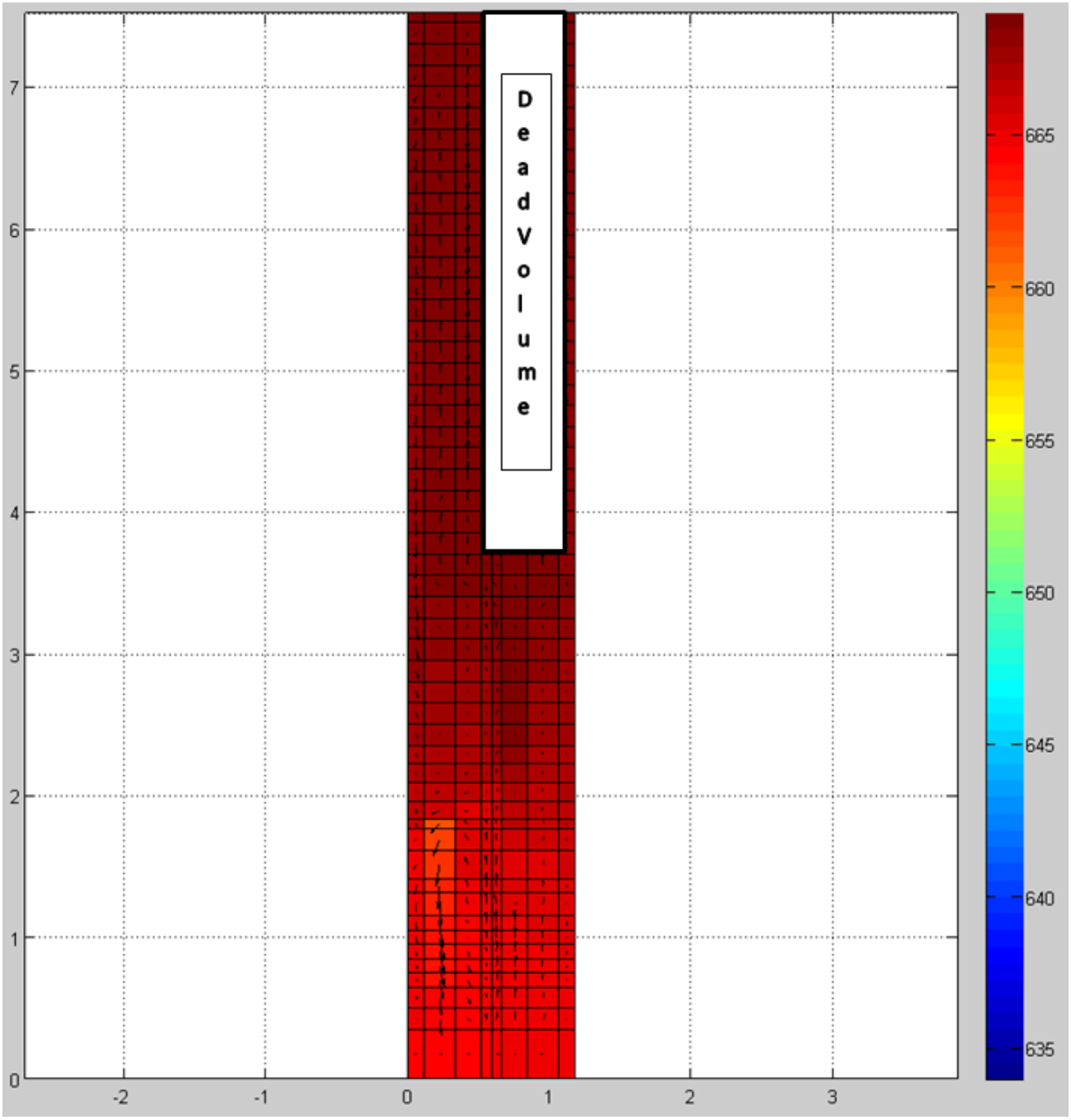

Fig. 63 – HERO-CIRCE transient, LBE the thermal stratification and the velocity in the pool: 6500 seconds

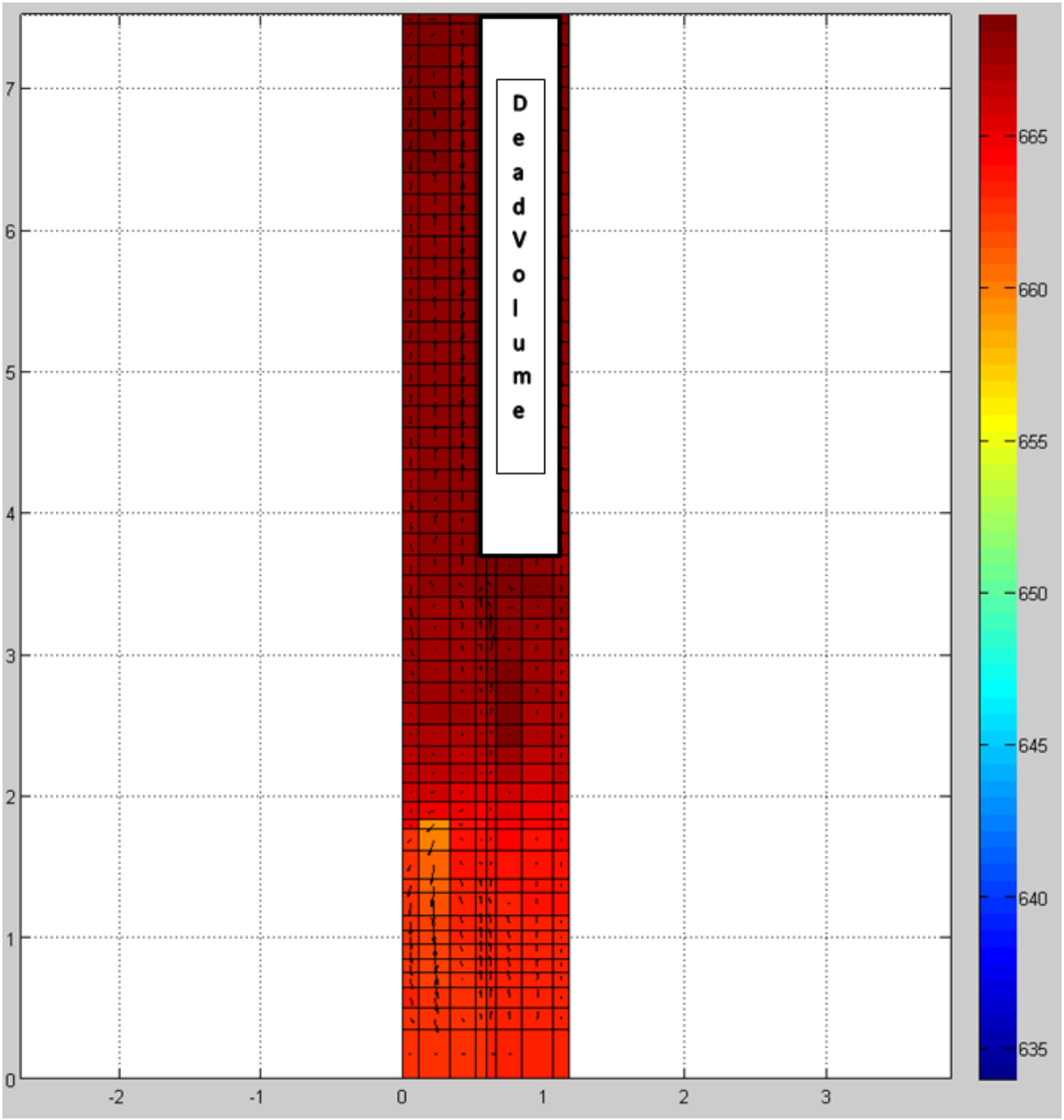

Fig. 64 – HERO-CIRCE transient, LBE the thermal stratification and the velocity in the pool: 6800 seconds

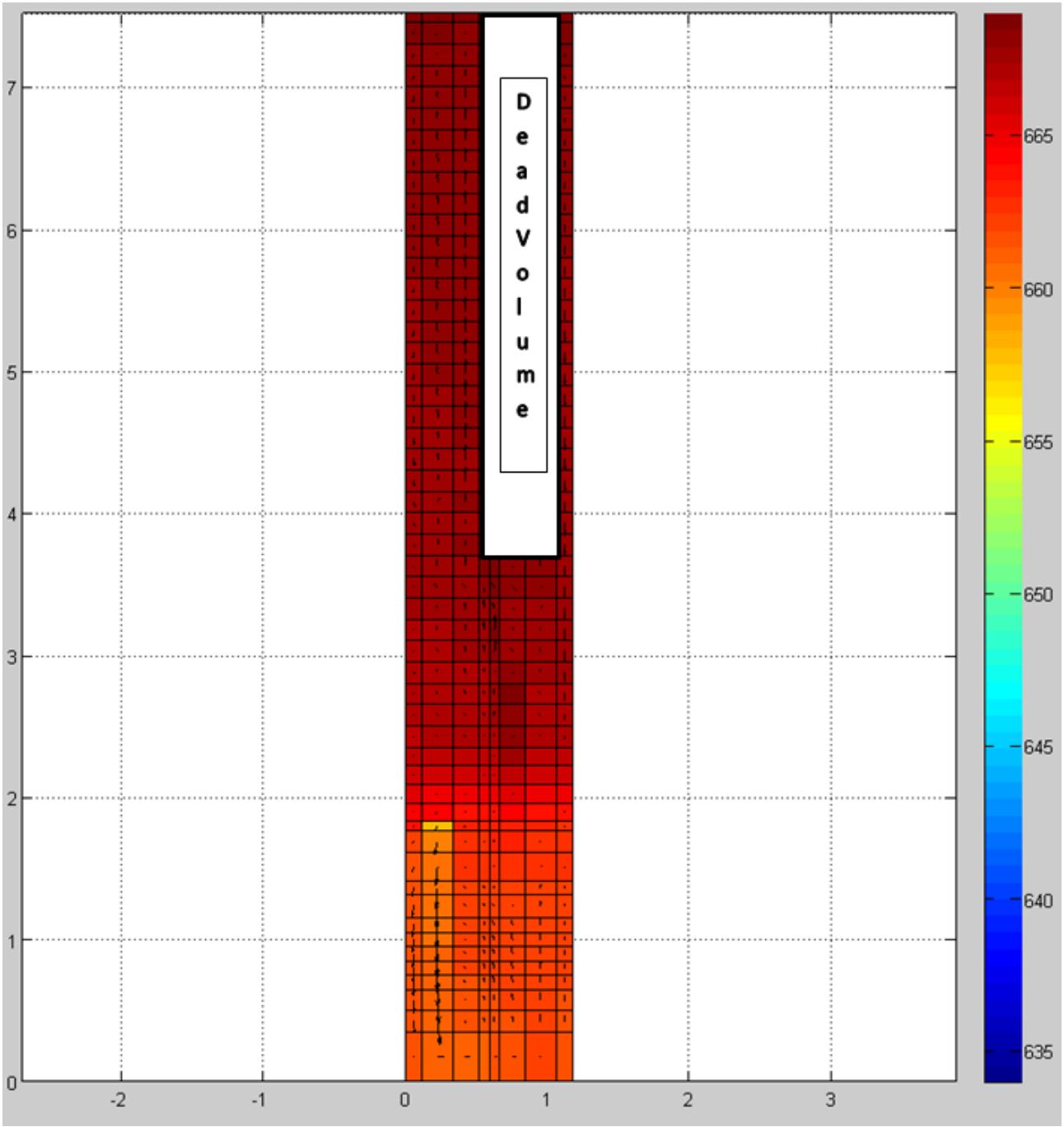

Fig. 65 – HERO-CIRCE transient, LBE the thermal stratification and the velocity in the pool: 7000 seconds

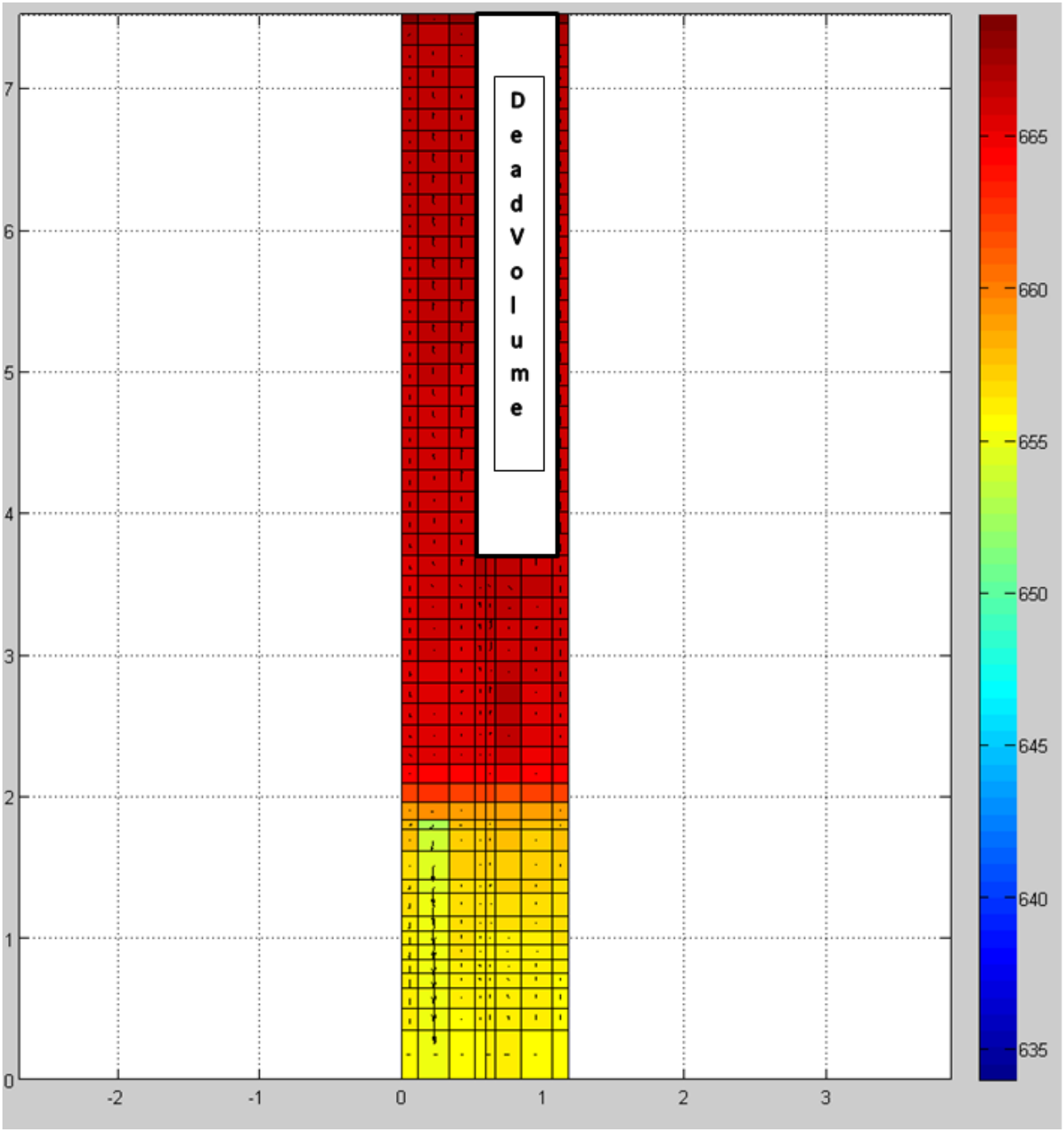

Fig. 66 – HERO-CIRCE transient, LBE the thermal stratification and the velocity in the pool: 8000 seconds

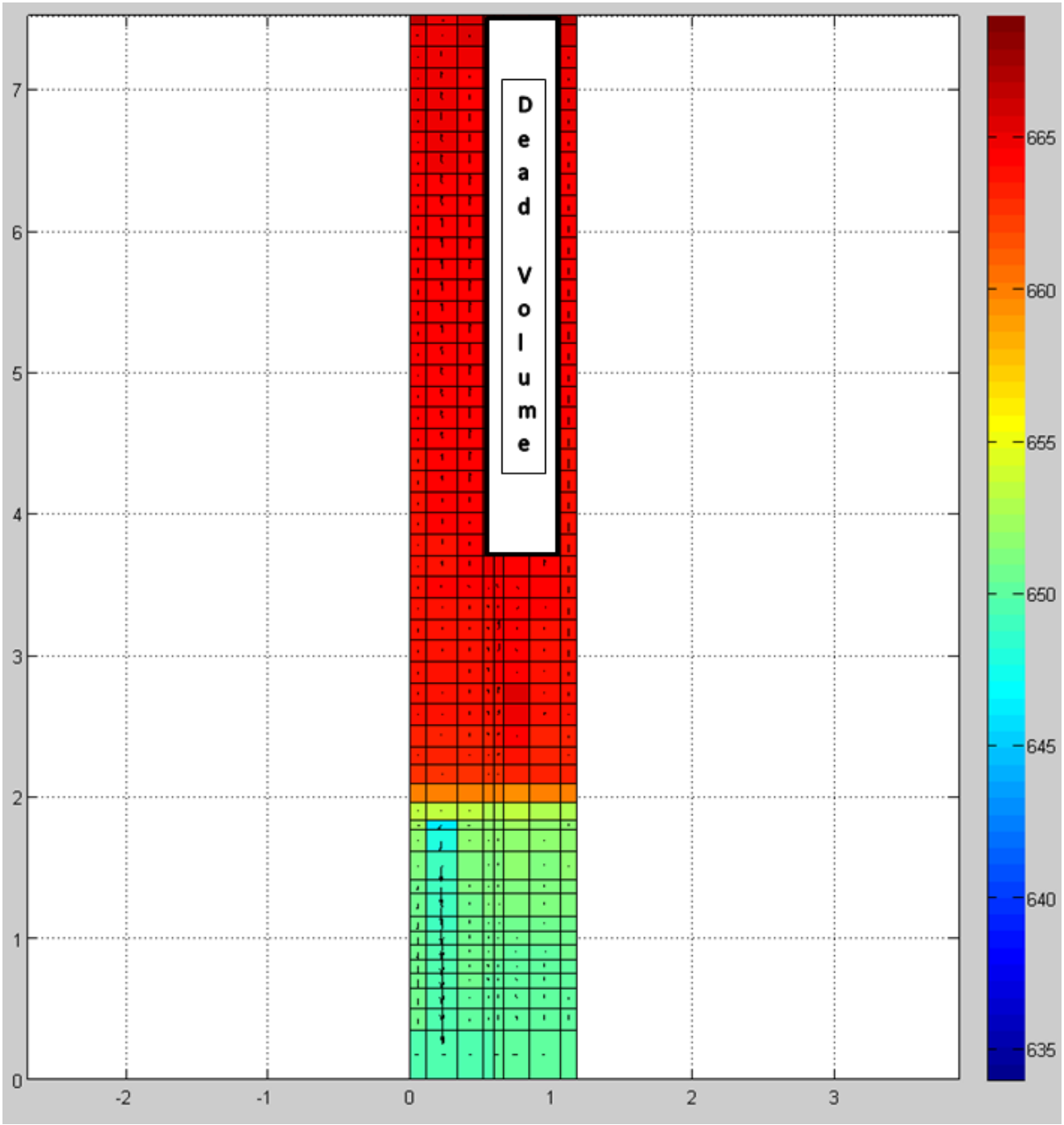

Fig. 67 – HERO-CIRCE transient, LBE the thermal stratification and the velocity in the pool: 9000 seconds

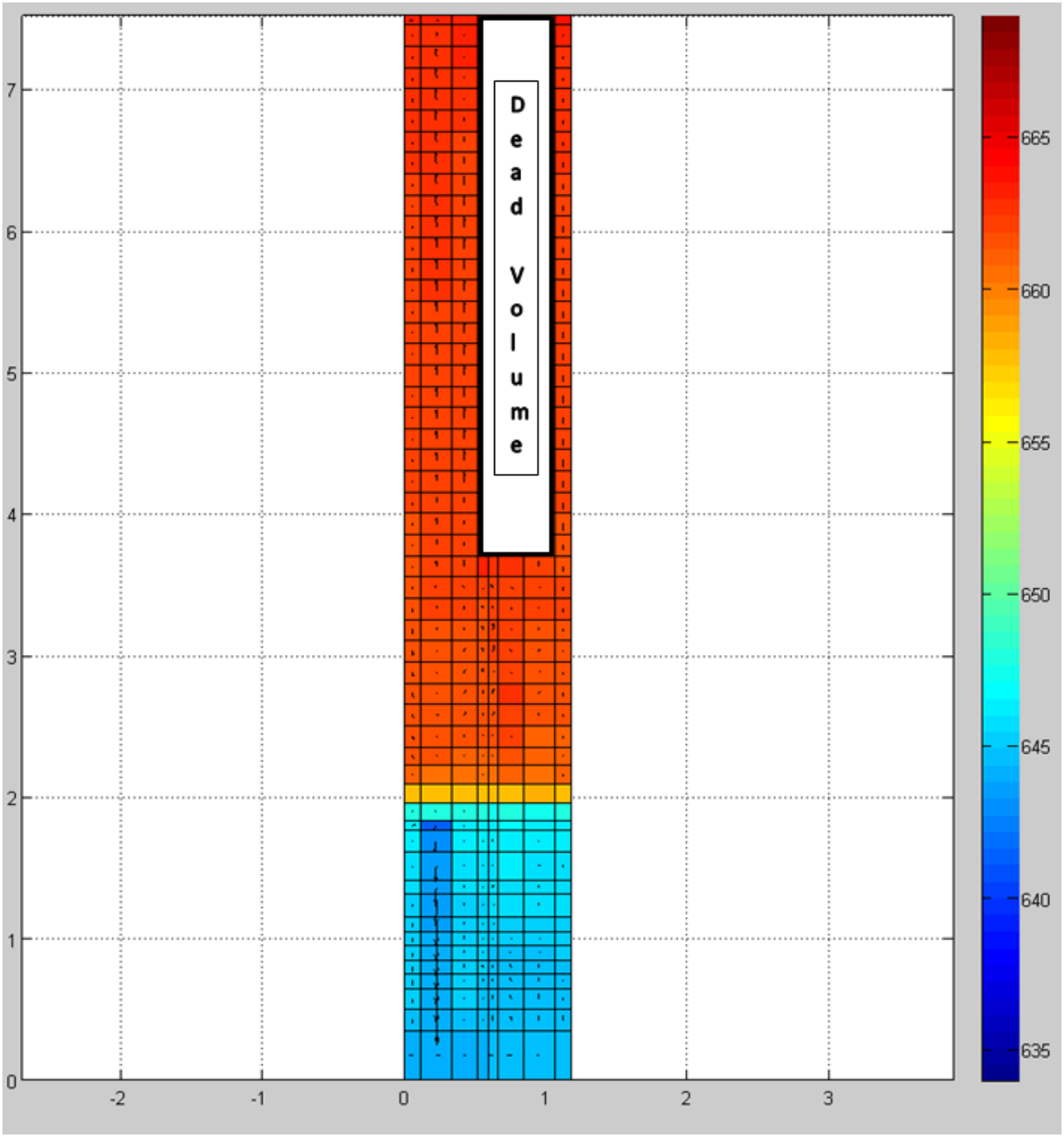

Fig. 68 – HERO-CIRCE transient, LBE the thermal stratification and the velocity in the pool: 10000 seconds

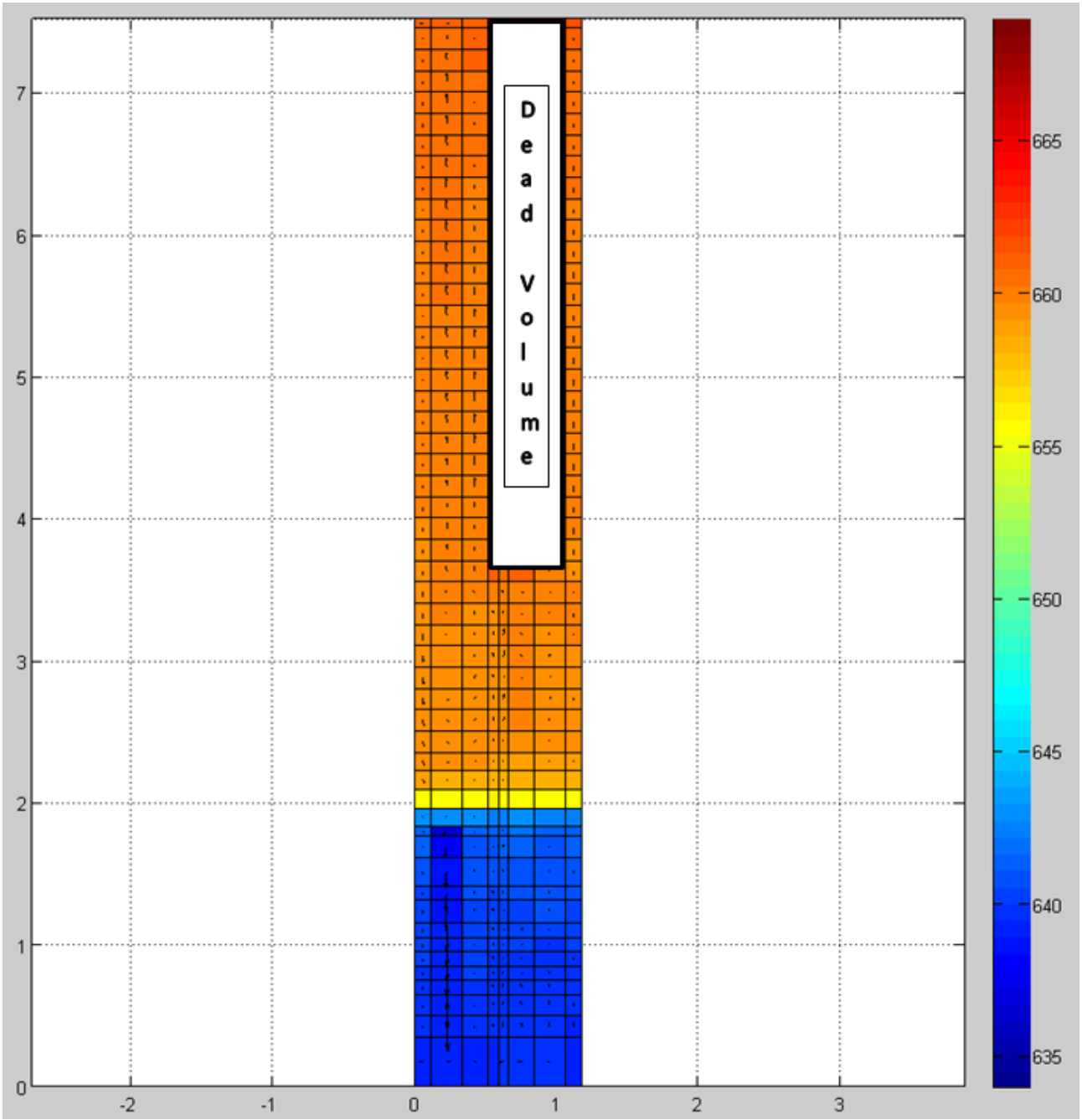

Fig. 69 – HERO-CIRCE transient, LBE the thermal stratification and the velocity in the pool: 11000 seconds

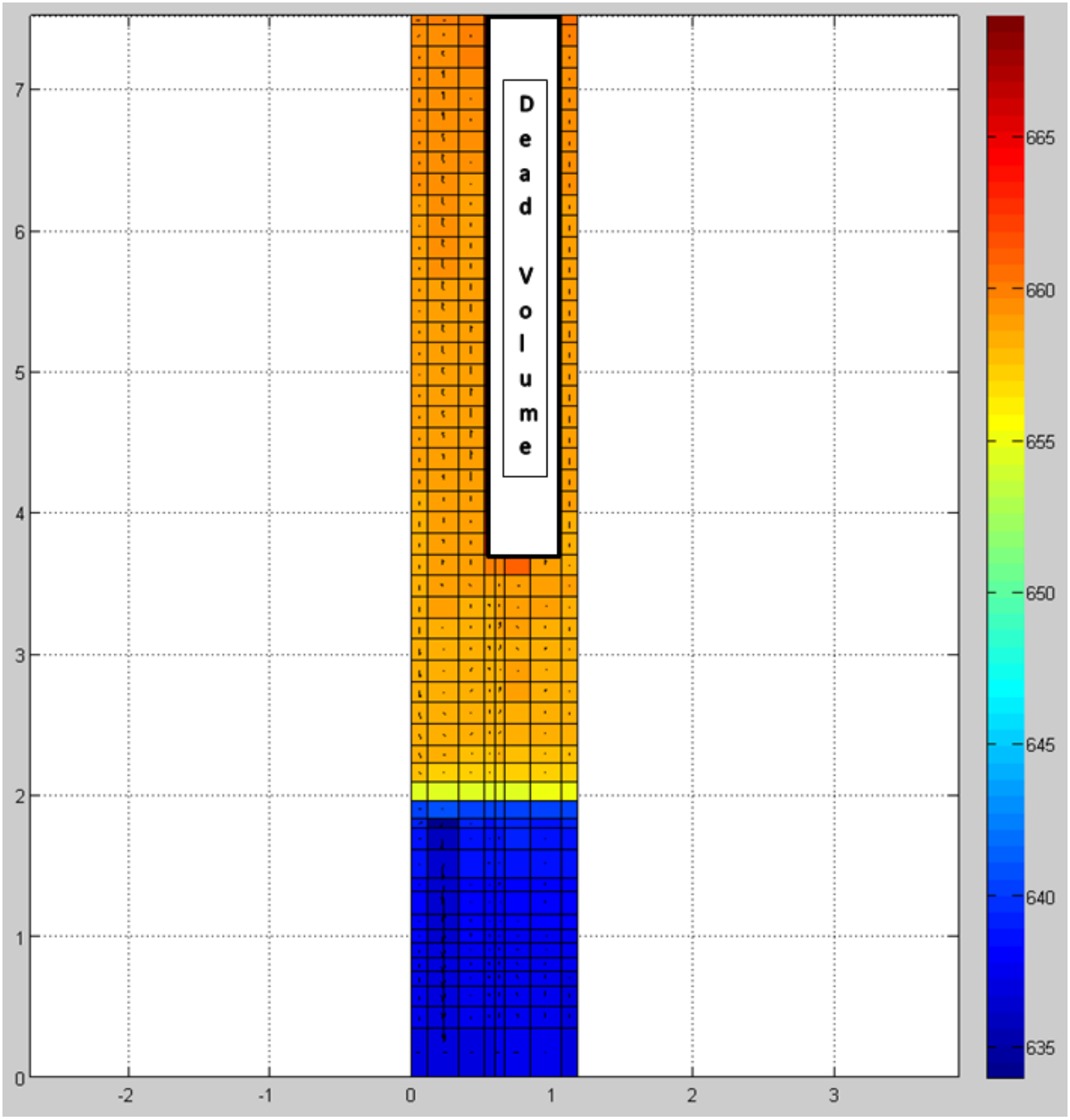

Fig. 70 – HERO-CIRCE transient, LBE the thermal stratification and the velocity in the pool: 11500 seconds

4.3 Sensitivity analysis

This paragraph shows a preliminary sensitivity analysis carried out on the results described above.

Fig. 71 shows how the thermal situation changes with different correlation of the convective coefficient. The previous simulations are performed with Ushakov correlation[8] and the following result is obtained with Todreas and Kazimi correlation[9]. At first the Fig. shows a more pronounced peak temperature at the inlet of the FPS during the first instants of the transient. After 6500 seconds from the begin of the transient, the FPS and HERO channel LBE inlet-outlet temperatures are slightly in lower than in the previous case.

The sensitivity analysis is also performed on the LBE properties used. The following time trends are obtained using the results of the article [10].

Fig. 72 and Fig. 73 highlight the results obtained for case 1 of steady state simulation.

Fig. 72 shows the evolutions of the LBE temperatures at FPS inlet (tempf 40020000), FPS outlet (tempf 40120000), HERO channel inlet (tempf 300010000) and HERO channel outlet (tempf 300400000) comparing the RELAP5-3D default thermophysical properties (red line) and the new properties[10]. The time trend highlights that the temperature gap at FPS and HERO channels are increased with new properties. In particular the ΔT between inlet and outlet section of FPS increase of 3 K and the ΔT between inlet and outlet section of HERO channels increase of 2 K. This differences are due to a smaller value of c_p obtained with new thermophysical properties.

Fig. 73 depicts the LBE mass flow rate at HERO channel inlet. The results show an increase of 0.4% to the value of LBE flow rate. Furthermore the new properties show a lower numerical instability at equal time step.

Fig. 74 and Fig. 75 describe the results obtained for transient simulation.

Fig. 74 highlights the evolution of temperature for 4500 seconds from the transient start up. The results are comparable and the discrepancy is reduced but the new properties show a lower numerical instability at equal time step. During the first instant of the transient, the temperatures at the inlet section of FPS highlight a similar peak.

Fig. 75 depicts the LBE mass flow rate at HERO channel inlets. this time trend highlights the same features shown in Fig. 73.

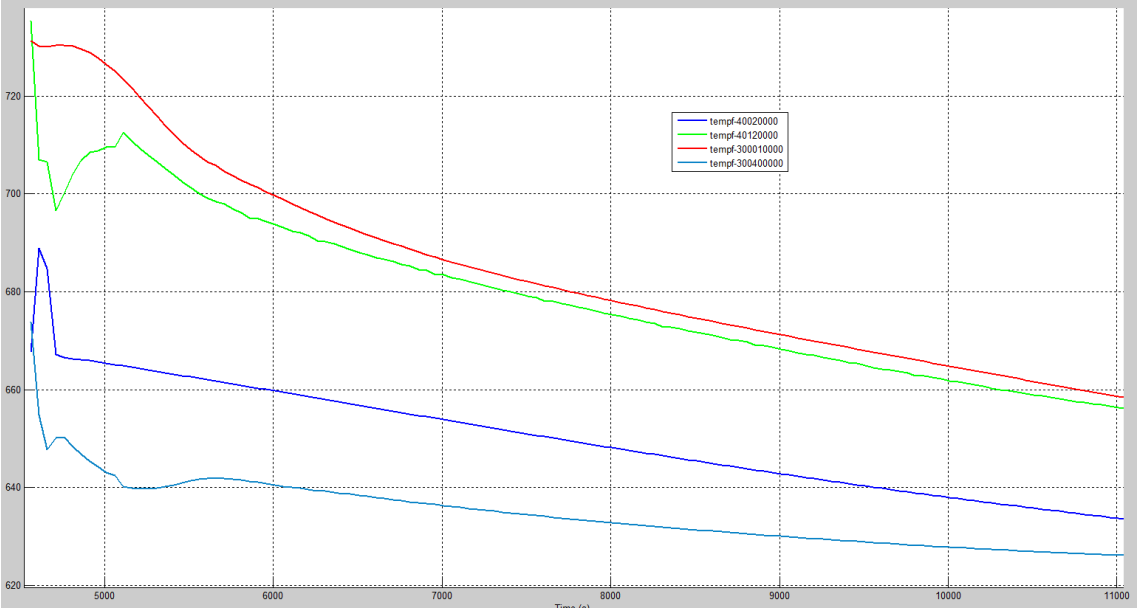

Fig. 71 – HERO-CIRCE transient, FPS and HERO channel LBE inlet-outlet temperatures. Todreas and Kazimi correlation

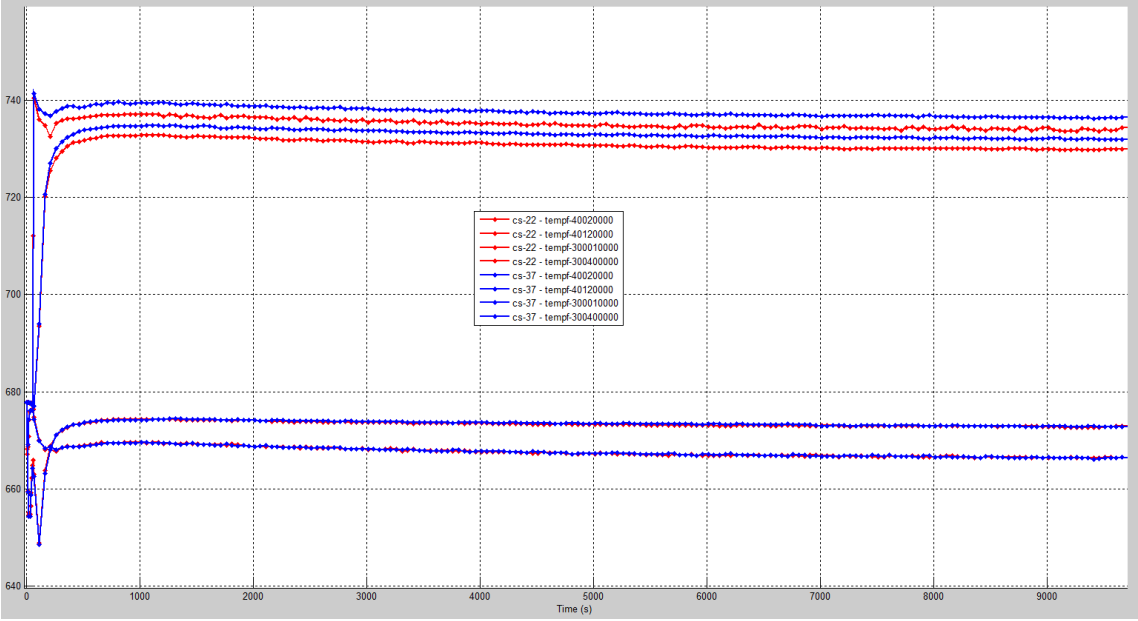

Fig. 72 – Case 1: HERO-CIRCE full power steady state preliminary simulations, LBE temperatures at FPS and HERO channels inlet/outlet; comparison between different properties

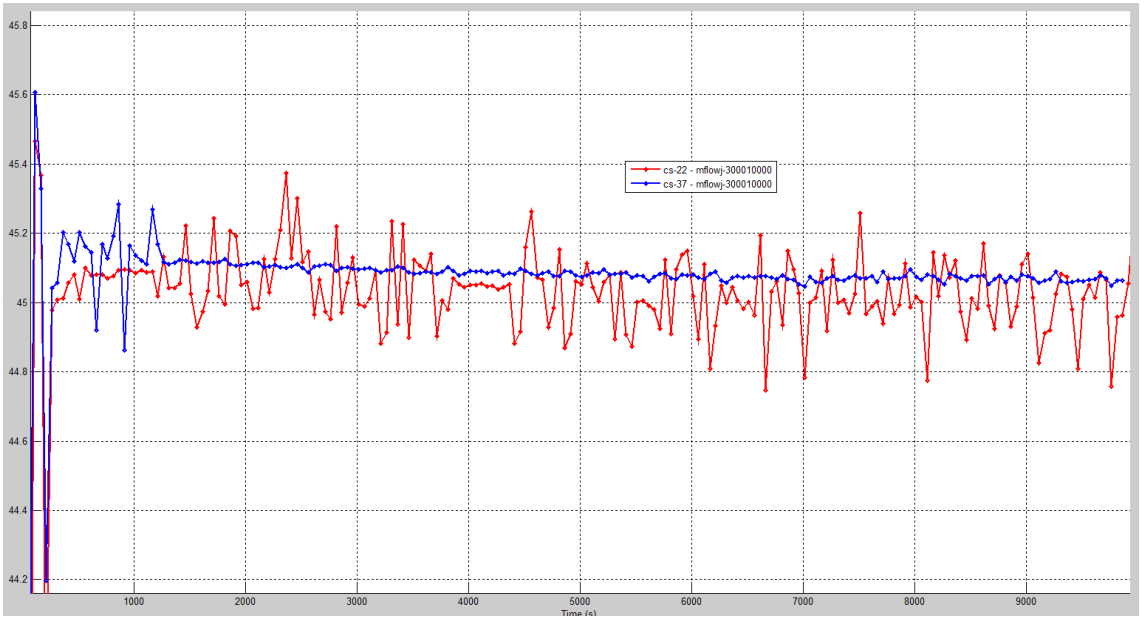

Fig. 73 – Case 1: HERO-CIRCE full power steady state preliminary simulations, LBE mass flow rate at HERO channel inlet; comparison between different properties

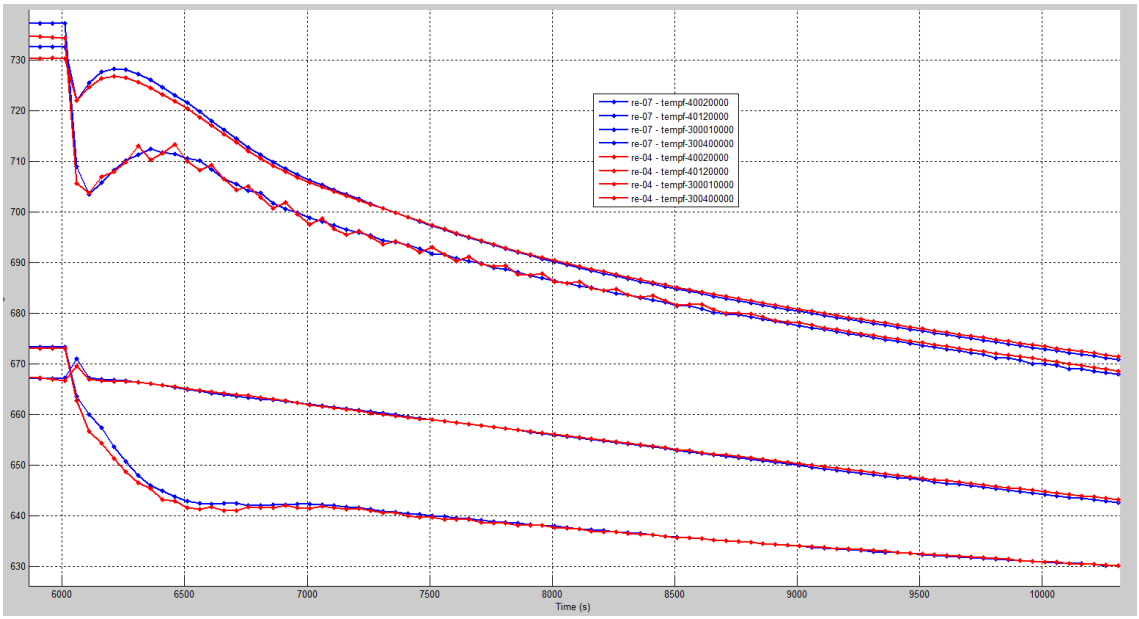

Fig. 74 – HERO-CIRCE transient, FPS and HERO channel LBE inlet-outlet temperatures; comparison between different properties

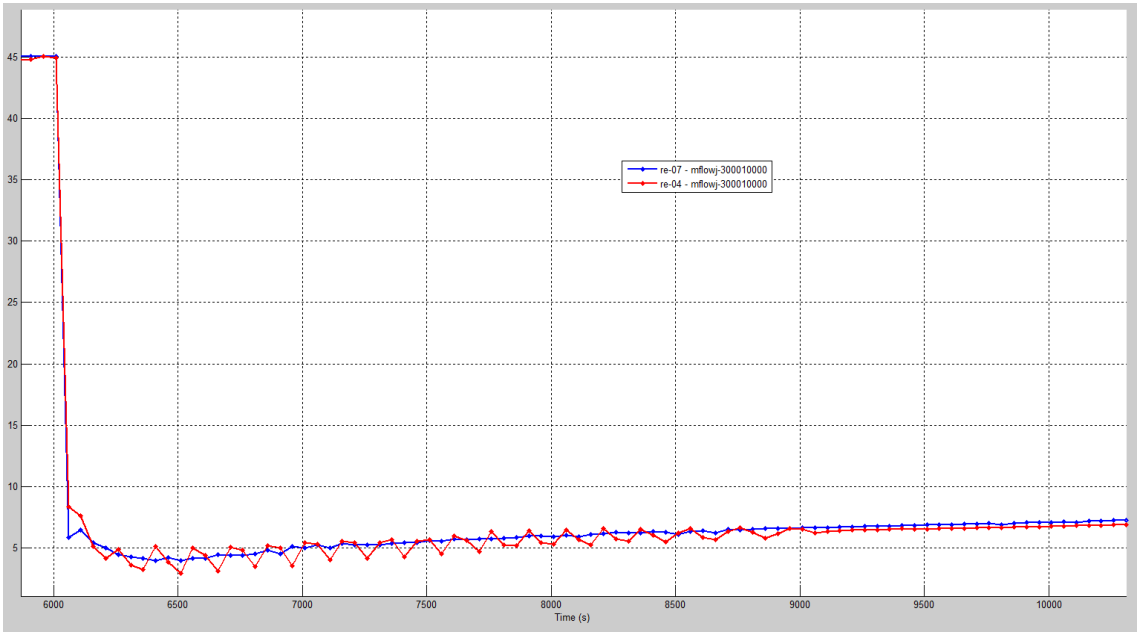

Fig. 75 – HERO-CIRCE transient, LBE mass flow rate at HERO LBE channel inlet; comparison between different properties

5 Modeling HERO-CIRCE by RELAP5/Mod3.3

RELAP5/Mod3.3 is a light water reactor transient analysis code developed by the U.S. Nuclear Regulatory Commission (NRC) for use in rulemaking, licensing audit calculations, evaluation of operator guidelines and as a basis for a nuclear plant analyzer. It is a highly generic code that, in addition to calculating the behavior of a reactor coolant system during a transient, can be used for simulation of a wide variety of hydraulic and thermal transients in both nuclear and non-nuclear systems involving mixtures of steam, water, non-condensable and solute [11][12][13]. In particular the version 5.3.3 has the capability to include the lead and LBE as coolant material.

5.1 Hydraulic model

The hydraulic nodalization of HERO-CIRCE can be divided into 11 macro-regions, Fig. 76 and Fig. 77.

- Region #1: it is kept as axial origin. It includes the feeding conduit, the FPS and it ends with the bifurcation that connects the heating zone to the LBE riser and the dead volume. It is connected to region #9 and region #2.
- Region #2: it models the LBE channel riser and it includes the Ar injection system. It is connected to region #1 and region #3.
- Region #3: models the separator that connect the LBE riser to the HERO LBE channel. It is connected to region #2, region #4 and region #5.
- Region #4: models the CIRCE gas cover. It is connected to region #3, region #5 and region #6.
- Region #5: models the HERO LBE channel. It is connected to region #3, region #4 and region #8.
- Region #6: models the CIRCE upper pool. It includes the DHR LBE channel, the HERO LBE dead zone, the upper-central pool. It consists of a connection to the CIRCE gas plenum and two levels at which parallel pipes or branches are provided to simulate the upper pool. It is connected to region #3, region #4 and region #7.
- Region #7: represents the CIRCE central pool. It consists of five levels at which parallel pipes or branches are provided to simulate the central pool. It is connected to the DHR LBE channel outlet and to the HERO LBE dead zone outlet. It is linked to region #6, and region #8.
- Region #8: represents the CIRCE lower pool. It consists of two levels at which parallel pipes or branches are provided to simulate the lower pool. It is connected to the HERO LBE channel outlet. It is linked to region #5, region #7 and region #9.
- Region #9: represents the CIRCE lower plenum. It consist of a branch at connected to region #8 and region #1.
- Region #10: simulates the HERO-SGBT steam/water side.
- Region #11: accounts for the DHR air side.

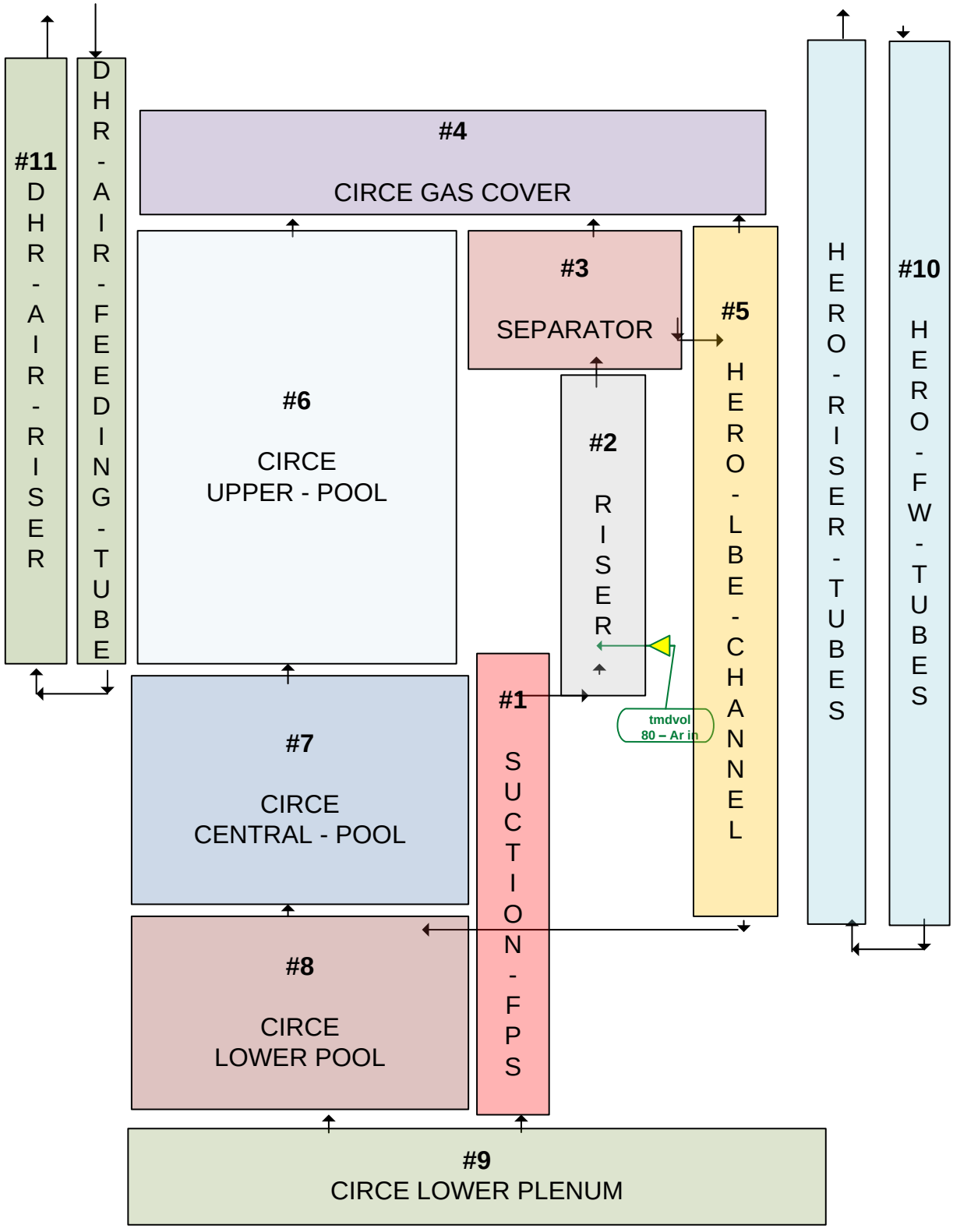

Fig. 76 – HERO-CIRCE RELAP5/Mod3.3 macro-regions.

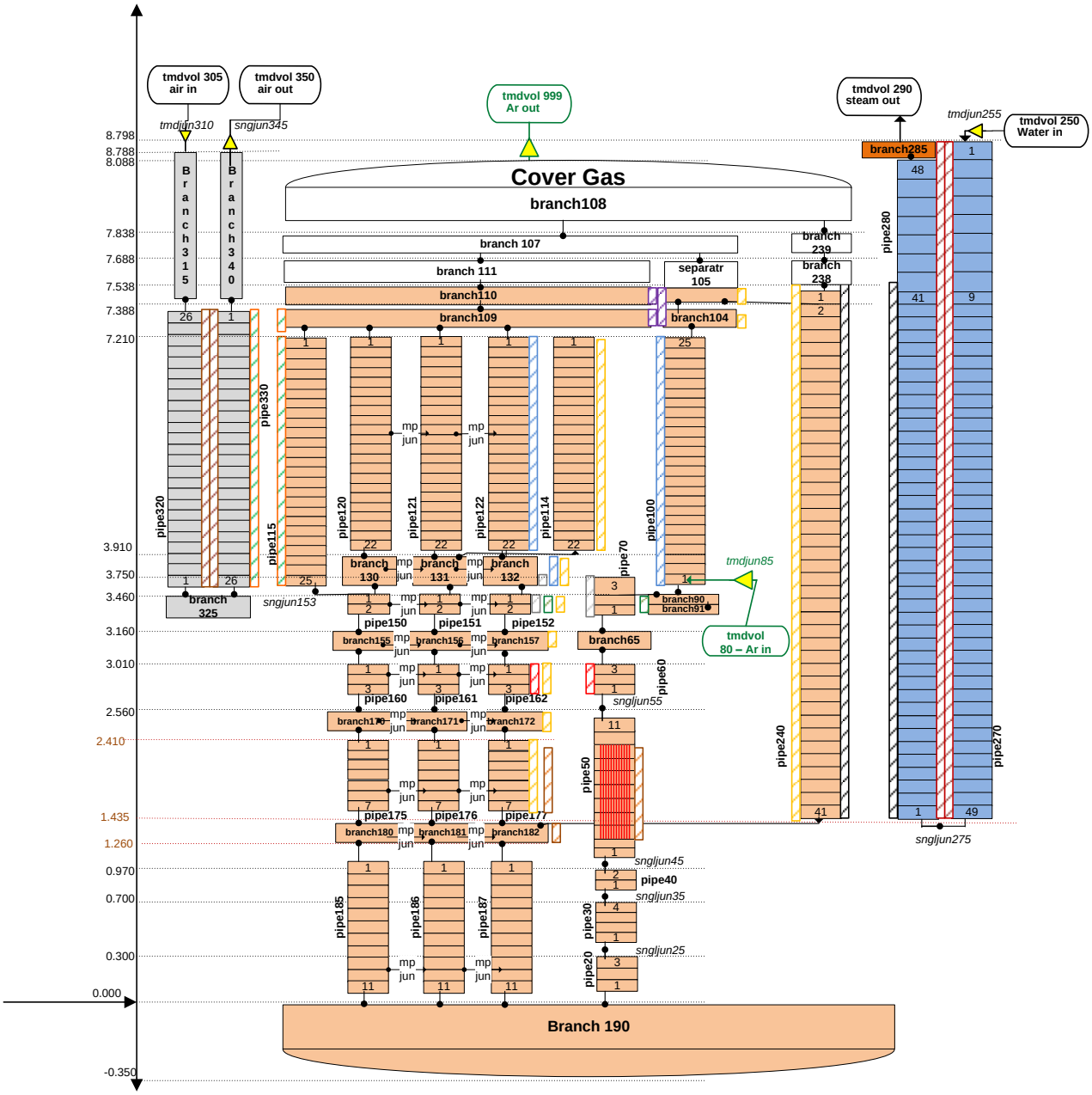

Fig. 77 – HERO-CIRCE RELAP5/Mod3.3 nodalization.

5.1.1 Region #1: suction and FPS

The region (Fig. 77) includes:

- Pipe 20 (0.3 m long, 3 nodes), which is the LBE feeding conduit initial part,
- The FPS lower plenum zone modeled by pipe 30 (0.4 m long, 4 nodes) and pipe 40 (0.27 m long, 2 nodes),
- The FPS pipe 50 (1.590 m long, 11 nodes, active length from node 3 to node 8) whose grids are modeled with concentrated pressure drop coefficient at the corresponding junctions,
- The FPS upper plenum pipe 60 (0.45 m long, 3 nodes),
- The connection among the heating zone and the bifurcation is modeled by branch 65 (0.15 m long, 2 junctions)

- The bifurcation that models the fitting volume between the LBE riser and the dead volume (which contains heating cable ends and instrumentation and is not fed by LBE) by pipe 70 (0.59 m long, 3 nodes).
- Appropriate single junctions to connect pipe components. In particular, sngjun 25 account for the pressure drop due to the Venturi flow meter.

5.1.2 Region #2: riser and Ar injection

The region consists of (Fig. 77):

- The Ar injection system which is represented by tmdvol 80 and tmdjun85 that injects Ar directly at the LBE riser inlet (pipe 100),
- The connection between the bifurcation (pipe 70) and the LBE riser inlet by Branch 90 and branch 91,
- The LBE riser pipe 100 (3.75 m long, 25 nodes).

5.1.3 Region #3: separator

It is constituted by branch 104 and separatr 105, Fig. 77. Branch 104 is connected to the LBE riser outlet and with the separatr 105. This last component has three connections. The first one is at its inlet with the LBE-Ar mixture coming from the LBE riser outlet. The second, is again at its inlet and connects the single phase LBE to the HERO channel (pipe 240) at the inlet of its second node. The last one is at its outlet and connects the single phase Ar to the gas CIRCE gas plenum (branch 107).

5.1.4 Region #4: CIRCE cover gas

It is constituted by branch 107 and branch 108. This last branch is connected to a tmdvol to fix the Ar pressure inside the gas plenum (Fig. 77).

5.1.5 Region #5: HERO LBE channel

The region includes (Fig. 77):

- Branch 238 and branch 239 that model the gas cover of the HERO LBE channel and connect it to the CIRCE cover.
- Pipe 240 represents the HERO LBE channel. It includes 41 nodes and 40 junctions. In order to account for the grids, four concentrated pressure drops coefficients have been implemented at the corresponding junctions.

5.1.6 Region #6: CIRCE upper pool

It consists of a connection to the CIRCE gas plenum and two levels at which the upper pool and its structures are modeled by parallel pipes or branches. In particular, it includes (Fig. 77):

- An upper part constituted by branch 111 and branch 110 that connects branch 109 to the CIRCE gas plenum. Branch 109 that connects the upper pool level-0 (four pipes: pipe 120, 121, 122, 115) to branch 110.
- The CIRCE pool level-0 is modeled by pipe 120, pipe 121 and pipe 122. Each pipe (3.3 m long) is constituted by 22 identical axial nodes. In order to represent open pool effects, they are connected each other's by 21 x 3 lateral junctions (120 to 121, 120 to 122 and 121 to 122).
- The CIRCE DHR channel (pipe 115) is connected at level-0 by branch 109. This pipe (3.75 m long) is constituted by 25 axial nodes (it ends in the region #7, level 0).
- The LBE dead zone (pipe 114) which is the annular zone below the separator between the HERO – SG and the descending shell). This zone is not connected to the upper part (branch 109) even if it starts at the elevation of level-0.

- The upper pool level-1 is constituted by three branches: 130, 131 and 132. They are connected respectively to pipes 120, 121, and 122 at their inlet and ends into pipes 150, 151 and 152 (which are described in the central pool region #8). These branch are connected each other's horizontally (130 to 131, 130 to 132 and 131 to 132). Branch 132 inlet is connected to pipe 114 outlet (LBE dead zone) in order to connect the dead zone to the pool at its bottom.

5.1.7 Region #7: CIRCE central pool

It consists of five levels at which the central pool and its structures are modeled by parallel pipes or branches. In particular, it includes (Fig. 77):

- The central pool level-0 is composed of 3 parallel pipes (pipe 150, 151 and 152). Each pipe is 0.3 m long, 2 nodes. These pipes are connected each other's horizontally (150 to 151, 150 to 152 and 151 to 152). Pipe 150 inlet is connected to the DHR LBE channel outlet (pipe 115) in order to provide connection between the central pool and the LBE that feed DHR channel.
- The central pool level-1 is composed of 3 parallel branches (branch 155, 165 and 157). Their inlets are connected respectively to pipes 150, 151 and 152. Their outlets are connected to three pipes that constitute level-2 (pipe 160, 161, 162). These branches are connected each other's horizontally (155 to 156, 155 to 157 and 156 to 157).
- The central pool level-2 is composed of 3 parallel pipes (pipe 160, 161 and 162). Each pipe is 0.45 m long, 3 nodes. These pipes are connected each other's horizontally (160 to 161, 160 to 162 and 161 to 162).
- The central pool level-3 is composed of 3 parallel branches (branch 170, 171 and 172). Their inlets are connected respectively to pipes 160, 161 and 162. Their outlets are connected to three pipes that constitute level-4 (pipe 175, 176, 177). These branches are connected each other's horizontally (170 to 171, 170 to 172 and 171to 172).
- The central pool level-4 is composed of 3 parallel pipes (pipe 175, 176 and 177). Each pipe is 0.975 m long, 7 nodes. These pipes are connected each other's horizontally (175 to 176, 175 to 177 and 176 to 177).

5.1.8 Region #8: CIRCE lower pool

It consists of two levels at which the lower pool and its structures are modeled by parallel pipes or branches. In particular, it includes (Fig. 77):

- The lower pool level-0 is composed of 3 parallel branches (branch 180, 181 and 182). Their inlets are connected respectively to pipes 175, 176 and 177 (region #7). Their outlets are connected to three pipes that constitute lower pool level-1 (pipe 185, 186, 187). These branches are connected each other's horizontally (180 to 181, 180 to 182 and 181 to 182). Branch 182 inlet is connected to the LBE channel (pipe 240, region #5) to connect the LBE that leaves the HERO SGBT to the CIRCE lower pool.
- The lower pool level-1 is composed of 3 parallel pipes (pipe 185, 186 and 187). Each pipe is 1.26 m long, 11 nodes. These pipes are connected each other's horizontally (185 to 186, 185 to 187 and 186 to 187).

5.1.9 Region #9: CIRCE lower plenum

It is constituted by branch 190, Fig. 77. Branch 190 inlet is connected to the lower pool at the outlets of pipes 185, 186 and 187 and is connected to the feeding conduit (pipe 20, region #1) inlet.

1.1.1 Region #10: HERO-SGBT steam/water side

The model concentrates 7 bayonet tubes into a single equivalent tube. It includes the feed-water inlet (tmdvol 250, tmdjun 255), the feed-descending tube (pipe 270, 49 nodes), the water/steam annular riser

(pipe 280, 48 nodes), the steam plenum (branch 285) and the steam outlet (tmdvol 290) (Fig. 77). Pipe 270 is connected to pipe 280 by a single junction (sngjun 275). The active length is located between node 1 and node 41 (pipe 280).

1.1.1 Region #11: DHR air side

It includes the air inlet (tmdvol 305, tmdjun 310), the inlet air plenum branch 315, the descending tube (pipe 320, 26 nodes), branch 325, the air annular riser (pipe 330, 26 nodes), the air outlet plenum (branch 340) and the air outlet (tmdvol 340). The active length embed all the pipe component length. The non-active length is modeled in branch components 310 / 340 (Fig. 77).

1.2 Heat structures model

Heat structures consists in six main zones (Fig. 77):

1. FPS zone includes an external heating source to provide the power to the LBE and models the heat exchange between the FPS and its upper structure, the fitting volume (bifurcation) and the surrounding pool.
2. The second zone simulates the heat exchange between the riser, the separator and their correspondent surrounding LBE channels located in the pool.
3. The third zone models the HERO SGBT tubes that separate the descending water from the water steam riser (insulated pipe AISI – vacuum – AISI).
4. The fourth zone accounts for the pipes that allow the heat exchange between LBE – water-steam (double pipe with intermediate powder under He pressurized atmosphere).
5. The fifth zone is the SGBT insulated shell (double wall with intermediate air gap).
6. The last zone model the DHR air – air side and the DHR air – LBE side.

6 Pre-Test Calculations

6.1 Identification of full power steady state conditions

6.1.1 Preliminary calculations

Several calculations were performed to identify the initial conditions required to achieve full power steady state.

RUN#1:

- Duration [s] 1000, FPS power [kW] 450, Pool initial temperature [°C] 400.0, Ar mass flow [kg/s] 0.0027455, Feed-water pressure [bar] 172, Feed-water inlet temperature [°C] 335.0, Feed-water mass flow [kg/s] 0.3307850,Heat losses are not considered

RUN#2:, RUN#3, RUN#4 and RUN#5

- As RUN#1 except
- Ar mass flow respectively: [kg/s] 0.0024709, [kg/s] 0.0021964, [kg/s] 0.0019218, [kg/s] 0.0020100

RUN#6:

- As RUN#1 except
- Feed-water mass flow [kg/s] 0.45054

RUN#7:

- As RUN#1 except
- Ar mass flow [kg/s] 0.0020100, pool initial temperature [°C] 412.0

RUN#8:

- As RUN#1 except
- Ar mass flow [kg/s] 0.0022030, pool initial temperature [°C] 412.0

RUN#99

- As RUN#8 except
- Duration [s] 6000

RUN#100

- As RUN#8 except
- Duration [s] 6000, component “Separatr 105” modeled as “branch 105” to check its influence on the LBE mass flow rate in the HERO channel, Ar mass flow rate [kg/s] 0.002410 (increased in order to reach a LBE flow of 44.7 kg/s)

Simulations at 1000s:The main results are reported in Fig. 78 (FPS temperature drop) Fig. 79 (LBE-HERO temperature drop) Fig. 80 (LBE HERO mass flow rate) Fig. 81 (SGBT HERO maximum steam temperature) and Tab. 14 (summary). RUN#7 and 8 fit the operational parameters identified in Tab. 13. The trend of the main variables result stable up-to 1000s. RUN#1 to RUN#6 highlight a slight increase of the temperature at FPS inlet that still remains up-to 1000 s. This is due to the initialization of the temperature in the pool (it was slight lower than the HERO LBE channel outlet temperature).

Simulations at 6000s:The main results are depicted in Fig. 82, Fig. 83 and summarized in Tab. 15. The simulations are based on RUN#8 and confirm the achievement of steady state conditions up to 6000s. The main outcome of this set of analysis is the introduction of the branch component to model the LBE that feed the HERO channel.

Description	Unit	Steam line	Helium line	LBE side
Fluid	--	Water - steam	Helium	LBE
Circulation mechanism	--	Axial pump + accumulator	Storage tank for leakage refilling	Gas enhanced
Main components	--	7 bayonet tubes, steam chamber	Helium chamber	SGBT unit shell
Bundle type and P/D	-	Triangular	--	Shell
Removed power	kW	450	--	--
Operating inlet temperature	°C	335	--	480
Operating mass flow	kg/s	0.330785	stagnant	44.573529
Design pressure	bar	180	5.0	As CIRCE
Operating pressure	bar	172	4.5	Hydraulic head
Hydraulic head in design condition	bar	0.7	--	--
Hydraulic head in test condition	bar	0.7	--	--
Test pressure	bar	180	--	--
Design temperature	°C	432	432	As CIRCE
Volume	m^3	0.0083	0.0054	--
Empty weight	kg	135	--	--
Code	--	EN13445	--	--
Welding joint efficiency	--	1	--	--
Notified body	--	TUV0948	--	--
Welding specification	--	WKF/3479/1	--	--
Serial number	--	13173	--	--
CE - PED	--	III Category	B1+F Module	--

Tab. 13 – HERO-CIRCE SGBT unit, main data.

			RUN #							
Description			1	2	3	4	5	6	7	8
Initial conditions	I1	Duration [s]	1000	1000	1000	1000	1000	1000	1000	1000
	I2	FPS power [kW]	450	450	450	450	450	450	450	450
	I3	Pool initial T. [°C]	400.0	400.0	400.0	400.0	400.0	400	412	412
	I4	Ar mass flow [kg/s]	0.0027455	0.0024709	0.0021964	0.0019218	0.0020100	0.0027455	0.0020100	0.0022030
	I5	Feed-water pressure [bar]	172	172	172	172	172	172	172	172
	I6	Feed-water inlet T. [°C]	335.0	335.0	335.0	335.0	335.0	335.0	335.0	335.0
	I7	Feed-water mass flow [kg/s]	0.3307850	0.3307850	0.330785	0.330785	0.330785	0.45054	0.330785	0.330785
Results	R1	FPS inlet T. [°C]	399.1	398.8	398.4	397.9	398.1	397.8	406.9	407.2
	R2	FPS outlet T. [°C]	465.4	467.1	469.4	472.1	471.2	464.0	479.6	477.8
	R3	LBE – HERO inlet T. [°C]	459.5	461.3	463.2	465.6	464.8	458.0	474.1	472.5
	R4	LBE – HERO outlet T. [°C]	402.1	402.0	401.6	401.1	401.2	399.2	406.7	407.2
	R5	LBE mass flow HERO inlet [kg/s]	47.117	45.647	43.950	42.081	42.693	47.136	42.996	44.295
	R6	Steam max outlet temp T. [°C]	384.1	383.9	384.6	385.5	385.2	358.6	394.3	393.9
Trend	R00	Stable	R6	R6	R6	R6	R6	R6	From R1 to R6	From R1 to R6
	R0+	Increasing trend	From R1 to R5	From R1 to R5	From R1 to R5	From R1 to R5	From R1 to R5			
	R0-	Decreasing trend						From R1 to R5		

Tab. 14 – HERO-CIRCE summary of the full power steady state simulations at 1000s.

			RUN #	
Description			99-separatr105	100-branch105
Initial conditions	I1	Duration [s]	6000	6000
	I2	FPS power [kW]	450	450
	I3	Pool initial T. [°C]	412.0	412.0
	I4	Ar mass flow [kg/s]	0.0022030	0.002403
	I5	Feed-water pressure [bar]	172	172
	I6	Feed-water inlet T. [°C]	335.0	335.0
	I7	Feed-water mass flow [kg/s]	0.3307850	0.3307850
Results	R1	FPS inlet T. [°C]	408.7	408.9
	R2	FPS outlet T. [°C]	479.4	478.5
	R3	LBE – HERO inlet T. [°C]	475.2	474.3
	R4	LBE – HERO outlet T. [°C]	408.9	409.1
	R5	LBE mass flow HERO inlet [kg/s]	44.373	44.800
	R6	Steam max outlet temp T. [°C]	395.3	395.1
	R7	Lower pool avg T. [°C]	408.8	409.0
	R8	Central pool avg T. [°C]	411.4	415.0

Tab. 15 – HERO-CIRCE summary of the full power steady state simulations at 6000s.

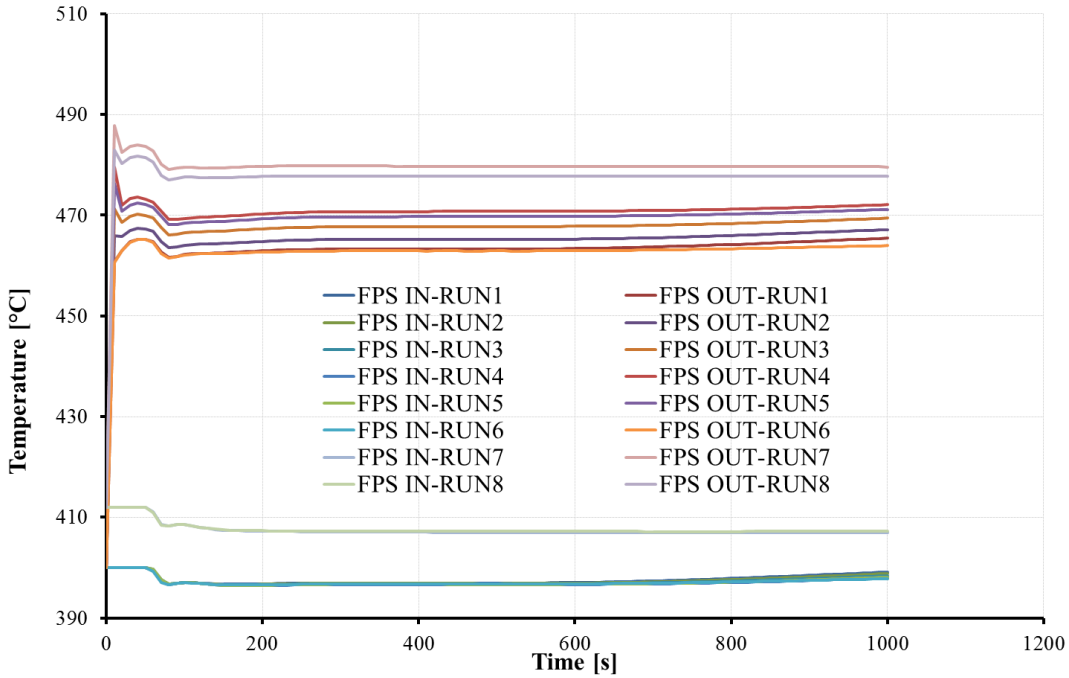

Fig. 78 – HERO-CIRCE full power steady state preliminary simulations, LBE temperatures at FPS channel inlet/outlet.

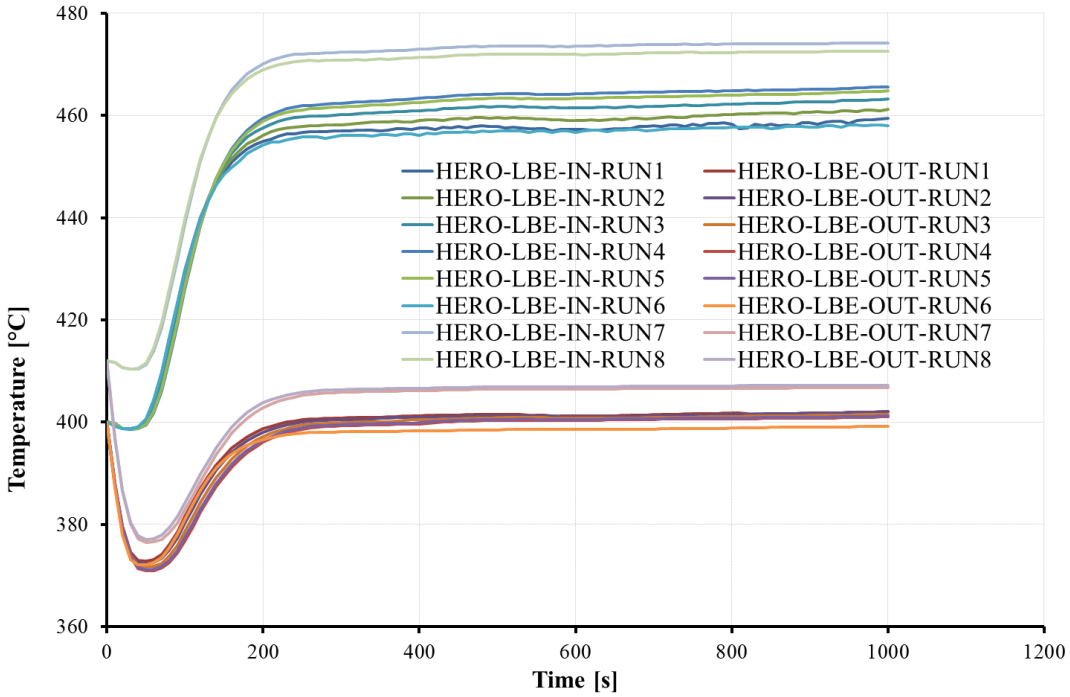

Fig. 79 – HERO-CIRCE full power steady state preliminary simulations, LBE temperatures at HERO channel inlet/outlet.

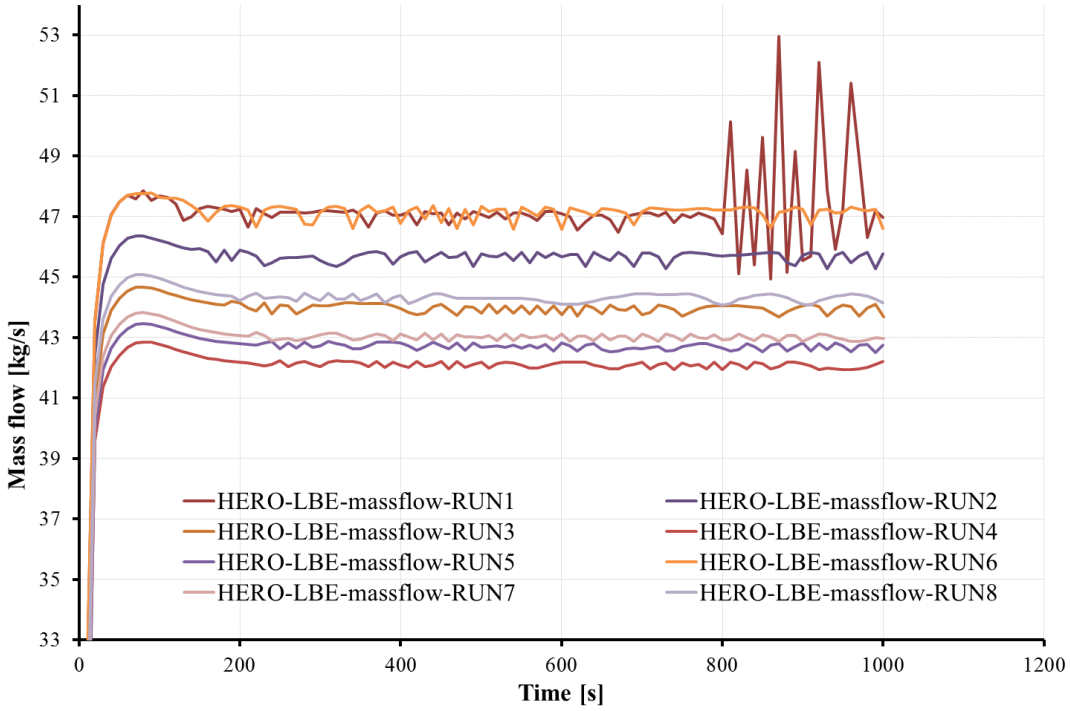

Fig. 80 – HERO-CIRCE full power steady state preliminary simulations, LBE mass flow rate at at HERO channel inlet.

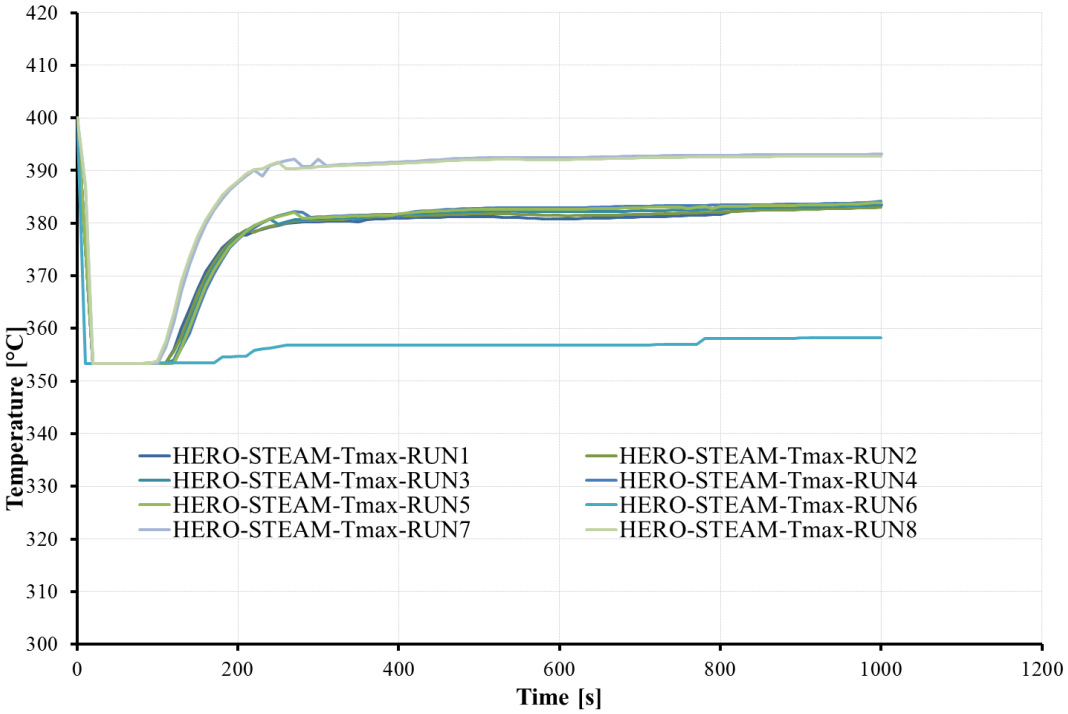

Fig. 81 – HERO-CIRCE full power steady state preliminary simulations, HERO SGBT maximum steam temperature.

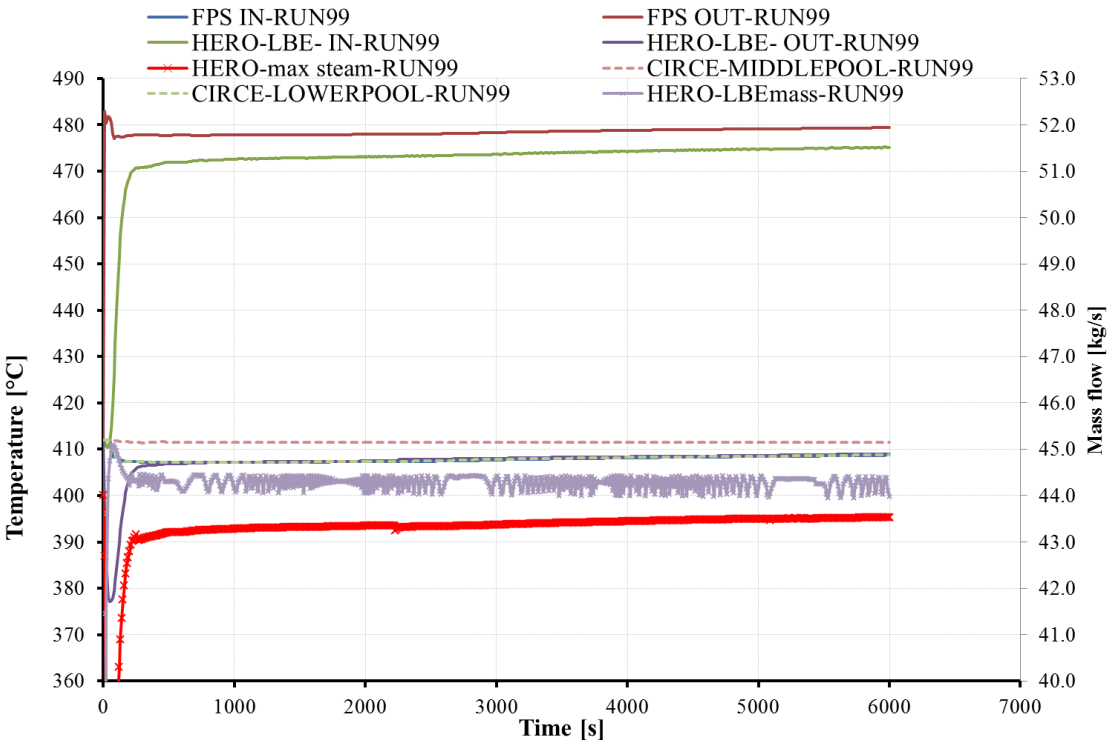

Fig. 82 – HERO-CIRCE full power steady state simulations, HERO SGBT RUN#99.

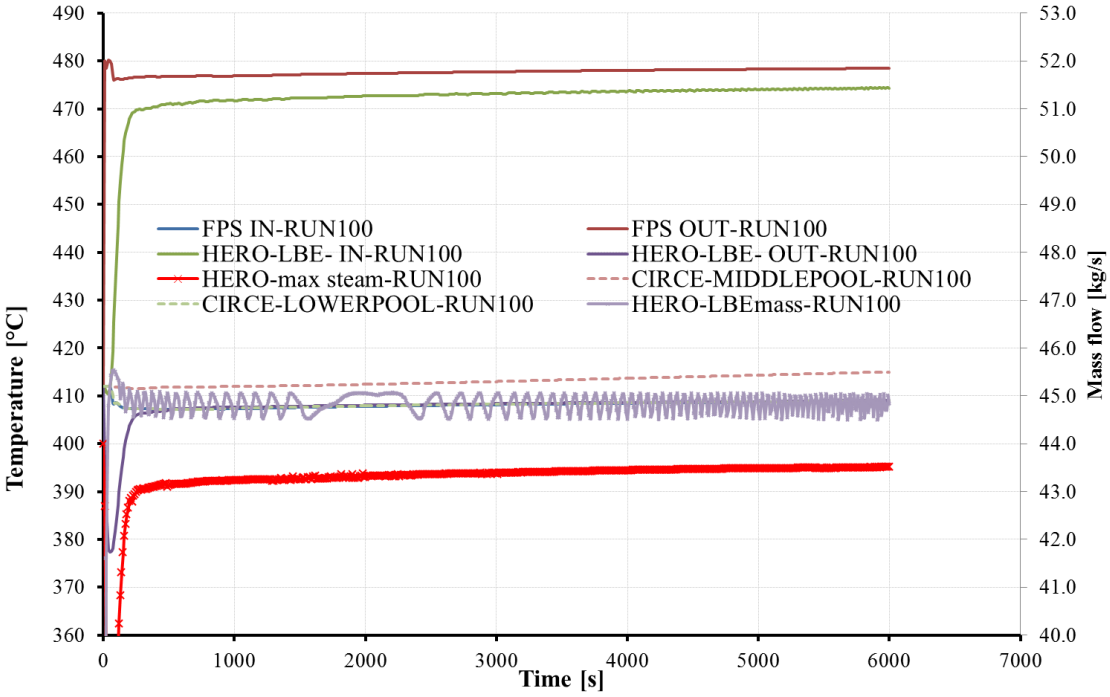

Fig. 83 – HERO-CIRCE full power steady state simulations, HERO SGBT RUN#100.

6.1.2 Steady state operation at full power

This set of simulations is based on section 6.1.1. Their main aim is to provide steady state simulations at full power considering two different cases and the heat losses effects. The following cases are analyzed:

- Case1: Fixed LBE mass flow rate at HERO inlet (44.7 kg/s), heat losses equal to 45 kW (conservatively).
- Case 2: Fixed LBE temperature drop across the FPS (80 °C), heat losses equal to 45 kW (conservatively).

The main results are summarized in Tab. 16.

Fig. 84 highlights the evolutions of the LBE temperatures at FPS inlet (tempf 05001), FPS outlet (tempf 05011), HERO channel inlet (tempf 10401) and HERO channel outlet (tempf 24041) comparing case 1 to case 2.

Fig. 85 reports the trend of temperatures at the HERO secondary water/steam inlet (tempf 27001) and outlet (tempg 28501) versus the HERO LBE channel temperature drop. Bothe Case 1 and Case 2 are expected to generate steam at about 374-376°C.

Fig. 86 depicts the LBE temperature trend in the CIRCE pool. According to the nomenclature indicated in Fig. 77, tempf 190 represents the LBE temperature in the CIRCE lower plenum. Tempf 187 and tempf 182 represent the zone above the lower plenum. Tempf 177, tempf 172 tempf 152 and tempf 132 highlight the middle part of the pool. Tempf 122, 109 and are representative of the upper pool up to the LBE level zone which is represented by tempf 111. The temperature trend in the pool is included between 400 -405 °C except the upper part below the LBE level zone that reaches 438 – 460 °C and the LBE fee level zone that decreases down to 200 – 230 °C. This is reflected in a temperature decrease in the gas plenum (Fig. 87). Should be mentioned that the heat losses at the LBE free level and at the gas

plenum have been modeled as for the rest of the pool with a constant heat transfer coefficient since they are not known. It is therefore expected that did not fully represent the effective situation.

Fig. 88 depicts the LBE mass flow rate at HERO channel outlet (mflowj 24040). Case 1 is fixed as boundary condition at 47.4 kg/s whereas case 2 reaches a LBE flow rate of about 38.2 kg/s.

The last Fig. (Fig. 89) reports the generated / removed powers at FPS (cntrlvar 60), HERO channel (cntrlvar 124), heat losses form CIRCE walls (cntrlvar 115, imposed at 45kW), and transferred by the HERO and DHR wraps to the pool (respectively cntrlvar 094 and 132)

Description			**RUN # Case1**	**RUN # Case2**
Initial conditions	I1	Duration [s]	1000	1000
	I2	FPS power [kW]	450	450
	I3	Pool initial T. [°C]	404.6	404.6
	I4	Ar mass flow [kg/s]	0.002410	0.001510
	I5	Feed-water pressure [bar]	172	172
	I6	Feed-water inlet T. [°C]	335.0	335.0
	I7	Feed-water mass flow [kg/s]	0.3307850	0.330785
	I8	Heat losses [kW]	45	45
Results	R1	FPS inlet T. [°C]	399.7	398.7
	R2	FPS outlet T. [°C]	469.6	480.4
	R3	LBE – HERO inlet T. [°C]	465.5	474.8
	R4	LBE – HERO outlet T. [°C]	402.7	400.6
	R5	LBE mass flow HERO inlet [kg/s]	44.7	38.2
	R6	Steam max temp T. [°C]	385.8	388.2
	R7	Steam outlet temp T. [°C]	374.2	376.5
	R8	Power removed by HERO [kW]	403.3	408.4
	R9	Power removed by heat losses [kW]	45.0	45.0
	R10	LBE temperature central pool [°C]	400 – 405	400 – 405
	R11	LBE temperature upper pool [°C]	438.3	462.0
	R12	Gas plenum temperature [°C]	310.4	453.0

Tab. 16 – HERO-CIRCE summary of the full power steady state simulations.

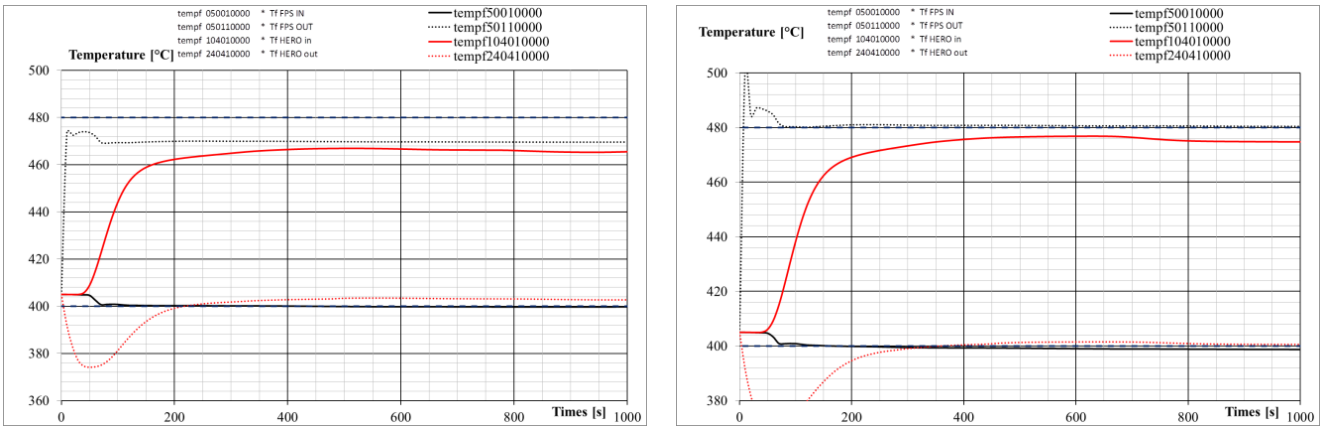

RUN # Case1 RUN # Case2

Fig. 84 – HERO-CIRCE FPS and HERO channel LBE inlet-outlet temperatures.

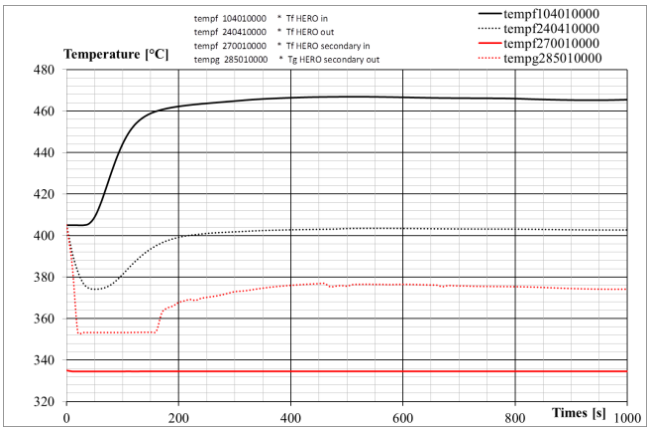

RUN # Case1

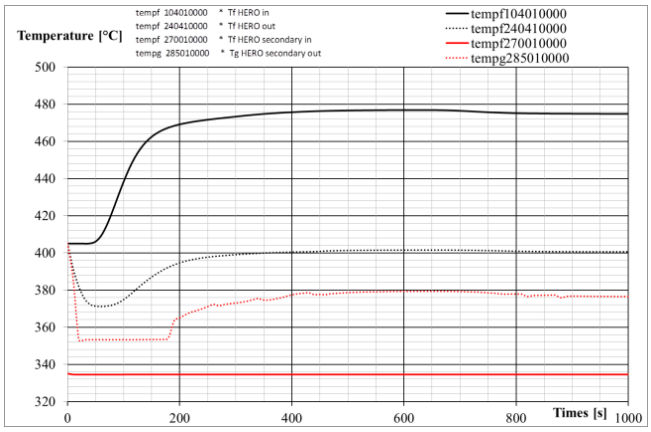

RUN # Case2

Fig. 85 – HERO-CIRCE HERO channel LBE inlet-outlet and water/steam inlet outlet temperatures.

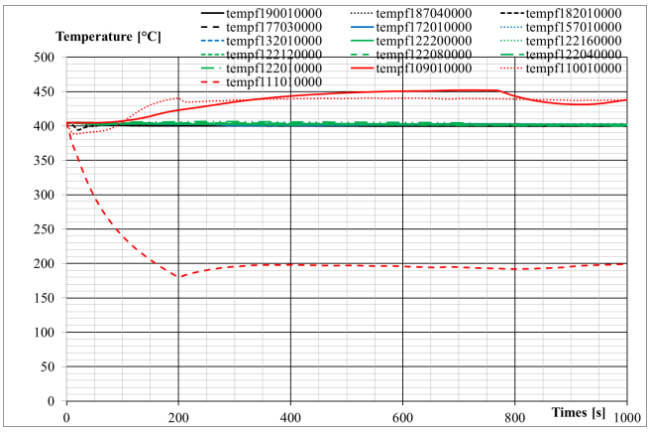

RUN # Case1

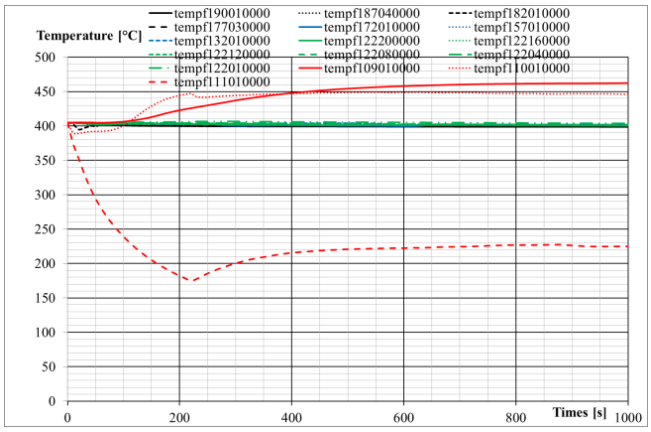

RUN # Case2

Fig. 86 – HERO-CIRCE LBE temperatures in the pool.

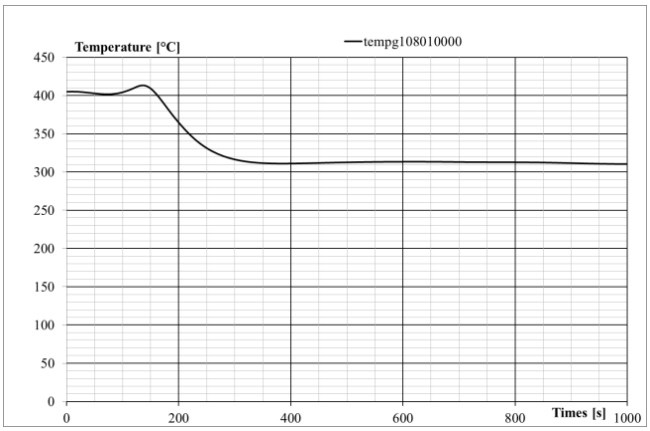

RUN # Case1

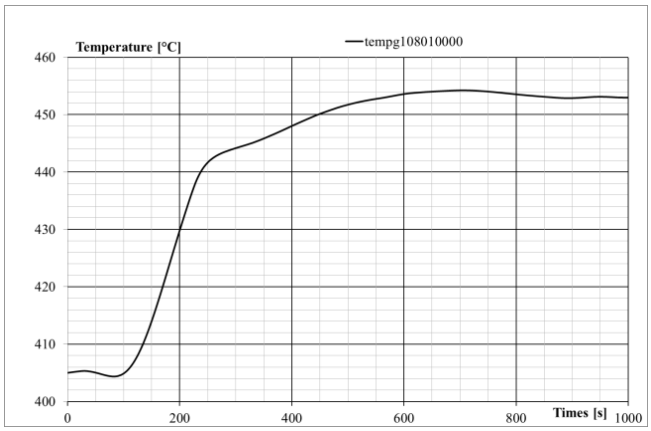

RUN # Case2

Fig. 87 – HERO-CIRCE Ar temperature in the gas plenum.

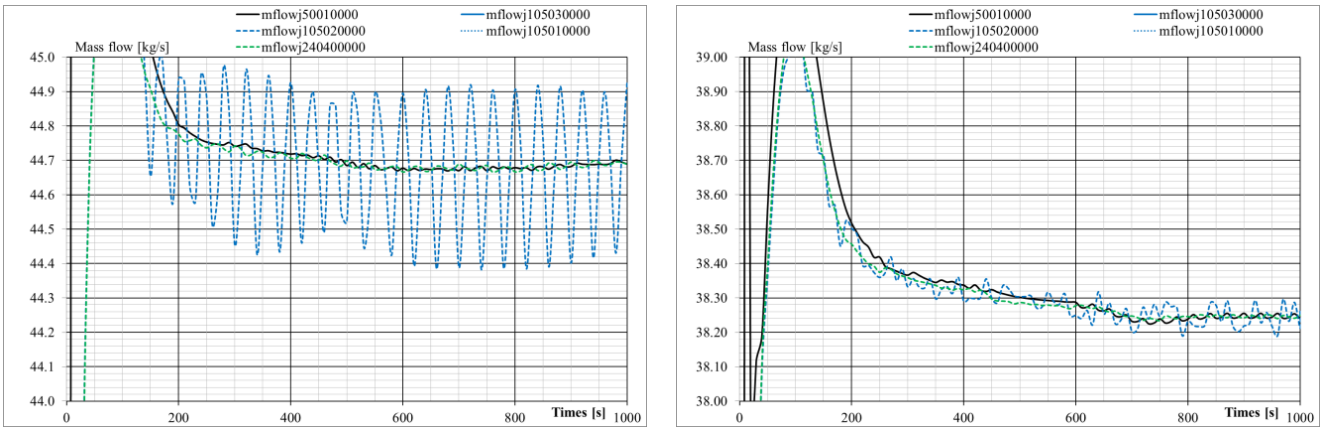

RUN # Case1 RUN # Case2

Fig. 88 – HERO-CIRCE LBE mass flow rate.

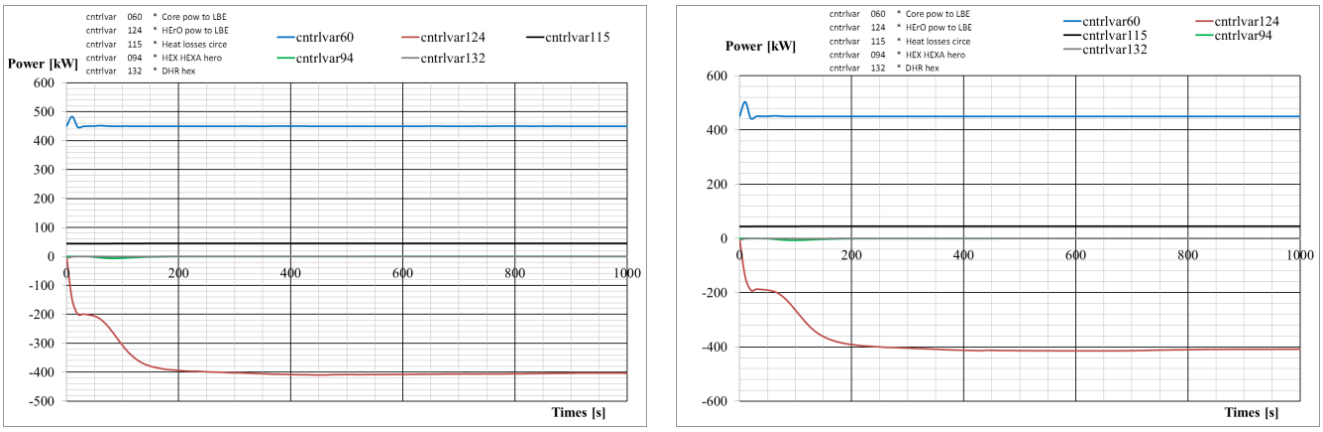

RUN # Case1 RUN # Case2

Fig. 89 – HERO-CIRCE removed powers.

6.2 Transient analysis

6.2.1 Test description

The starting point for transient test is considered case 2 (Tab. 16). The test basically consists in a protected loss of feed-water plus loss of LBE pump: the FPS power decrease down to 7% (representative of decay heat), loss of feed-water and loss of Ar injection will occur followed by the activation of the air cooled DHR.

The FPS power decreases in 900s according to Fig. 90. The compensated FPS power accounts for the decay heat power and the heat losses from CIRCE (that are assumed 20 kW during the transient). The Ar injection decreases linearly in 10 seconds from 0.001510 kg/s to zero, the feed-water falls in from 0.330785000 to zero linearly in 5 seconds while the DHR is activated after 50 seconds (air flow rate 0.225 kg/s), Tab. 18.

Time [s]	Power shutdown curve [kW]	Compensated FPS power [kW]	Heat losses [kW]
0	450	450	45
1000	450	450	45
1001	96.99	116.99	20
1002	83.482	103.482	20
1003.5	71.073	91.073	20
1005	62.513	82.513	20
1007.5	52.932	72.932	20
1010	46.728	66.728	20
1015	38.639	58.639	20
1022.5	31.571	51.571	20
1030	27.173	47.173	20
1040	23.01	43.01	20
1050	19.948	39.948	20
1060	17.749	37.749	20
1090	13.979	33.979	20
1120	11.937	31.937	20
1180	9.738	29.738	20
1240	8.717	28.717	20
1300	8.168	28.168	20
1360	7.618	27.618	20
1420	7.225	27.225	20
1480	6.99	26.99	20
1540	6.754	26.754	20
1600	6.518	26.518	20
1660	6.283	26.283	20
1720	6.047	26.047	20
1780	5.969	25.969	20
1840	5.733	25.733	20
1900	5.576	25.576	20

Tab. 17 – HERO-CIRCE transient, FPS power.

Time [s]	Power [kW]	Feed-water flow [kg/s]	Ar mass flow [kg/s]	Air mass flow [kg/s]
0	450	0.330785000	0.001510	0
1000	450	0.330785000	0.001510	0
1005	82.513	0	0.000755	0
1010	66.728	0	0	0
1050	39.948	0	0	0.225
1900	25.576	0	0	0.225
1e6	25.576	0	0	0.225

Tab. 18 – HERO-CIRCE transient, sequence of main events.

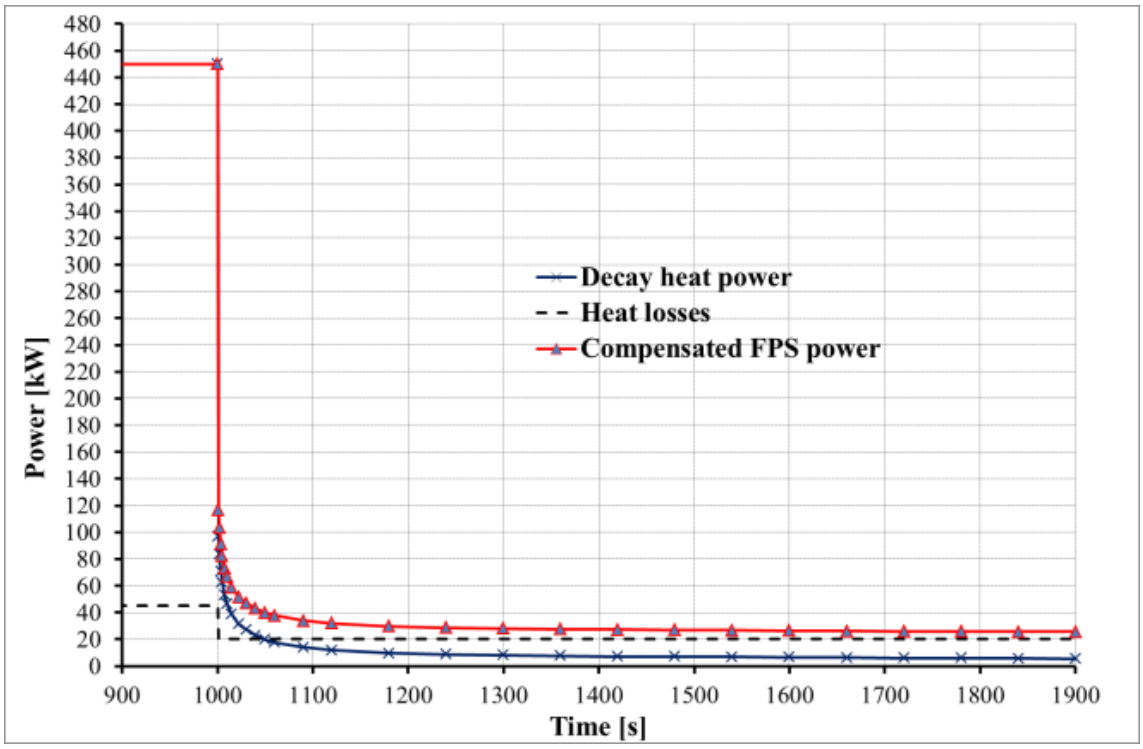

Fig. 90 – HERO-CIRCE transient, FPS power.

6.2.2 Results

Fig. 53 highlights the evolutions of temperatures for 5000 seconds from the transient start up.

0-80 seconds (Fig. 92-a): FPS outlet temperature (tempf 05011) decreases below 420 °C in the first 10 seconds then it stabilizes at 420°C. FPS inlet temperature (tempf 05001) remains constant at 400 °C. The temperatures at the HERO channel inlet (tempf 10401) slightly begins to decrease (and remains above the FPS outlet temperature) while it increases at its outlet because the feed-water goes to zero in the first 5 seconds (tempf 24041). Similarly to the HERO channel inlet, the LBE temperature slightly decreases along the riser (tempf 100, and remains above the FPS outlet temperature).

80-200 seconds (Fig. 92-b): FPS inlet temperature (tempf 05001) increases and overpasses the FPS outlet temperature after about 95 seconds. The spike reaches 440°C and then it decreases again to 400 °C. As results, FPS outlet temperature (tempf 05011) increases from 420 °C to 505°C then it stabilizes at 480°C. The temperatures at the HERO channel inlet (tempf 10401) slightly continue to decrease (and falls below the FPS outlet temperature after about 125 seconds) while it follows the FPS outlet temperature trend at its outlet (tempf 24041). Similarly to the HERO channel inlet, the LBE temperature slightly decreases along the riser (tempf 100, and falls below the FPS outlet temperature after about 125 seconds). Conditions for flow reversal seems to be obtained between 80 – 120 seconds even if this could be related to REAP modelling since un-physical stratification of LBE inside HERO is predicted (local flow reversal could in principle occur avoiding global flow reverse).

200-900 seconds (Fig. 92-c): FPS outlet temperature (tempf 05011) increases again due to a reduction of mass flow rate from 480 °C to 520°C then it decreases down to 480°C (LBE mass flow will increase again). The temperatures at the HERO channel inlet (tempf 10401) slightly continue to decrease (and remains below the FPS outlet temperature) while it follows the FPS outlet temperature trend at its outlet

(tempf 24041). Similarly to the HERO channel inlet, the LBE temperature slightly decreases along the riser (tempf 100).

900-1200 seconds (Fig. 92-d): FPS outlet temperature (tempf 05011) decreases and goes below the temperature at the HERO channel inlet and the riser.

1200-1600 seconds (Fig. 92-e): FPS outlet temperature (tempf 05011) have a spike at about 1260-1290 seconds and overpasses the temperature at the HERO channel inlet and the riser. The FPS inlet temperature has smooth spike too (indicating possible initiation of reversal of mass flow which is not completed since the inlet temperature remains below the outlet temperature).

1600-5000 seconds (Fig. 92-f): FPS outlet temperature (tempf 05011) increase constantly (the mass flow rate induced by NC decreases constantly).

Fig. 93 highlights the behavior of the DHR. The LBE enters the DHR (tempf 10901) at about 400 °C and leaves it at about 375 °C. The air heats up from 20 °C to about 200 °C.

Fig. 94 reports the temperature trends in the pool: constant decrease of temperature is observed because of heat losses and DHR effects.

LBE mass flow rates at FPS and HERO channel inlets/outlets are given in Fig. 95.

0-80 seconds (Fig. 96-a): LBE mass flow rate across the HERO and FPS decreases to a minimum of about 7 kg/s and then in increases up to about 11.3 kg/s.

80-200 seconds (Fig. 96-b): LBE mass flow rate across the HERO and FPS falls to low values and flow reversal is predicted to occur after 87 second and last up to 115 seconds.

200-900 seconds (Fig. 96-c): LBE mass flow rate across the HERO and FPS remains low at about 2 kg/s.

900-1200 seconds (Fig. 96-d): LBE mass flow rate across the HERO and FPS increases up to 10 kg/s.

1200-1600 seconds (Fig. 96-e): mass flow reversal inception is reached two times, however it seems to do not develop.

1600-5000 seconds (Fig. 96-f): mass flow constantly decreases down to 2 kg/s. Oscillations are observed at LBE channel outlet.
LBE DHR channel mass flow rate is depicted in Fig. 97. The mass flow rate stabilizes at about 10.5 kg/s after 1500 seconds.

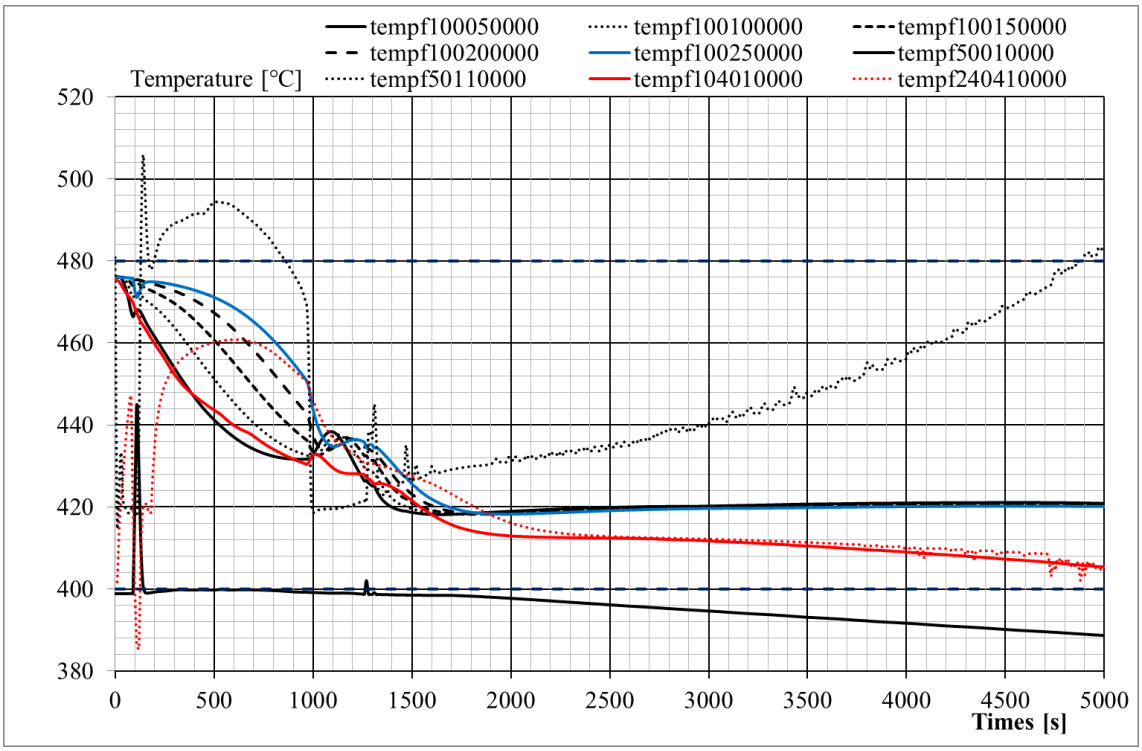

Fig. 91 – HERO-CIRCE transient, R-5 3.3 simulation, FPS, HERO LBE channel and riser temperatures.

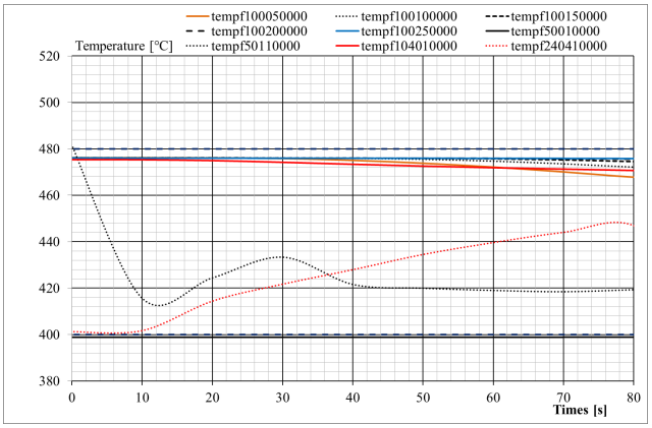

(a) 0-80 seconds

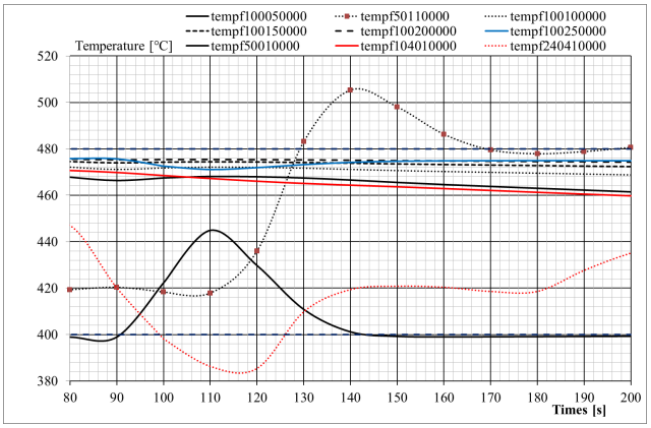

(b) 80-200 seconds

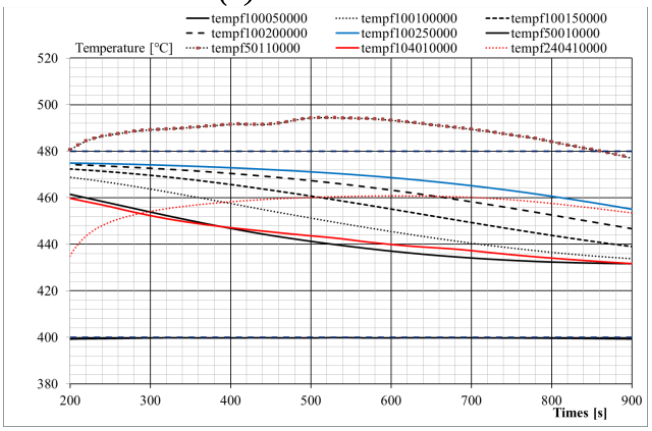

(c) 200-900 seconds

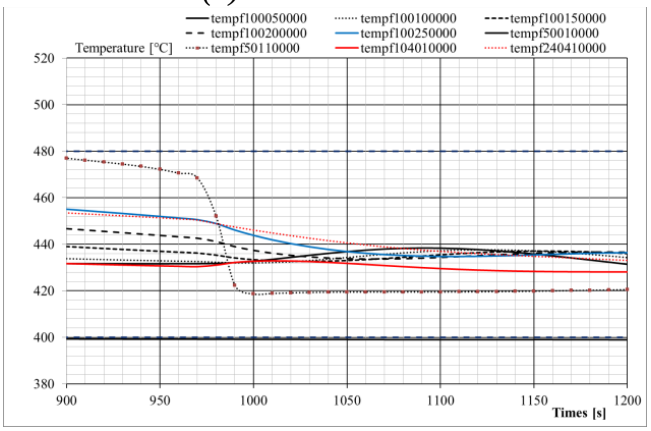

(d) 900-1200 seconds

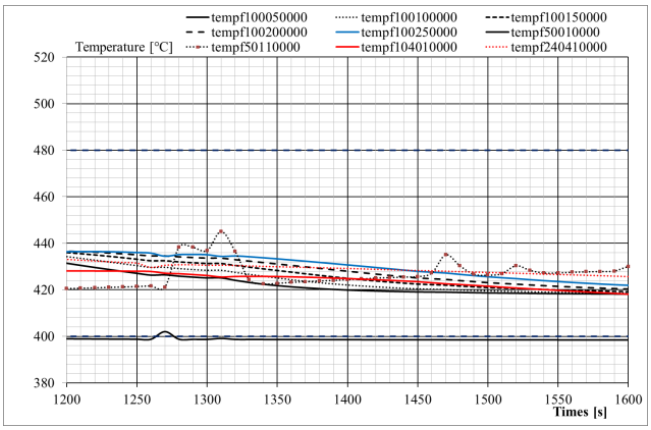

(e) 1200-1600 seconds

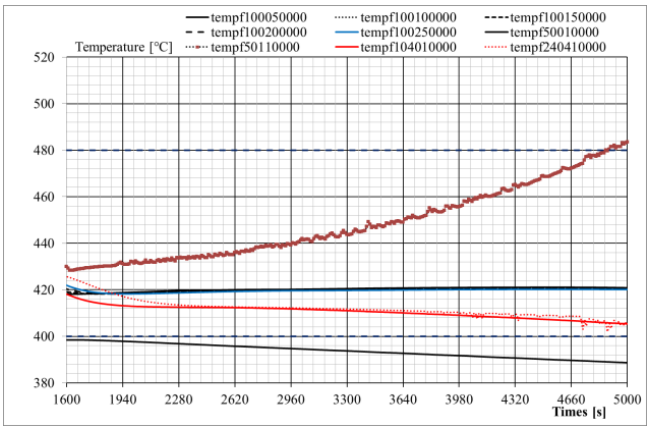

(e) 1600-5000 seconds

Fig. 92 – HERO-CIRCE transient, R-5 3.3 simulation, FPS, HERO LBE channel and riser temperatures zoom.

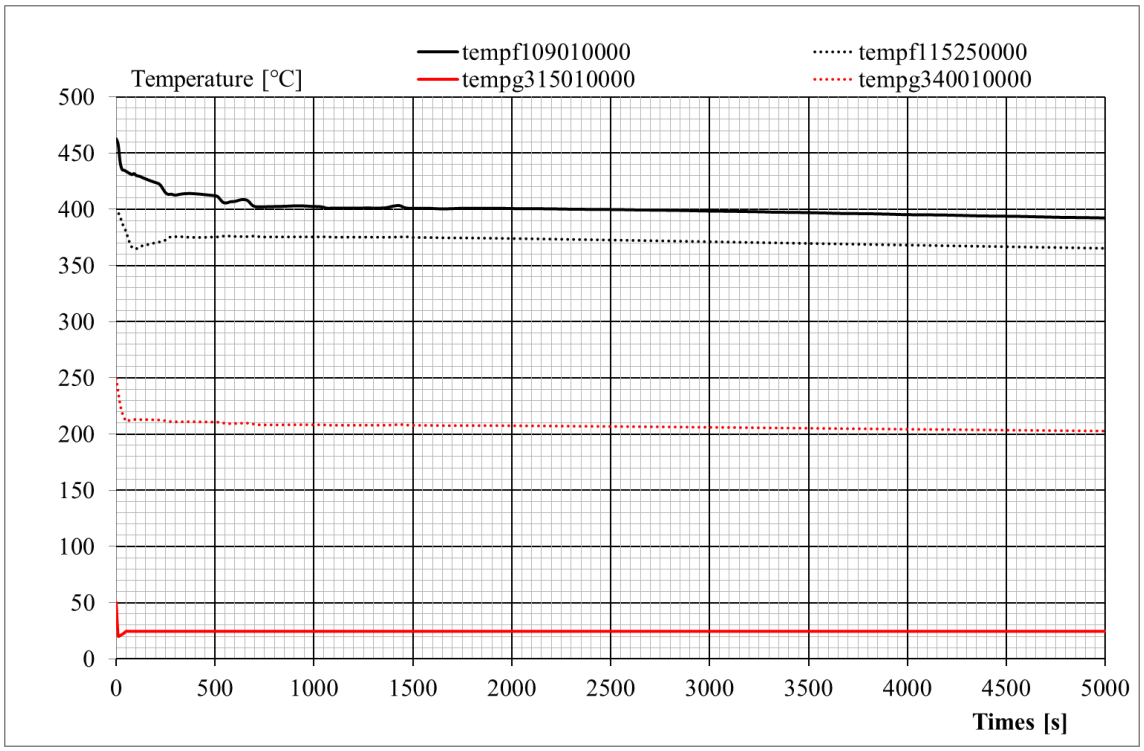

Fig. 93 – HERO-CIRCE transient, R-5 3.3 simulation, DHR LBE channel and air side temperatures.

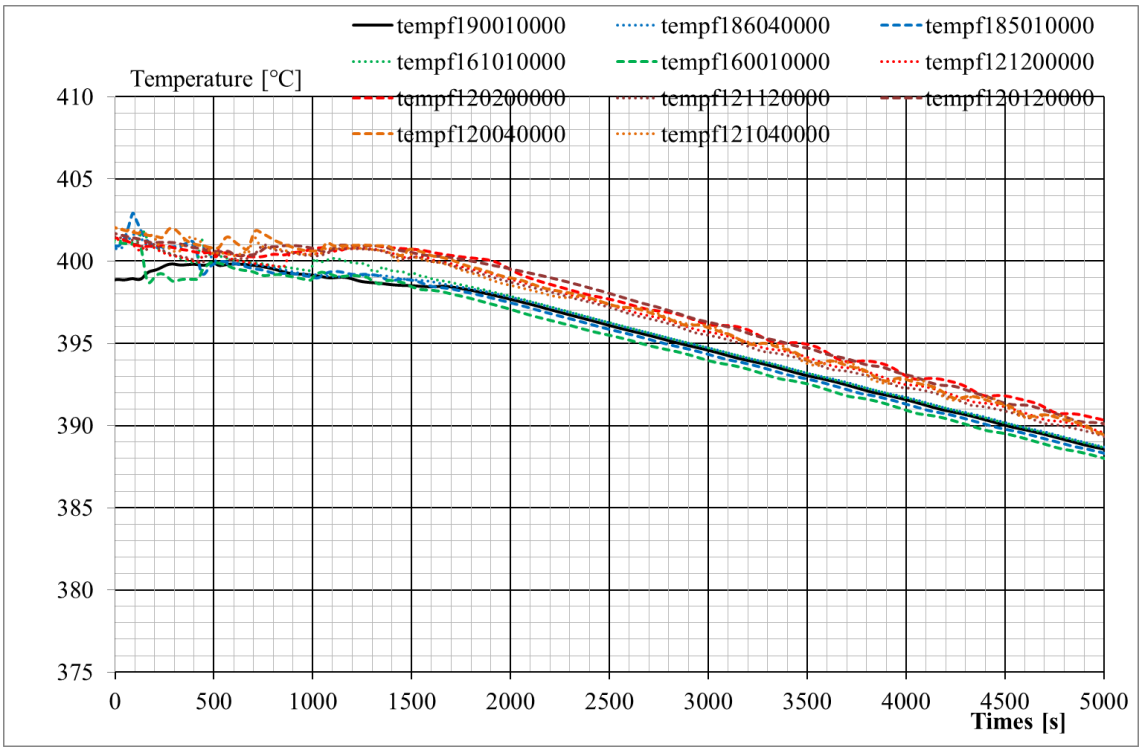

Fig. 94 – HERO-CIRCE transient, R-5 3.3 simulation, LBE pool temperatures.

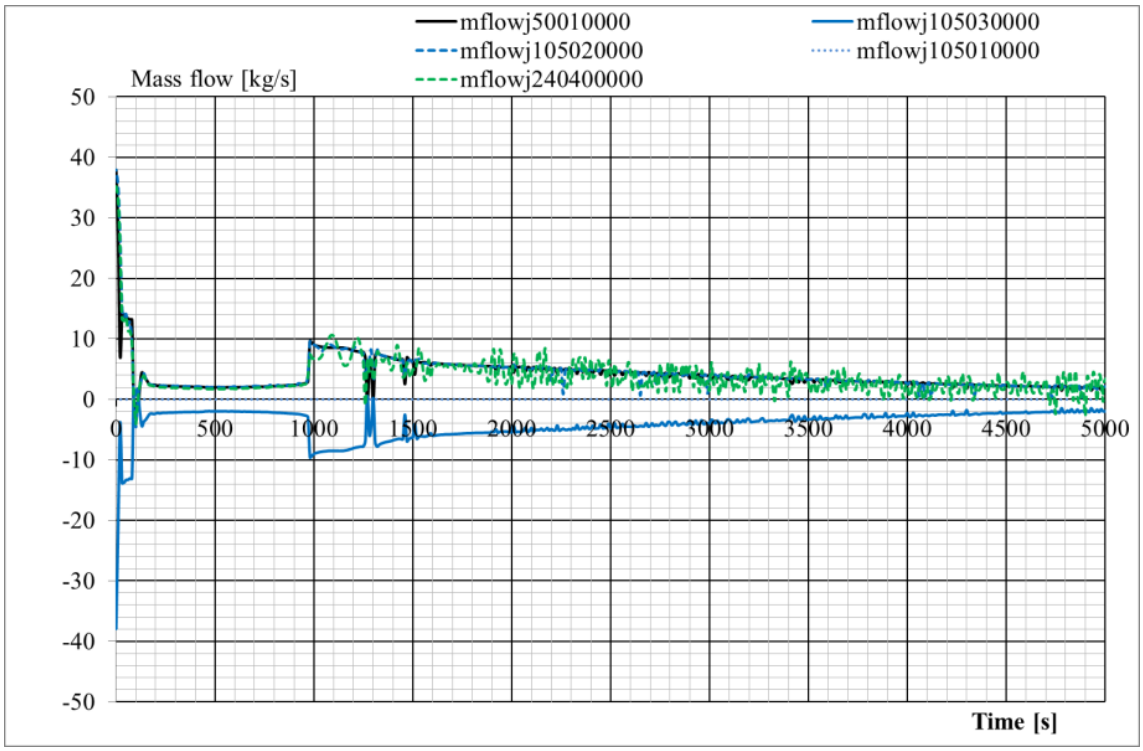

Fig. 95 – HERO-CIRCE transient, R-5 3.3 simulation, LBE mass flow rates at FPS outlet/inlet and HERO LBE channel inlet/outlet.

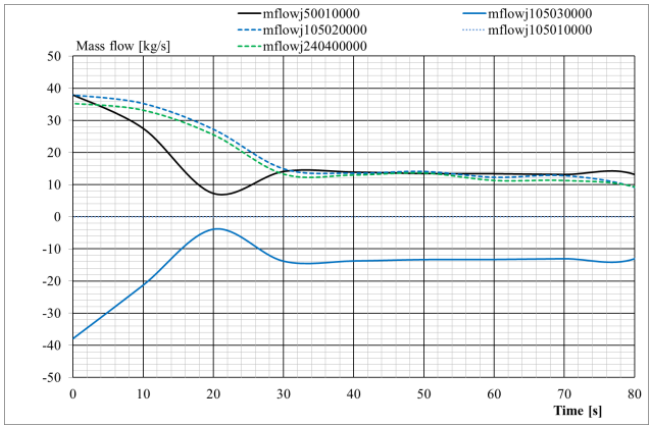

(a) 0-80 seconds

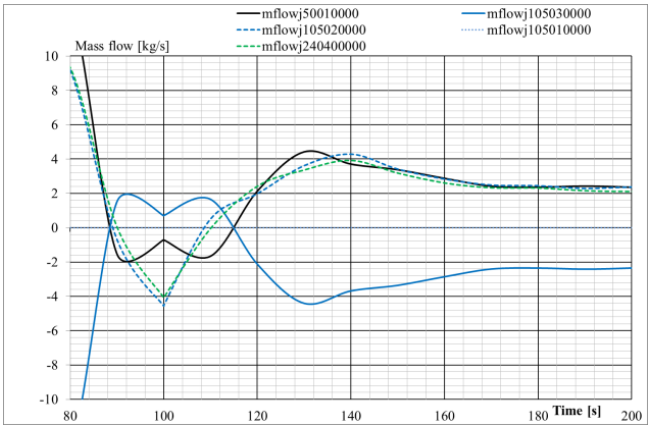

(b) 80-200 seconds

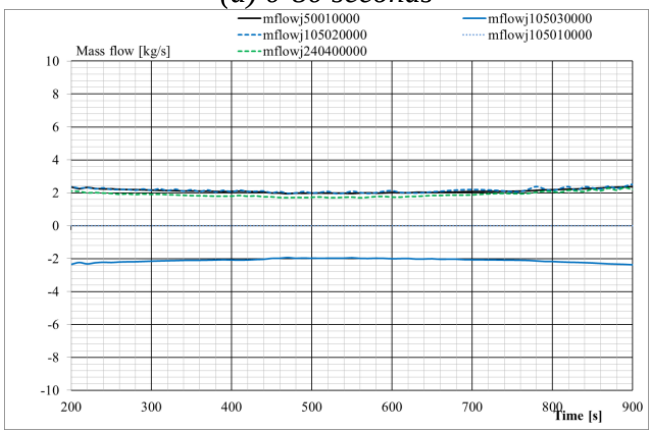

(c) 200-900 seconds

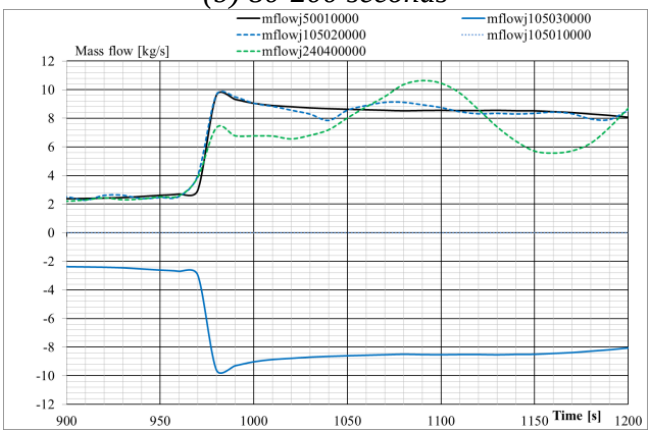

(d) 900-1200 seconds

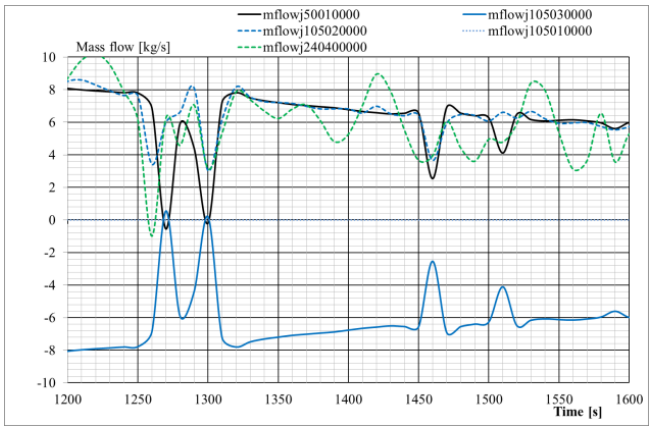

(e) 1200-1600 seconds

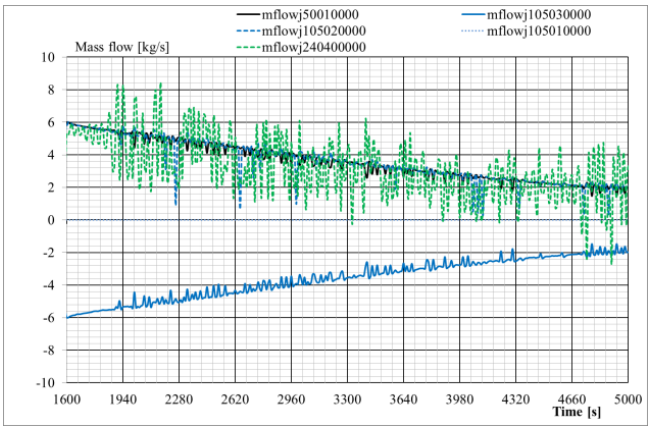

(f) 1600-5000 seconds

Fig. 96 – HERO-CIRCE transient, R-5 3.3 simulation, LBE mass flow rates at FPS outlet/inlet and HERO LBE channel inlet/outlet zoom.

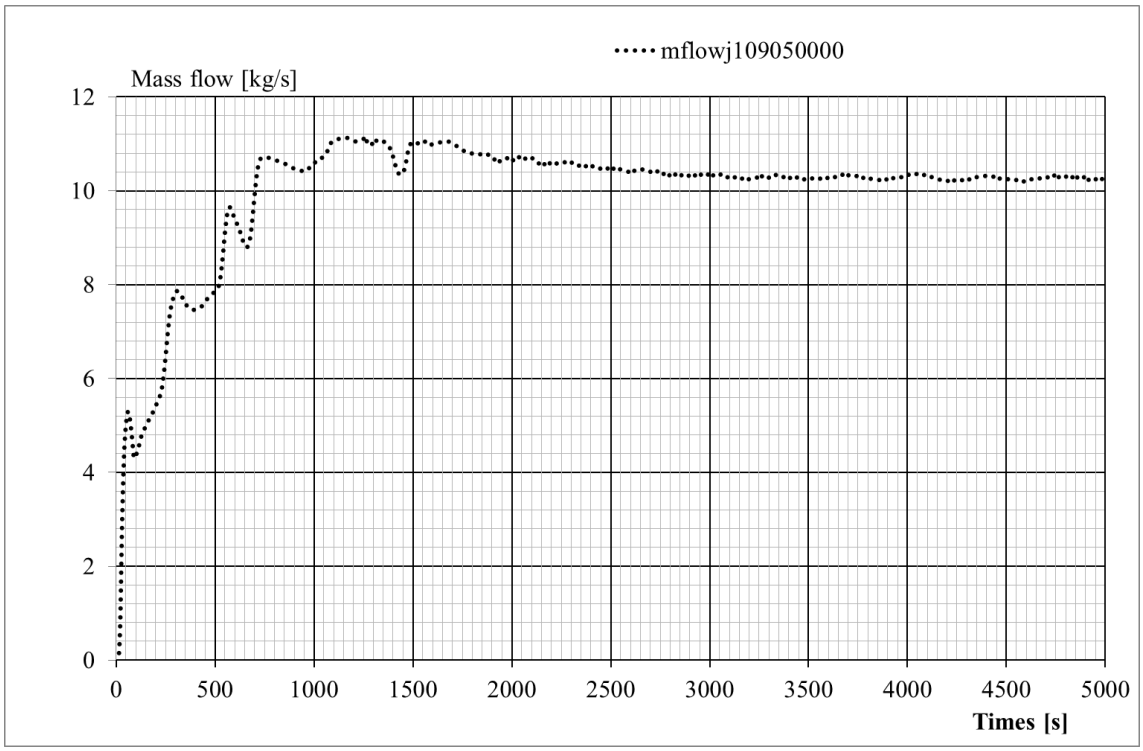

Fig. 97 – HERO-CIRCE transient, R-5 3.3 simulation, LBE mass flow rates at DHR inlet.

7 Conclusions

ENEA designed and constructed the HERO (Heavy liquid mEtal pRessurized water cOoled tubes) test section. This device is actually located in CIRCE and consists of seven double wall bayonet tubes that represent, as much as possible, the ALFRED SG tubes (1:1 in length).

The report describes HERO-CIRCE Pre-test STH calculations by means of RELAP5-3D and RELAP5/Mod3.3

RELAP5-3D v4.3.4 pre-test analyses: two steady state and a transient tests have been investigated.

Two steady state conditions are analysed:

- Case 1, setting up to obtain a constant LBE mass flow rate across the SGBT section equal to 44.7kg/s (representative of the scaled down SG of ALFRED), and
- Case 2, setting to achieve a constant temperature drop across the FPS equal to 80°C in the range 400-480°C (representative of the temperature drop across the core ALFRED).

RELAP5/Mod3.3 pre-test analyses.
Two steady state conditions are investigated:

- Case 1: Full power (450kW) and constant LBE mass flow rate at HERO inlet
- Case 2: Full power (450kW) and constant temperature drop (of about 80°C) across the FPS

These plant status have been characterized assuming the heat losses at CIRCE walls (conservative value has been applied). In both these cases HERO is predicted to generate steam at about 374-376°C.

Starting from Case 2 a transient test has been simulated. The test basically consists in a protected loss of feed-water plus loss of LBE pump: the FPS power decrease down to 7% (representative of decay heat plus heat losses compensation), loss of feed-water and loss of Ar injection will then occur followed by the activation of the air cooled DHR.

The simulation highlights that low natural circulation (in the order of 2-5 kg/s) will take place in the HERO test section. This is basically due to the length of this component (its inlet is close to the FPS inlet). The code predicts a reversal of mass flow after about 80 seconds that lasts about 30 seconds. This phenomenon seems to be related to R-5 capabilities (it does not account for local reverse inside the HERO channel).

REFERENCES

[1] www.gen-4.org, GEN-IV technology website.

[2] www.leader-fp7.eu. LEADER Project website.

[3] A. Alemberti, S M. Grattarola. Project Presentation. LEADER Project WP0 – DEL 035-2010, July 2010.

[4] D. Rozzia, A. Toti, M. Tarantino, Double-wall Bayonet Tube Steam Generator for LFR Application. Preliminary Characterization, NNFISS – LP3 – 032, September 2011.

[5] D. Rozzia, D. Martelli, N. Forgione M. Moretti, A. Naviglio, D. Vitale Di Maio A. Del Nevo, M. Tarantino Activities in Support to the Assessment of SG Bayonet Tubes, for GEN-IV Applications ENEA, NNFISS - LP3 - 054, 2012

[6] D. Rozzia, A. Del Nevo, M. Tarantino, P. Gaggini, D. Vitale Di Maio, G. Caruso, L. Gramiccia, "Fornitura Scambiatore di Calore a Tubi a Baionetta" ADPFISS-LP2_028, 2013.

[7] D. Rozzia, Del Nevo A., Tarantino M., V. Narcisi, D. Vitale Di Maio, F. Giannetti, ALFRED-SGBT. Preliminary characterization by the HERO test section, ADPFISS-LP2-100, september 2015.

[8] Ushakov, P.A., Zhukov, A.V., Matyukhin, M.M., 1977. Heat transfer to liquid metals in regular arrays of fuel elements. High Temperature 15, 868–873 (translated from Teplofizika Vysokikh Temperatur 15 (1977), 1027–1033).

[9] Kazimi, M.S., Carelli, M.D., 1976. Clinch River Breeder Reactor Plant Heat Transfer Correlation for Analysis of CRBRP Assemblies, Westinghouse, CRBRP-ARD-0034.

[10] Balestra, P., Giannetti, F., Caruso, G., Alfonsi, A., 2016. New RELAP5-3D Lead and LBE Thermophysical Properties Implementation for Safety Analysis of Gen IV Reactors, Science and Technology of Nuclear Installations, vol. 2016, Article ID 1687946. http://dx.doi.org/10.1155/2016/1687946.

[11] NUREG/CR-5535, RELAP5/MOD3.3 Code Manual, Volume IV: Models and Correlations, Information Systems Laboratories Inc., December 2001.

[12] NUREG/CR-5535, RELAP5/MOD3.3 Code Manual, Volume I: Code Structure, System Model, and Solution Methods, Information Systems Laboratories Inc., March 2003.

[13] NUREG/CR-5535, RELAP5/MOD3.3 Code Manual, Volume II Appendix A: Input Requirements, Information Systems Laboratories Inc., June 2004.

Curriculum del personale CIRTEN

Il gruppo di lavoro di "Sapienza" Università di Roma che ha collaborato alla presente attività di ricerca è composto da:

Vincenzo Narcisi received his Bachelor's degree in Energy Engineering in 2013 from the "Sapienza" University of Rome. He obtained his degree (M.S. level) in Energy Engineering in 2016 from the the "Sapienza" University of Rome. The master thesis "Pre-test simulations of experimental campaign in the CIRCE-HERO facility" was performed in collaboration with ENEA Brasimone Research Center. During this period he acquired capability in the safety analysis and TH best-estimate transient calculations with the aid pf RELAP5-3D computer programs. His currently research activity is focused on two-phase thermal hydraulic transient analysis, based on system TH computer programs, code Verification and Validation, Sensitivity Analisys and Uncertainty Quantification.

Fabio Giannetti received his degree (M.S. level) in Energy Engineering in 2010 and his Ph.D. in Energy in 2014 from the "Sapienza" University of Rome. He is currently research fellow at "Sapienza" University of Rome. His research activity is focused on two-phase thermal hydraulic transient analysis based on system TH computer programs. He is member of UIT (Italian Union of Thermal Fluid Dynamics).
He acquired capability mainly in the safety analysis and TH best-estimate transient calculations, with the aid of RELAP5/mod3.3, RELAP5-3D, TRACE and MELCOR computer programs, to enhance the safety performances for nuclear reactors (GEN II, GEN III, GEN IV and fusion) and relative sensitivity analysis, as well through RAVEN.
He acquired also expertise in the following topics: advanced thermal-hydraulics; severe accidents analysis; alternative energy and energy saving; design of components and systems for energy production plants; thermodynamic cycles of nuclear power plants.

Gianfranco Caruso received his degree (M.S. level) in Nuclear Engineering in 1984, his Ph.D. in Energy in 1988 and obtained a Postgraduate certificate in Industrial Safety and Protection in 1992 from the "Sapienza" University of Rome. Lecturer in Nuclear Plants from 1986 to 2000, he was Adjunct Professor from 2000 to 2006 and then Assistant Professor in Applied Physics and in Nuclear Plants at the same University. He is member of the ICHMT (International Centre for Heat and Mass Transfer) Scientific Council (1998-2006 and 2012-2016) and member of UIT (Italian Union of Thermal Fluid Dynamics). He is author of two textbooks and more than 120 scientific publications in major journals and conferences. From 1984 he acquired particular expertise in the following topics: advanced thermal-hydraulics in nuclear plants; alternative energy and energy saving; air heating and conditioning; two-phases heat transfer; design of components and systems for energy production plants; studies on physical properties of fluids; heat exchange equipment; thermodynamic cycles of nuclear power plants; industrial safety.